

A STUDY ON SLIDING MODE
STATE ESTIMATION

By

JINHEE CHOI

Bachelor of Science in Engineering
Seoul National University
Seoul, Korea
1979

Master of Science in Engineering
Korea Advanced Institute of Science and Technology
Seoul, Korea
1981

Submitted to the Faculty of the Graduate College
of the Oklahoma State University
in partial fulfillment of the requirements
for the Degree of
DOCTOR OF PHILOSOPHY
May, 1993

COPYRIGHT

by

CHOI, JINHEE

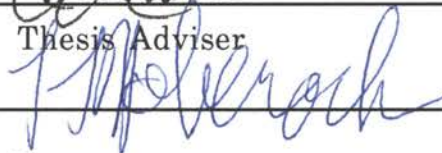
May 1993

A STUDY ON SLIDING MODE
STATE ESTIMATION

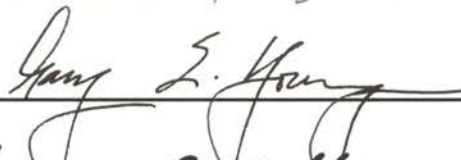
Thesis Approved:



Thesis Adviser



Mark T. Hazan





Dean of the Graduate College

ACKNOWLEDGMENTS

I would like to express my sincere appreciation to my advisor, Dr. Eduardo A. Misawa, for his excellence in guiding and encouragement throughout the course of this research. I am indebted to him for his valuable suggestions and inspiration. I would also like to thank Dr. Gary E. Young, Dr. Lawrence L. Hoberock and Dr. Martin T. Hagan for their helpful comments and discussions.

To my parents, JongKwan Choi and KeumSoon Kim, my deepest thanks for their immeasurable love. My special thanks go to my wife HeeWon for her sacrifice and praying for me. Also, I am deeply grateful to my parents in law and our pastors for their praying.

I want to thank the financial supports provided by the Republic of Korea.

TABLE OF CONTENTS

Chapter	Page
I. INTRODUCTION.....	1
1.1 Overview	1
1.1.1 Scope	1
1.1.2 Contributions of the Thesis.....	2
1.1.3 Problem Definition	3
1.2 Literature Survey	4
1.2.1 Nonlinear Observer	4
1.2.2 Stability Theory and Robust Controls	7
1.3 Differential Equations with Discontinuous Right-Hand Side	8
1.3.1 1-order Examples	8
1.3.3 2-order Examples	10
II. FUNDAMENTALS OF SLIDING OBSERVERS.....	14
2.1 Systems and Problem Statement	14
2.2 Solutions of Discontinuous Differential Equations	16
2.2.1 Sliding and Passing Conditions	16
2.2.2 Switching System.....	18
2.3 Sliding Observer Dynamics	20
2.3.1 Reaching Dynamics	20
2.3.2 Sliding Dynamics.....	22
2.4 Coordinate Transformation.....	23
2.4.1 Shifted-coordinate System	23
2.4.2 Sliding Observer Error Dynamics in the Shifted-coordinate.....	25
2.4.3 Passing Points on the Hyperplane	28

Chapter	Page
III. STABILITY ANALYSIS	31
3.1 Worst-case Analysis	31
3.1.1 Worst-case Analysis of Switching System	31
3.1.2 Example	35
3.2 Worst-Direction in the shifted-coordinate	37
3.2.1 2-Dimension Reaching Dynamics	37
3.2.2 Worst Direction in the Velocity Field	38
3.2.3 Numeric Search	41
3.2.4 Approximate Worst Direction	43
3.2.5 General Remarks	49
3.3 Lyapunov-like Function	49
3.3.1 Introduction	49
3.3.2 Lyapunov-like Function Theorem	50
3.3.3 Passing Jump of Lyapunov-like Function	53
3.4 Lyapunov-like Stability Analysis	56
3.4.1 Lyapunov-like Stability Theorem	56
3.4.2 Contour of Lyapunov-like Function	69
IV. DESIGN OF SLIDING OBSERVERS	75
4.1 Reaching Dynamics Response	75
4.1.1 Reaching Dynamics Response	75
4.1.2 Conceptual Comparisons of Stability Theorems	78
4.1.3 Sliding Observer Design Algorithm	79
4.2 Comparative Example with VSS Observer	81
4.2.1 Sliding Observer	81
4.2.2 VSS Observer	83
4.3 Inverted Pendulum	85
4.4 Nonlinear Mass-Spring System with Friction	88
4.5 Super-tanker Lateral Dynamics	92
V. ROBOT CONTROL BASED ON SLIDING OBSERVERS	97
5.1 Sliding Observer for Multiple Measurement	97

Chapter		Page
5.2	Robots Dynamics	99
5.2.1	Dynamics of Rigid Robots	99
5.2.2	Two link Manipulator.....	100
5.3	The Case with No Parameter Uncertainty.....	103
5.3.1	The Design of the Sliding Observer.....	103
5.3.2	Feedback Linearization Control	105
5.4	The Case with Parameter Uncertainty.....	108
5.4.1	The Design of the Sliding Observer	108
5.4.2	Adaptive Control	109
5.4.3	Sliding Control.....	112
VI.	STOCHASTIC SLIDING OBSERVER DESIGN	115
6.1	Introduction.....	115
6.2	Sliding Observer Design for Noisy Measurements.....	116
6.3	1st Order System Example.....	119
6.4	2nd Order System Example	121
6.5	Prediction and Simulation.....	123
6.5.1	Effect of Measurement Noise	123
6.5.2	Effect of Process Noise.....	125
6.5.3	Effect of Parametric Mismatch	127
VII.	CONCLUSION AND FUTURE RESEARCH	130
7.1	Summary and Conclusion.....	130
7.1.1	Thesis Summary.....	130
7.1.2	Conclusion	132
7.2	Future Research	133
7.2.1	Design Algorithm by Lyapunov-like Stability	133
7.2.2	Worst-case Lyapunov-like Function Search	135
7.2.3	Design procedure Based on the Lyapunov-like Stability Theorem	136
7.2.4	Design Algorithm for Noisy Measurement.....	137
7.2.5	Using Nonlinear Terms in the Observer	137

Chapter	Page
BIBLIOGRAPHY.....	139
APPENDIXES.....	151
APPENDIX A - MATHEMATICAL BACKGROUND.....	154
APPENDIX B - STABILITY THEOREMS.....	159
APPENDIX C - SIGN EQUALIZATION OF PASSING STATES.....	174

LIST OF FIGURES

Figure	Page
1.1 Comparison between linear and nonlinear systems.....	9
1.2 Luenberger observer error dynamics	10
1.3 Sliding observer error dynamics.....	10
1.4 Plotting of sign and saturation function	11
1.5 A linear system with high gains	11
2.1 Shifted-coordinate and sliding patch.....	26
2.2 Passing points on the hyperplane	27
3.1 Worst-case analysis in 2-dimensional phase plane	32
3.2 Stable region by the stability criterion.....	34
3.3 The templet (dotted lines) and disturbed trajectories	36
3.4 The worst-case: $w_1 = 0.8 \cdot \text{sign}(x_2 - k_1 \cdot \text{sgn}(x_1))$	36
3.5 Velocity field and the worst trajectory	37
3.6 Conception of the velocity field.....	39
3.7 Unimodal functions.....	41
3.8 Block diagram of the optimization algorithm	42
3.9 The simulation results of the numeric search.....	43
3.10 The trajectory of solution point and velocity field.....	45
3.11 A solution point shows passing right through the hyperplane	55
3.12 Passing points on the hyperplane	57

Figure	Page
3.13 Phase plane and Lyapunov-like function	61
3.14 Phase plane and Lyapunov-like function	64
3.15 Equivalent eigenvalues.....	64
3.16 Phase plane and Lyapunov-like function	68
3.17 Contour of Lyapunov-like functions	70
3.18 Contour of Lyapunov-like function on the hyperplane	71
3.19 Contour of large Lyapunov-like function case.....	71
3.20 Contour of small Lyapunov-like function case.....	72
3.21 Contour of badly designed case.....	73
3.22 Contour of suggested case.....	73
4.1 Conceptual comparison of stability theorems	77
4.2 Lyapunov-like function contour on the hyperplane	78
4.3 Simulation results of SOON	83
4.4 Sliding observer simulation results	83
4.5 VSS observer simulation results.....	84
4.6 Inverted pendulum with a moving support.....	85
4.7 Simulation results of SOON	87
4.8 Sliding observer simulation results	88
4.9 Simulation results of SOON	90
4.10 Simulation results: time domain plot of 1st states.....	90
4.11 Simulation results: time domain plot of 2st states	91
4.12 Worst reaching dynamics with $x^i = [0 \ 1.5 \ 0.5]$	90
4.13 Worst reaching dynamics with $x^i = [0 \ 1.5 \ 0]$	91
4.14 The actual and estimated states of super-tanker.....	95

Figure	Page
5.1 Two link Manipulator	101
5.2 The simulated results of the sliding observer	105
5.3 The simulated results of feedback linearization control based on the sliding observer.....	107
5.4 The simulated results of feedback linearization control based on the sliding observer with uncertain parameters.....	109
5.5 The simulated results of adaptive control based on the sliding observer with uncertain parameter.....	111
5.6 The simulated results of sliding control based on the sliding observer with uncertain parameter.....	114
6.1 Effect of measurement noise: SO vs. KF (for the 1st order system).....	123
6.2 Effect of measurement noise: SO vs. KF (for the 2nd order system)	124
6.3 Effect of process noise: SO vs. KF (for the 1st order system)	126
6.4 Effect of process noise: SO vs. KF (for the 2nd order system).....	126
6.5 Effect of parameter mismatch: SO vs. KF (for the 1st order system).....	128
6.6 Effect of parameter mismatch: SO vs. KF (for the 2-order system).....	128
7.1 Lyapunov-like function and the passing jump.....	134
7.2 Conception of the velocity field and Lyapunov-like function.....	135
A.1 The velocity field near the hyperplane	153
A.2 Fourier series expansion of square wave and signum function	154
A.4 A saturation function.....	157
A.3 Differential of the Fourier series of square wave.....	155
B.1 The equivalent gain profile	161
B.2 Estimation error dynamics.....	163

Figure	Page
C.1 Transient responses of the reaching dynamics	177
C.2 The conceptual diagram of the reaching time	178
C.3 Convexity and concavity of the function	186
C.4 Convexity of the state and Sign change of the state.....	187

NOMENCLATURE

A	Upper diagonal system matrix
A_m	Meta system matrix
A°	Nominal system value
\tilde{A}	Difference between the system and nominal system
c_{ijk}	Coriolis and centrifugal terms
C_s	Fictitious step advancing constant.
d_{kj}	Coefficient of inertia matrix $D(q)$
g	Nonlinear vector function,
g	Gravitational constant: 9.8 m/sec^2
h^*	Kalman filter optimal gain
H	Linear correction coefficient: $H^T = [h_1^T, h_2^T, \dots, h_n^T]$, $H \in \mathcal{R}^{n \times m}$
K	Switching coefficient: $K^T = [k_1^T, k_2^T, \dots, k_n^T]$, $K \in \mathcal{R}^{n \times m}$
K_s	Shifted switching coefficient
N_1	RIDF of 1_s and the function of statistics of \tilde{y}
P_{2^*}	Fictitious advancing point
P	Unique positive-definite solution to the Lyapunov equation.
p_i	Right eigenvector of A associated with λ_i .
q_i	Left eigenvector of A associated with λ_i .
q_j	Generalized coordinate that is the joint angle
q_r	Reference velocity

Q	Process noise intensity
R	Measurement noise intensity
s	Signs: +,- or 0
s^*	Different sign from s : $\text{sign}(s) \neq \text{sign}(s^*)$
$s_+^i(\tau_j)$	Initial state on the hyperplane at time τ_j
\dot{s}_i	Time derivative of sliding surface
u_d	Sliding observer error dynamics disturbance input
u	Control input vector
v	Measurement noise vectors
w	Input or disturbance input
W	$W = \{0, \dots, 0 \ w\}^T$
x_+	Shifted coordinate ($x_1 > 0$)
x_-	Shifted coordinate ($x_1 < 0$)
x^i	Initial state at the passing point.
y	Measurement vector
\tilde{y}	Output error vector
$Y(q, \dot{q}, \ddot{q})$	Regressor and q is an r -order vector of parameters.
z	System state vector
δ	Rudder angle (degree)
$\delta(x_1)$	Dirac delta function
$\delta\xi$	Magnitude of velocity difference
ϕ_k	Gravitational forces and torques
Φ	State transition matrix: $\Phi = \text{diag}(Q, R)$.

θ	System parameter
$\sigma_+^i(\tau_j)$	Initial state on the hyperplane in the shifted coordinate
τ_i	Control inputs
w	Process noise vectors
Ω_0	Sliding zone in the hyperplane ($x_1 = 0$ and $ x_2 \leq k_1$)
Ω_+	Right half space ($x_1 > 0$)
Ω_-	Left half space ($x_1 < 0$)
ψ	Yaw angle (degree)
$\dot{\psi}$	Yaw rate (degree/sec)

CHAPTER I

INTRODUCTION

1.1 Overview

1.1.1 Scope

A considerable amount of work has been done in the field of state estimation since the late forties. For nonlinear systems, the observers have mainly relied on the precise knowledge of the plant. Recently, state estimation of nonlinear system in the presence of uncertainty has attracted much attention. This attention, of course, is due to the fundamental importance of the issue. There are several robust observers for the uncertain systems, for example, sliding observers, VSS observers, adaptive observers etc. [Misawa, 1989]. However, choosing a proper observer is not easy because, in many cases, the observer design is problem-dependent.

Recently, price-reduced and powerful microprocessors have applied to nonlinear estimation techniques that require on-line calculations. However, the estimation schemes, for example, with the computation of the coupled covariance and filter equations are burdensome on applicable capabilities of the microprocessors in practice. Hence, this study aims at developing a simple structure observer so that it can be implemented using microprocessors.

1.1.2 Contributions of the Thesis

For nonlinear/uncertain systems, adaptive and robust observers have been proposed. Since the robustness of the variable structure system is known, nonlinear observers using "sliding mode" technique have been studied in several ways. An approach using the dual concept of the variable structure system requires the so-called "matching condition." Misawa et al., proposed a sliding observer that can be designed without the matching condition. They proposed two design procedures: the first one is for the case of the strictly positive real system and the other one is based on the absolute stability theorem. With the absolute stability theorem, the sliding observer utilizes a saturation function instead of a sign function.

This study focuses on the robust features of the sliding observer by introducing a Lyapunov-like function theorem. The main works are summarized as follows: first, the fundamentals of the sliding observer were reviewed and explained systematically for the robust features including the shearing effects. For the stability of the observer, the worst case was analyzed so that an algebraic stability condition was derived for the 2-order case. By introducing a coordinate transformation, it is found that the sliding observer can be interpreted in the light of a linear system theory. Stability theorems combined this coordinate transformation and the Lyapunov-like theorem were proved for the stability of the observer. Consequently, a robust nonlinear observer design algorithm, "Sliding Observer design by worst reaching dynamics for Nonlinear/ uncertain system" (SOON) is developed for a phase variable canonical form system. Several comparative examples show the strong points of the sliding observer.

The sliding observer for multiple measurements was developed and

applied to designing an observer based controller for a SCARA robot.

In order to realize the optimal Kalman-Bucy filter, we should know the exact intensities of noise which compose the state error covariance matrix, i.e., the Riccati equation. Practically, however, the noises are not measurable, and the noise intensities may be changed according to the variation of operating conditions. With the nominal statistical properties of the sensor noises, Misawa[1988] applied the method of statistical linearization in designing a suboptimal stochastic sliding observer. In his study, the method was applied to the first order Markov process. The extension from the first order Markov process of the previous work [Misawa, 1988] to the second order Markov process was performed. The extension work includes the parameter mismatch cases in which the optimal solution of the Lyapunov equation was numerically obtained by the steep decent method.

1.1.3 Problem Definition

A nonlinear dynamic system can usually be represented by a set of nonlinear differential equations in this form:

$$\dot{z} = g(z, u, t, w, \theta) \quad (1.1)$$

$$y = h(z, u, t, v, \theta) \quad (1.2)$$

where $g(z, u, t, w, \theta)$ is an $n \times 1$ nonlinear vector function, and z is the internal state vector; y is the measurement vector, u is the control input vector, and w and v are the process and measurement noise vectors. θ is the system parameter, and the system is explicitly time dependent.

A state estimation problem can be interpreted as a composition of a dynamical system that estimates the state z from the measurement y and possibly including the input u . In this study, we are interested in a simple

and robust observer that will guarantee a priori stability and convergence with some relaxed knowledge of the system. Practically, the observer will be implemented using microprocessors or computers and will be corrupted with measurement noise and process noise. With this scope, the ideal state estimation problem can be described as designing a simple observer that can be implemented with desired accuracy and stability in the noise and uncertain environment. For practical situations, the class of problems will be specified. In the study, the plant is assumed to be described by systems of first order differential equations in the canonical form:

$$\begin{cases} \dot{z}_1 = z_2 \\ \dot{z}_2 = z_3 \\ \dots \\ \dot{z}_{n-1} = z_n \\ \dot{z}_n = g(z, u, t, w, \theta) \\ y(t) = C z(t) \end{cases} \quad (1.3)$$

$$\quad \quad \quad \begin{cases} \dot{z}_n = g(z, u, t, w, \theta) \\ y(t) = C z(t) \end{cases} \quad (1.4)$$

where $z \in \mathbb{R}^n$, $y \in \mathbb{R}$, $C \in \mathbb{R}^{1 \times n}$ and $g(z, u, t, w, \theta)$ is a nonlinear/uncertain function.

1.2 Literature Survey

A literature survey was performed on the nonlinear observers and the related fields such as stability theories and robust control. The nonlinear observer survey includes a brief summary of Misawa and Hedrick's recent paper (see detail Misawa [1989]) and is updated with the papers published since 1989.

1.2.1 Nonlinear Observers

Since the cornerstone of modern estimation theories, the Wiener filter and the celebrated Kalman filter, the estimation theory has been a very vigorous research topic. In the case of a linear plant and a linear relationship

between the unknown state and the noisy observations, the estimation problem has been solved by Kalman and Bucy [Kalman, 1960; Kalman, 1961]. Furthermore the Kalman filter is so easily installed in computers that it has been widely used.

In the non-linear case, the Extended Kalman filter [Gelb, 1974; Sorenson, 1985] has a analogous structure to the Kalman filter. The Extended Kalman filter uses both the nonlinear and linear models, and it assumes that the system is perfectly known. The computation of the coupled covariance and filter equation imposes considerable real-time computational efforts [Wishner, 1969; Misawa, 1989]. To avoid the computational load, the approximation of the Extended Kalman filter's residual-gain was precomputed in the Constant Gain Extended Kalman filter [Safonov, 1978; Safonov, 1980]. This method has the guaranteed robustness as the mathematical dual of the LQG controller. This method assumes that the system matrix is Gateaux differentiable [Holzman, 1970], nonanticipative, dynamical nonlinear operators with finite incremental gain so that has limitation on hard nonlinearities.

Phaneuf [1968] developed a Statistically Linearized filter [Gelb, 1974] that uses the describing function. It requires the probability density function to determine the describing function. Beaman [1984] suggests the new scheme to lessen the computational burden due to the error covariance equation. A priori performance and robustness cannot be guaranteed without exactly knowledge of the statistics of x .

The concept of Global Linearization Methods was introduced by Bestle and Zeitz [1983] and extended to the multiple output case by Krener et al. [Krener, 1985; Walcott, 1987]. With the assumption of the existence of a nonlinear transformation $T(x^*)$ that in the new coordinate x^* , the system

may be transformed into a linear observer canonical form. Following the arguments involving the starting vector of Bestle and Zeitz [1983], Walcott et al., showed the necessary transformation for a single output case. This method transforms a system into a simple linear system but cannot guarantee the existence of the transformation.

Another approach is the Extended Linearization Method, which falls into the category of gain scheduling methods. Baumann and Rugh [1986] introduce an observer-design technique for non-linear systems that yields constant eigenvalues for the error differential equation linearized about fixed equilibrium points. The method of extended linearization requires that the system dynamics be known exactly, and this method cannot guarantee the performance and stability except in the neighborhood of constant operating points.

One major idea in designing the nonlinear observer is linearizing the system about a nominal trajectory so that the linear observer technique is applied. Another way to design the nonlinear observer is to use a transformation technique that expresses the system in observable canonical form that simplifies the design process.

However, most of the schemes of nonlinear observers have relied on an exact knowledge of the system. Recently, the robustness of observer for a nonlinear system has been pursued by using the dual concept of Variable Structure System [Drakunov, 1986; Slotine, 1987; Misawa, 1988; Misawa, 1989; Walcott, 1986; Walcott, 1987; Chen, 1987; Chen, 1990]. A nonlinear observer using the sliding mode technique was analyzed for a stochastic case by Drakunov [1986] and for a deterministic case by Slotine, Hedrick and Misawa [1986]. Another approach to estimation of uncertain nonlinear systems is the adaptive observer [Hori, 1988; Chen, 1988; Chen, 1990]. The

drawbacks of the adaptive observer are that it requires the so-called matching conditions, and the estimation error cannot be guaranteed to converge but only to be bounded.

1.2.2 Stability Theory and Robust Controls

Several references can be found on the Lyapunov theory applied to nonlinear systems with discontinuous functions [Alimov, 1960, 1961; Bockman, 1991; Peleties, 1991; Stalford, 1981]. Passivity interpretations of adaptive control laws are discussed in the book of Landau [1979]. The reader is referred to Vidyasagar's book [1978] for a detailed discussion of absolute stability. The circle criterion and its extensions to non-autonomous systems were derived by Narendra [1973], and Zames [1966].

The idea of variable structure systems and sliding surfaces [Filippov, 1964] has been investigated mostly in the Soviet literature [Utkin, 1984; Utkin, 1977; Utkin, 1978; Itkis, 1976]. It is well known that VSS shows robustness, i.e., disturbance rejection property. The undesirable feature, chattering is remedied by plugging a boundary layer into a neighboring sliding surface [Slotine, 1983; Slotine, 1984]. The sliding observer is motivated by the dual concept of sliding control to give the inherent robustness to the nonlinear estimation. Plant uncertainty is the main reason why we need feedback. However, plant uncertainty was largely neglected by modern control [Bryson, 1969] during the 1960s and 1970s. The optimal controllers based on LQG have shown poor performance and even instability in real systems because of high sensitivity to modelling errors [Doyle, 1981; Doyle, 1982]. Beginning in the late 1970s, the study of robust control systems by means of singular-value analysis is represented by the work of investigators centered at the MIT.

The earliest statement of the separation theorem in the literature of control theory was given by Joseph and Tou [Joseph, 1961] on discrete-time systems in 1961. The separation theorem for discrete-time systems was so reasonable and convenient that it was immediately adopted, without rigorous proof, for continuous-time systems [Friedland, 1986; Walcott, 1988]. It is well known that the separation principle cannot be applied directly to uncertain nonlinear systems. Esfandiari and Khalil [1989] used the singular perturbation technique to prove the stability of the observer-based closed-loop control in the presence of time-scaling.

The literature on the subject of computational considerations and robustness with model uncertainties [Safonov, 1978] is sparse. Schweppe [1973] discussed nonlinear estimation and provided a good intuitive understanding of the trade-off between computational requirements and residual-gain choice.

The references about the stochastic processes spread over a wide range of literature, according to the level of mathematical rigor. General textbooks [Papoulis, 1984; Friedland, 1986] are available. Jazwinski [1970] and Astrom [1970] give readable accounts of stochastic differential equations including the Ito and Straonovitch calculi. A higher level of mathematical rigor is found by Kushner [1967, 1984] and Anderson et al. [1986].

1.3 Differential Equations with Discontinuous Right-Hand Sides

1.3.1 1-order Examples

A linear time invariant system with a pole at -3 is asymptotically stable and its nonzero initial state decays to origin exponentially. If a disturbance

is applied, then the system shows state error as in Figure 1.1 (a). The linear system is

$$\dot{x} = -3x + w \quad (1.5)$$

Let us consider a first-order differential equation with a discontinuous right-hand side.

$$\dot{x} = -3 \operatorname{sgn}(x) + w \quad (1.6)$$

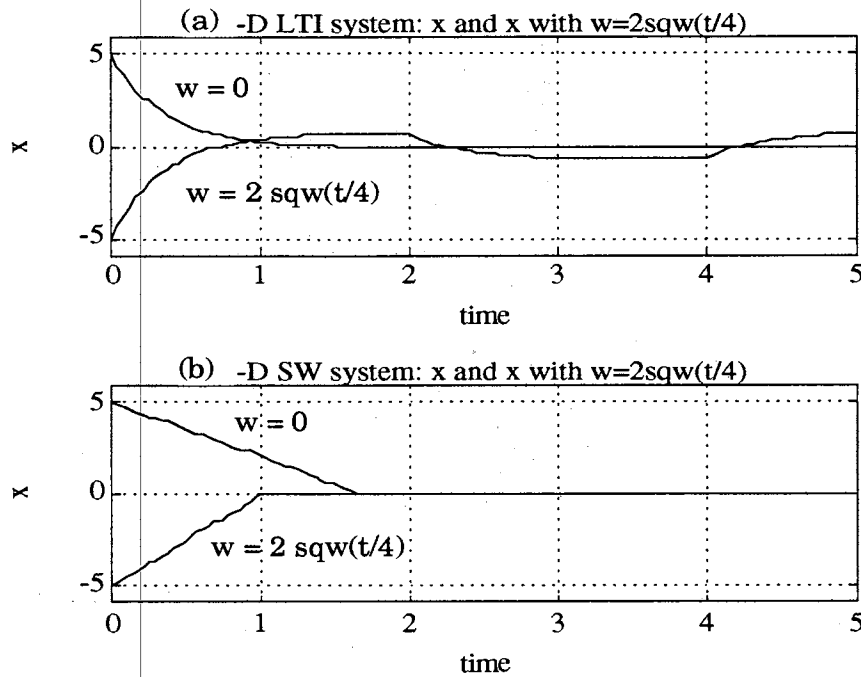


Figure 1.1 Comparison between linear and nonlinear systems

(a) Linear system (b) nonlinear switching system

Without the disturbance input, the switching system, with initial condition $x^i=5$, decays 3 per second. The approaching slope of this nonlinear system is constant, compared to the asymptotic behavior of the linear system.

The velocity field of this system with the bounded disturbance ($|w| < 3$) is

$$\begin{cases} \dot{x} < 0, & \text{for } x > 0 \\ \dot{x} > 0, & \text{for } x < 0 \end{cases} \quad (1.7)$$

This velocity field composes a sliding motion at the switching plane. With a disturbance less than the switching coefficient, this switching system does not leave the sliding surface. The robust feature of the system with a discontinuous right-hand side is mainly owing to this sliding motion. Until arriving at the switching plane $x=0$, the signum function is constant. While staying in the switching plane, the instant time mean of the signum function has the value between $-1 \leq \zeta \leq 1$, i.e., from the Filippov's equivalent dynamics.

1.3.3 2-order Examples

Let us consider a nonlinear system that is a 2-order linear canonical form system with switching functions.

$$\begin{cases} \dot{x}_1 = -h_1 x_1 + x_2 - k_1 1_s(x_1) \\ \dot{x}_2 = -h_2 x_1 - k_2 1_s(x_1) + w \end{cases} \quad (1.8)$$

where w is a input or disturbance input and $h_1:2$, $h_2:2$, $k_1:0.1$, $k_2:2$, $w=\sin(t)$, $1_s(x_1) = \text{sign}(x_1)$ or $\text{sat}(x_1)$

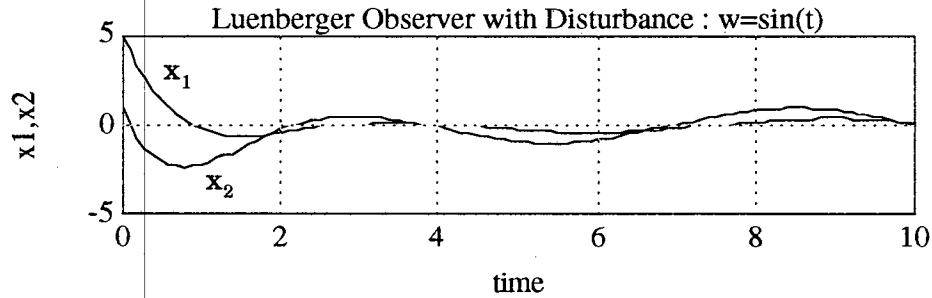


Figure 1.2 Luenberger observer error dynamics

If the system has only linear correction terms, then it is the same as the error dynamics of the Luenberger observer. If switching terms are added to the system then it becomes a nonlinear sliding observer error dynamics.

When the disturbance is applied to the system, the linear system shows the state error according to the disturbances as shown in Figure 1.2. Compared to the linear system, the nonlinear system with additional switching terms compensates the disturbance and quickly diminishes state errors as in Figure 1.3. These properties are the robust features that is essential to observers.

We can see the sliding motion begins at approximately 4 seconds. The switching term looks like the control action of "pulse width modulation control." The saturation function looks like the control action of "amplitude modulation control" and it has the opposite sign of disturbance.

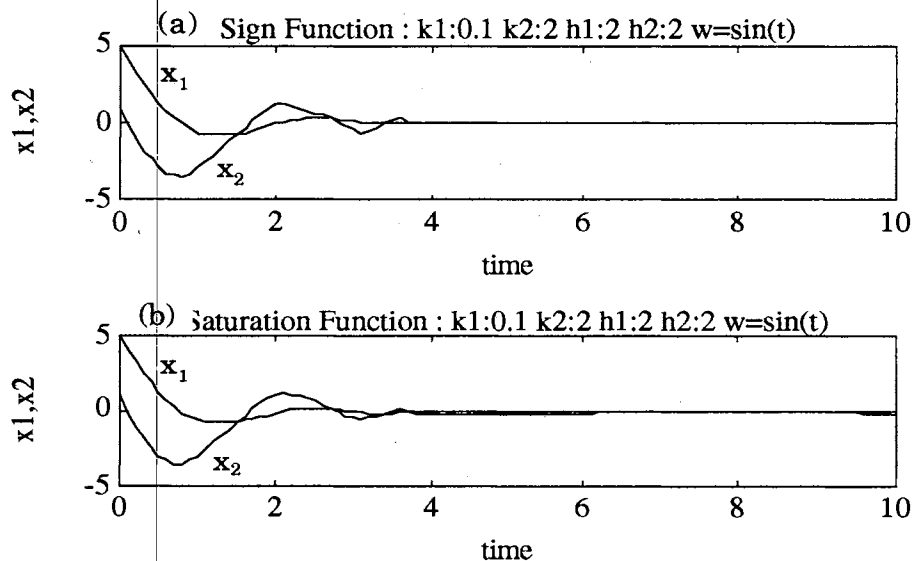


Figure 1.3 Sliding observer error dynamics

(a) Sign function case (b) Saturation function case

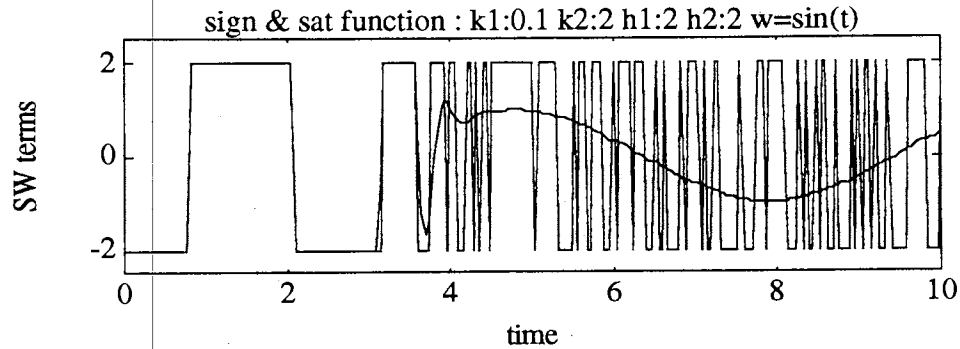


Figure 1.4 Plotting of sign and saturation function

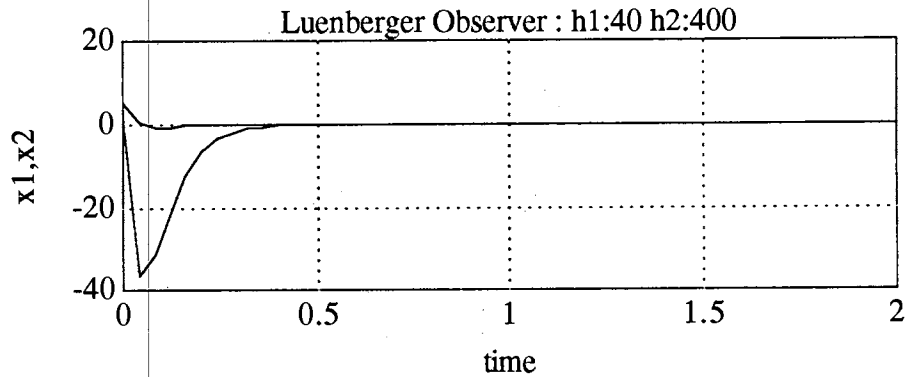


Figure 1.5 A linear system with high gains

The linear system with high gain has a big overshoot compared to the former ones. It is well known that the sensor noise is also amplified by the same gains. The signum function in the nonlinear system has "adaptive" features that behave as a high gain function near the origin and as a low gain function far from the origin.

A nonlinear observer that just had switching terms added to it shows desirable robust features. Since the signum function does not satisfy the Lipschitz condition, the stability of the system with the signum function has

been usually studied by the Lyapunov stability theory. Hence, if the Lyapunov function is not found for the nonlinear observers with the signum function, then the nonlinear observers have been designed with quadratic Lyapunov function which required the matching condition [Walcott, 1986] or can be designed only for a strictly positive real system [Misawa, 1988]. This study aims developing a sliding observer without the matching condition.

CHAPTER II

FUNDAMENTALS OF SLIDING OBSERVERS

2.1 Systems and Problem Statement

It is assumed that the plant is described by a set of first order differential equations in the canonical form:

$$\begin{cases} \dot{z}_1 = z_2 \\ \dot{z}_2 = z_3 \\ \dots \\ \dot{z}_{n-1} = z_n \\ \dot{z}_n = g(z, u, t, w, \theta) \end{cases} \quad (2.1)$$

$$y(t) = C z(t) \quad (2.2)$$

where $z \in \mathbb{R}^n$, $y \in \mathbb{R}^m$, $C \in \mathbb{R}^{m \times n}$, $g(z, u, t, w, \theta)$ is a nonlinear/uncertain function of the state, input, time, disturbance, and system parameter. With this system, the sliding observer is suggested as follows:

$$\dot{\hat{z}} = \begin{pmatrix} \hat{z}_2 \\ \vdots \\ \hat{z}_n \\ \hat{g} \end{pmatrix} + H (y - C \hat{z}) + K l_s(\tilde{y}) \quad (2.3)$$

where $\tilde{y} = y - C \hat{z}$

$$\begin{aligned} H^T &= [h_1^T, h_2^T, \dots, h_n^T], \quad H \in \mathcal{R}^{n \times m} \\ K^T &= [k_1^T, k_2^T, \dots, k_n^T], \quad K \in \mathcal{R}^{n \times m} \end{aligned} \quad (2.4)$$

$\hat{g}(\hat{z}, u, t, w, \hat{\theta})$ is the estimated function of the nonlinear/uncertain function $g(z, u, t, w, \theta)$. The estimated function $\hat{g}(\hat{z}, u, t, w, \hat{\theta})$ is function of the estimated state, input, time, disturbance, and the estimated system parameter. The

function $1_s(\tilde{y})$ is the multivariable generalization of switching functions: $1_s(\tilde{y}) = [\text{sgn}(\tilde{y}_1) \text{sgn}(\tilde{y}_2) \dots \text{sgn}(\tilde{y}_m)]^T$. With this state estimator, the error dynamics is obtained by subtracting equation (2.3) from equation (2.1):

$$\dot{x} = (A - HC)x - K 1_s(\tilde{y}) + \begin{pmatrix} 0 \\ \vdots \\ 0 \\ w \end{pmatrix} \quad (2.5)$$

where $x = z - \hat{z}$, $\tilde{y} = y - C\hat{z} = Cx$, $w = g(z, u, t, w, \theta) - \hat{g}(\hat{z}, u, t, w, \hat{\theta})$, $C = [1 \ 0 \ \dots \ 0]$, the system matrix of error dynamics A is $A = \begin{bmatrix} 0 & I \\ 0 & 0 \end{bmatrix}$.

Since the function $g(z, u, t, w, \theta)$ can be a nonlinear function of the state, it is not modeled into the system matrix. For sliding observer error dynamics, w is the disturbance input which includes the system modeling errors, neglected nonlinearities, parametric uncertainties, and noises. Since the disturbance input w is the difference between g and \hat{g} , its dynamics varies according to the modeling accuracy and the estimation error state [Slotine, 1987]. The estimated model complexity may depend on the acceptable computational burden. The bound of the disturbance input w is assumed to be known for the proper range of system state.

This sliding observer is basically the conventional Luenberger-like observer with an additional term of the signum functions or saturation functions. The "error dynamics" of the observers will be studied in the light of this viewpoint.

Rewriting the equation (2.5), in the case of single measurement available, the observer error structure is of the following form:

$$\begin{cases} \dot{x}_1 = x_2 - h_1 x_1 - k_1 \text{sgn}(x_1) \\ \dot{x}_2 = x_3 - h_2 x_1 - k_2 \text{sgn}(x_1) \\ \vdots \\ \dot{x}_n = -h_n x_1 - k_n \text{sgn}(x_1) + w \end{cases} \quad (2.6)$$

Throughout this study, the above equation (2.6) is used as the standard form of the sliding observer error dynamics with a single measurement.

2.2 Solutions of Discontinuous Differential Equations

2.2.1 Sliding and Passing Conditions

According to the solution of discontinuous differential equations (see Appendix A.1), one should discern the conditions between the two main cases: one is the reaching dynamics and the other is sliding dynamics. Consider the case where the function $f(x)$ is discontinuous on a smooth surface S given by the equation $y = Cx = 0$. The surface S separates its neighborhood in the state space into domains Ω_- and Ω_+ . For the point ξ approaching the point $x \in S$ from the domains Ω_- and Ω_+ , let the function $f(t, \xi)$ have the limit values: [Filippov, 1964]

$$\lim_{\substack{\xi \in \Omega_- \\ \xi \rightarrow x}} f(t, \xi) = f(t, x), \quad \lim_{\substack{\xi \in \Omega_+ \\ \xi \rightarrow x}} f(t, \xi) = f^+(t, x) \quad (2.7)$$

The functions f_N and f_N^+ are defined as the normal component of the vectors f and f^+ to the surface S at the point x . The positive sign is directed toward the domain Ω_+ . In this study, the velocity means \dot{x} in (2.6).

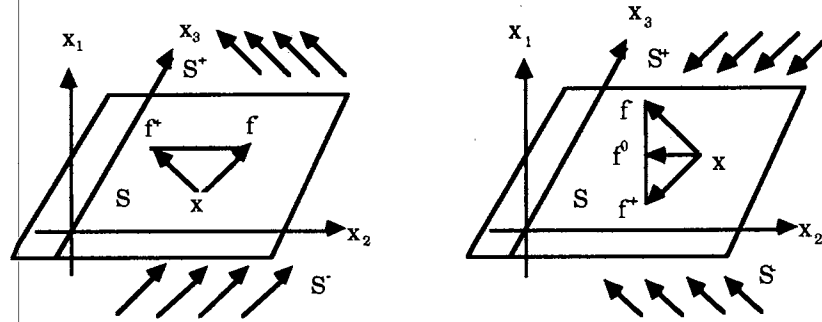


Figure 2.1 The velocity field near the hyperplane

Sliding Condition. If the velocity field $f(t,x)$ is directed to the surface S on both sides, i.e., $f_N(t,x) > 0$, $f_N^*(t,x) < 0$, then near surface S , all the solution points are approaching it from both sides as t increases, and they cannot leave it while the condition is satisfied. Let the hyperplane equation be $\phi(x) = 0$. For the sliding observer (2.6), $\phi(x) = x_1 = 0$ is the sliding surface, and the directional functions at the surface ($x_1=0$) are

$$\begin{cases} f_N = \frac{(\nabla\phi) \cdot f}{|\nabla\phi|} = \dot{x}_1 = x_2 - h_1 x_1 + k_1 = x_2 + k_1 \\ f_N^* = \frac{(\nabla\phi) \cdot f^*}{|\nabla\phi|} = \dot{x}_{1+} = x_2 - h_1 x_1 - k_1 = x_2 - k_1 \end{cases} \quad (2.8)$$

- The sliding condition for the system (2.6) is

$$x_1 \cdot \dot{x}_1 < 0 \quad (\text{at } x_1 = 0) \quad (2.9a)$$

Plug equation (2.7) in equation (2.8):

$$|x_2| < k_1 \quad (2.9b)$$

Passing Condition. If the velocity field $f(t,x)$ has the same signs, i.e., $f_N(t,x) < 0$, $f_N^*(t,x) < 0$ or $f_N(t,x) > 0$, $f_N^*(t,x) > 0$, then near surface S all the solution points are passing through the hyperplane $\phi(x) = x_1 = 0$ as t increases.

- The passing condition for the system (2.6) is

$$|x_2| > k_1 \quad (\text{at } x_1 = 0) \quad (2.10)$$

Suppose that for $t^i < t < t^f$ the trajectory of vector function $x(t)$ extends inside the region in which the right-hand side of equation (2.6) is continuous with respect to (t, x) . With this passing condition, the solution of this system is determined by the first case of the solution definition in Appendix A.1. Undoubtedly, if the velocity function $\dot{x} = f(t,x)$ is continuous at each half plane, then $x(t)$ is continuous. Consequently, the continuity of $x(t)$ is:

$$\mathbf{x}(t) = \mathbf{x}(t^i) + \int_{t^i}^t \mathbf{f}(\tau, \mathbf{x}(\tau)) d\tau \quad (2.11)$$

where \mathbf{x}^i is the initial state at the passing point.

Since the integral is continuous, the continuous derivative $\dot{\mathbf{x}} = \mathbf{f}(t, \mathbf{x})$ exists, for each half domains, for all $t \in (t^i, t^f)$, i.e., $\mathbf{x}(t)$ is a solution in the ordinary sense [Filippov, 1964] (see also Chapter 2.4.2).

2.2.2 Switching System

The suggested sliding observer is a linear system plus switching terms. The linear system has the linear correction term that corrects the velocity field proportional to the feedback state x_1 . On the contrary, the switching terms change the velocity field according to the sign of feedback states. In a linear system, the state transition matrix is in an exponential form. The solution of the switching system is compared with the usual definition of the solution of the differential equation with a continuous right-hand side.

The first order n-simultaneous switching system is

$$\begin{cases} \dot{x}_1 = x_2 - k_1 \operatorname{sgn}(x_1) \\ \dot{x}_2 = x_3 - k_2 \operatorname{sgn}(x_1) \\ \vdots \\ \dot{x}_n = -k_n \operatorname{sgn}(x_1) + w \end{cases} \quad (2.12)$$

While the state x_1 is not zero (in other words the solution point leaves the sliding surface and does not cross over the hyperplane), these dynamics are known as "reaching dynamics." In the 2-order case, it is easy to verify the trajectories of the switching system using a phase plane analysis. Unfortunately, however, this technique does not apply directly to higher order systems. For the general case, the state is obtained by integrating the first order simultaneous equations.

$$\left\{ \begin{array}{l}
 x_n = -k_n \operatorname{sgn}(x_1) t + \int_0^t w \, dt + x_n^i \\
 x_{n-1} = -\frac{k_n}{2!} \operatorname{sgn}(x_1) t^2 + \iint_0^t w \, dt \, dt + (x_n^i - k_{n-1} \operatorname{sgn}(x_1)) t + x_{n-1}^i \\
 \vdots \\
 x_2 = -\frac{k_n}{(n-1)!} \operatorname{sgn}(x_1) t^{n-1} + \iiint_0^t w \, dt^{n-1} + \frac{(x_n^i - k_{n-1} \operatorname{sgn}(x_1))}{(n-2)!} t^{n-2} + \dots + (x_3^i - k_2 \operatorname{sgn}(x_1)) t + x_2^i \\
 x_1 = -\frac{k_n}{n!} \operatorname{sgn}(x_1) t^n + \iiint_0^t w \, dt^n + \frac{(x_n^i - k_{n-1} \operatorname{sgn}(x_1))}{(n-1)!} t^{n-1} + \dots + (x_2^i - k_1 \operatorname{sgn}(x_1)) t + x_1^i
 \end{array} \right. \quad (2.13)$$

where x_j^i is the initial state of x_j and $\iiint w \, dt^n$ stands for n -multiple integral.

Let the bound of disturbance be $w=w(t)$ as follows:

$$-k_n \leq w_{\min} \leq w \leq w_{\max} \leq k_n \quad (2.14)$$

With the bounded initial state and disturbance, the bound of each state for the right half side of the switching plane ($x_1 > 0$) is as follows:

$$-k_n t + w_{\min} t + x_n^i \leq x_n \leq -k_n t + w_{\max} t + x_n^i \quad (2.15a)$$

$$-\frac{(k_n - w_{\min})}{2!} t^2 - (k_{n-1} - x_n^i) t + x_{n-1}^i \leq x_{n-1} \leq -\frac{(k_n - w_{\max})}{2!} t^2 - (k_{n-1} - x_n^i) t + x_{n-1}^i \quad (2.15b)$$

...

$$\begin{aligned}
 & \frac{(k_n - w_{\min})}{(n-1)!} t^{n-1} - \frac{(k_{n-1} - x_n^i)}{(n-2)!} t^{n-2} - \dots - (k_2 - x_3^i) t + x_2^i \leq x_2 \\
 & \leq \frac{(k_n - w_{\max})}{(n-1)!} t^{n-1} - \frac{(k_{n-1} - x_n^i)}{(n-2)!} t^{n-2} - \dots - (k_2 - x_3^i) t + x_2^i
 \end{aligned} \quad (2.15c)$$

$$\begin{aligned}
 0 & \leq -\frac{(k_n - w_{\min})}{n!} t^n - \frac{(k_{n-1} - x_n^i)}{(n-1)!} t^{n-1} - \dots - (k_1 - x_2^i) t + x_1^i \leq x_1 \\
 & \leq -\frac{(k_n - w_{\max})}{n!} t^n - \frac{(k_{n-1} - x_n^i)}{(n-1)!} t^{n-1} - \dots - (k_1 - x_2^i) t + x_1^i
 \end{aligned} \quad (2.15d)$$

ed

For the left half plane ($x_1 < 0$), the bound will be obtained the same way. We cannot conclude the stability of the system from the equations (2.15). However, the equations show that each state has modes of power of time. Particularly, the coefficient of the highest power term of each state has the opposite sign of x_1 .

2.3 Sliding Observer Dynamics

Since the sliding observer has both linear correction terms and switching terms, its dynamics may have characteristics of both. In this section, the sliding observer is compared with a linear system and a switching system and the sliding observer dynamics are reexamined as a composition of reaching dynamics and sliding dynamics.

2.3.1 Reaching dynamics

Linear Time Invariant (LTI) System. A LTI system in state space form is

$$\dot{z} = A z + B u, \quad z(t_0) = z_0 \quad (2.16)$$

The state solution is expressed in an exponential form of the state-transition matrix:

$$z(t) = e^{At} z_0 + \int_0^t e^{A(t-\tau)} B u(\tau) d\tau \quad (2.17)$$

The responses of a linear time-invariant dynamical system are dictated mainly by its modes, or equivalently, the eigenvalues of A . If an eigenvalue has a negative real part, its mode will approach zero exponentially as $t \rightarrow \infty$.

$$z(t) = \sum_i (p_i z_0) e^{\lambda_i t} q_i \quad (2.18)$$

where p_i and q_i are, respectively, a right and a left eigenvectors of A associated

with λ_i .

Switching System. The switching dynamics (2.15) is compared to the time invariant linear system dynamics. The state correction mechanism is compared to the LTI system as follows:

Switching system:

$$\begin{cases} \dot{x}_2 = \dot{x}_1 + k_1 \operatorname{sgn}(x_1) \\ \dot{x}_3 = \dot{x}_2 + k_2 \operatorname{sgn}(x_1) \\ \dots \\ \dot{x}_n = \dot{x}_{n-1} + k_{n-1} \operatorname{sgn}(x_1) \end{cases} \quad (2.19)$$

LTI system:

$$\begin{cases} \dot{x}_2 = \dot{x}_1 + h_1 x_1 \\ \dot{x}_3 = \dot{x}_2 + h_2 x_1 \\ \dots \\ \dot{x}_n = \dot{x}_{n-1} + h_{n-1} x_1 \end{cases} \quad (2.20)$$

Reaching Dynamics of the Sliding Observer. The sliding observer error dynamics is the same as the combination of two systems. Consider a 3-order case of the sliding observer with a passing condition:

$$\begin{cases} \dot{x}_1 = x_2 - h_1 x_1 - k_1 \operatorname{sgn}(x_1) \\ \dot{x}_2 = x_3 - h_2 x_1 - k_2 \operatorname{sgn}(x_1) \\ \dot{x}_3 = -h_3 x_1 - k_3 \operatorname{sgn}(x_1) + w \end{cases} \quad (2.21)$$

where $w = \omega(x, u, t, w, \theta)$

Differentiate \dot{x}_1 and plug in the second equation:

$$\ddot{x}_1 = -h_1 \dot{x}_1 - h_2 x_1 - k_1 \delta(x_1) \dot{x}_1 - k_2 \operatorname{sgn}(x_1) + x_3$$

where $\delta(x_1)$ is a dirac delta function (see Appendix A.2)

$$x_1^{(3)} = -h_1 \ddot{x}_1 - h_2 \dot{x}_1 - h_3 x_1 - k_1 \delta(x_1) \ddot{x}_1 - k_2 \delta(x_1) \dot{x}_1 - k_3 \operatorname{sgn}(x_1) + w \quad (2.22)$$

If a solution point does not cross over the hyperplane, i.e., reaching dynamics and x_1 is not zero, then the dynamics (2.22) is rewritten as:

$$\ddot{x}_1^{(3)} = -h_1 \ddot{x}_1 - h_2 \dot{x}_1 - h_3 x_1 - k_3 \operatorname{sgn}(x_1) + w \quad (2.23)$$

Near the switching plane, i.e., $|x_1| \ll 1$, the contribution of linear correction terms in the equation (2.21) is less than that of switching terms. However, the linear correction terms of the reaching dynamics cannot be neglected. Even though $|x_1| \ll 1$, we should notice that the differentiated terms may not be small. Hence, by using the linear correction terms, we can stabilize the system.

2.3.2 Sliding Dynamics

To get the sliding dynamics, the methodology of Lemma 1.1 in Appendix A.1 could be directly applied to the sliding observer [Filippov, 1964]. With a finite switching timing, the sliding dynamics includes chattering that may be harmful for sliding control in practice. For an observer problem, even though the chattering is only a numeric phenomenon, it is not desirable for the observer based controllers. With the linear correction terms, the sliding dynamics is obtained as the same method.

The $n-1$ poles associated with the sliding dynamics on the sliding patch are obtained by Slotine [1987]

$$\det \left(sI_{n-1} - \begin{bmatrix} -k_2/k_1 & 1 & 0 & \dots & 0 \\ -k_3/k_1 & 0 & 1 & \dots & 0 \\ \vdots & \vdots & \vdots & \ddots & \vdots \\ \vdots & \vdots & \vdots & \ddots & 1 \\ -k_n/k_1 & 0 & 0 & \dots & 0 \end{bmatrix} \right) = 0 \quad (2.24)$$

where the I_{n-1} is the identity matrix of order $n-1$. Thus the poles of the sliding dynamics can be placed arbitrarily by proper selection of the ratios k_i/k_1 , ($i=2, \dots, n$).

2.4 Coordinate Transformation

2.4.1 Shifted-coordinate System

The error dynamics (2.6) can be rewritten as:

$$\dot{x} = A_m x - K \operatorname{sgn}(x_1) + W \quad (2.25)$$

where $K = \{k_1, \dots, k_n\}^T$, $W = \{0, \dots, 0\}^T$ and

$$A_m = \begin{bmatrix} -h_1 & 1 & 0 & \dots & 0 & 0 \\ -h_2 & 0 & 1 & & & \\ \vdots & \vdots & \vdots & \ddots & \vdots & \\ \vdots & \vdots & \vdots & & 0 & 1 \\ -h_n & 0 & \vdots & \dots & 0 & 0 \end{bmatrix} = \left[\begin{array}{c|c} H & I \\ \hline \vdots & 0 \end{array} \right] \quad (2.26)$$

The equation (2.25) can be rewritten as:

$$\dot{x} = A_m x - \left[\begin{array}{c|c} I & 0 \\ \hline 0 & 0 \end{array} \right] K \operatorname{sgn}(x_1) + \begin{pmatrix} 0 \\ \vdots \\ 0 \\ u_d \end{pmatrix} \quad (2.27)$$

$$\text{where } u_d = w - k_n \operatorname{sgn}(x_1) \quad (2.28)$$

Observation 2.2 Matrix multiplication

$$\left[\begin{array}{c|c} H & I \\ \hline \vdots & 0 \end{array} \right] \left[\begin{array}{c|c} 0 & 0 \\ \hline I & 0 \end{array} \right] = \left[\begin{array}{c|c} I & 0 \\ \hline 0 & 0 \end{array} \right] \quad (2.29)$$

■

By using equation (2.29), rewrite equation (2.27):

$$\dot{\mathbf{x}} = \mathbf{A}_m \left(\mathbf{x} - \left[\begin{array}{c|c} 0 & 0 \\ \hline \mathbf{I} & 0 \end{array} \right] \mathbf{K} \operatorname{sgn}(\mathbf{x}_1) \right) + \begin{pmatrix} 0 \\ \vdots \\ 0 \\ \mathbf{u}_d \end{pmatrix} \quad (2.30)$$

The sliding observer can be rewritten:

$$\dot{\mathbf{x}} = \mathbf{A}_m (\mathbf{x} - \mathbf{K}_s \operatorname{sgn}(\mathbf{x}_1)) + \begin{pmatrix} 0 \\ \vdots \\ 0 \\ \mathbf{u}_d \end{pmatrix} \quad (2.31)$$

where $\mathbf{K}_s = \left[\begin{array}{c|c} 0 & 0 \\ \hline \mathbf{I} & 0 \end{array} \right] \mathbf{K}$: shifted switching coefficient (2.32)

Take a coordinate transformation:

$$\mathbf{x}_s = \mathbf{x} - \mathbf{K}_s \operatorname{sgn}(\mathbf{x}_1) \quad (2.33)$$

and differentiate it

$$\dot{\mathbf{x}}_s = \dot{\mathbf{x}} - \mathbf{K}_s \delta(\mathbf{x}) \dot{\mathbf{x}}_1 \quad (2.34)$$

Finally, in the shifted-coordinate system, the sliding observer is

$$\dot{\mathbf{x}}_s = \mathbf{A}_m \mathbf{x}_s + \begin{pmatrix} 0 \\ \vdots \\ 0 \\ \mathbf{u}_d \end{pmatrix} - \mathbf{K}_s \delta(\mathbf{x}) \dot{\mathbf{x}}_1 \quad (2.35)$$

For the reaching dynamics, the sliding observer in the shifted-coordinate is

$$\dot{\mathbf{x}}_s = \mathbf{A}_m \mathbf{x}_s + \begin{pmatrix} 0 \\ \vdots \\ 0 \\ \mathbf{u}_d \end{pmatrix} \quad (2.36)$$

where $u_d = w - k_n \text{sgn}(x_1)$

The shifted-coordinate transformation for each side of the domains Ω_+ and Ω_- are as follows:

$$x_s = \begin{cases} x_+ = x - K_s, & \text{for } \Omega_+ (x_1 > 0) \\ x_- = x + K_s, & \text{for } \Omega_- (x_1 < 0) \end{cases} \quad (2.37)$$

2.4.2 Sliding Observer Error Dynamics in the shifted coordinate

Compared to a LTI system, the sliding observer has three dynamics which are two reaching dynamics for $x_1 > 0$, $x_1 < 0$ in the shifted-coordinate and sliding dynamics at the hyperplane $x_1 = 0$.

i) Right Reaching Dynamics. The first mode is for $x_1 > 0$ space with passing condition:

$$\begin{cases} \dot{x}_1 = x_2 - h_1 x_1 - k_1 \\ \dot{x}_2 = x_3 - h_2 x_1 - k_2 \\ \dots \\ \dot{x}_n = w - h_n x_1 - k_n \end{cases} \quad (2.38)$$

Take the coordinate transformation:

$$\begin{cases} x_{1+} = x_1 \\ x_{2+} = x_2 - k_1 \text{sgn}(x_1) \\ \dots \\ x_{n+} = x_n - k_{n-1} \text{sgn}(x_1) \end{cases} \quad (2.39)$$

The right reaching dynamics is

$$\dot{x}_+ = \begin{bmatrix} -h_1 & 1 & 0 & \dots & 0 & 0 \\ -h_2 & 0 & 1 & & & \\ \vdots & \vdots & \vdots & \ddots & \vdots & \\ \vdots & \vdots & \vdots & & 0 & 1 \\ -h_n & 0 & \vdots & \dots & 0 & 0 \end{bmatrix} x_+ + \begin{bmatrix} 0 \\ \vdots \\ 0 \\ u_{d+} \end{bmatrix} \quad (2.40)$$

where $x_+ = [x_{1+} \dots x_{n+}]^T$, for $x_1 \neq 0$, $\delta(x_1) = 0$ and $u_{d+} = -k_n + w < 0$ for $k_n > |w|_{\max}$

The reaching dynamics is the second companion form in the linear

system theory. The equilibrium point is moved to:

$$\mathbf{x} = [0 \ k_1 \ k_2 \ \dots \ k_{n-1}]^T \quad (2.41)$$

The disturbance input u_{d+} will push the solution point into the sliding patch where the sliding mode occurs or the trajectory will cross the hyperplane.

ii) Left Reaching Dynamics. The second mode is for $x_1 < 0$ space with passing condition:

$$\begin{cases} \dot{x}_1 = x_2 - h_1 x_1 + k_1 \\ \dot{x}_2 = x_3 - h_2 x_1 + k_2 \\ \dots \\ \dot{x}_n = w - h_n x_1 + k_n \end{cases} \quad (2.42)$$

The shifted-coordinate transformation is

$$\begin{cases} x_{1-} = x_1 \\ x_{2-} = x_2 + k_1 \\ \dots \\ x_{n-} = x_n + k_{n-1} \end{cases} \quad (2.43)$$

The left reaching dynamics is

$$\dot{\mathbf{x}}_- = \begin{bmatrix} -h_1 & 1 & 0 & \dots & 0 & 0 \\ -h_2 & 0 & 1 & & & \\ \vdots & \vdots & \vdots & \ddots & \vdots & \\ & & & & 0 & 1 \\ -h_n & 0 & \dots & 0 & 0 & 0 \end{bmatrix} \mathbf{x}_- + \begin{bmatrix} 0 \\ \vdots \\ 0 \\ u_{d-} \end{bmatrix} \quad (2.44)$$

$$\text{where } \mathbf{x}_- = [x_{1-} \ \dots \ x_{n-}]^T \text{ and } u_{d-} = k_n + w > 0 \quad (2.45)$$

$$\text{The equilibrium point is moved to } \mathbf{x} = [0 \ -k_1 \ -k_2 \ \dots \ -k_{n-1}]^T. \quad (2.46)$$

The disturbance input u_{d-} will push the solution point into the sliding zone where the sliding mode occurs or the trajectory will cross the hyperplane.

iii) Sliding Dynamics. The third dynamics is the sliding dynamics that

is in the hyperplane $x_1 = 0$ with the sliding condition ($|x_2| < k_1$).

$$\begin{pmatrix} \dot{x}_2 \\ \dot{x}_3 \\ \vdots \\ \dot{x}_n \end{pmatrix} = \begin{bmatrix} -k_2/k_1 & 1 & 0 & \dots & 0 \\ -k_3/k_1 & 0 & 1 & \dots & 0 \\ \vdots & \vdots & \vdots & \ddots & \vdots \\ \vdots & \vdots & \vdots & \vdots & 1 \\ -k_n/k_1 & 0 & 0 & \dots & 0 \end{bmatrix} \begin{pmatrix} x_2 \\ x_3 \\ \vdots \\ x_n \end{pmatrix} + \begin{pmatrix} 0 \\ \vdots \\ 0 \\ w \end{pmatrix} \quad (2.47)$$

Steady State of the Sliding Dynamics. With the constant disturbance, the steady state with the sliding condition can be calculated from the condition:

$$\begin{cases} \dot{x}_1 = 0 \\ \dot{x}_2 = 0 \\ \vdots \\ \dot{x}_n = 0 \end{cases} \quad (2.52)$$

Plug this condition into the sliding observer (2.6) with $x_1 = 0$ and obtain:

$$\text{Time mean}[\text{sgn}(x_1)] = \frac{x_2}{k_1} = \frac{x_3}{k_2} = \dots = \frac{w}{k_n} \quad (2.53)$$

From this condition, the steady states are obtained as follows:

$$\begin{cases} x_{2ss} = \frac{k_1}{k_n} w \\ x_{3ss} = \frac{k_2}{k_n} w \\ \vdots \\ x_{nss} = \frac{k_{n-1}}{k_n} w \end{cases} \quad (2.54)$$

With the presumed condition $|w| \leq k_n$, the steady state is in the region $|x_{iss}| \leq k_{i-1}$; in other words the steady state is confined by the shifted-constant K_s . If the absolute of every state is less than the shifted constant, i.e., $|x_i| \leq k_{i-1}$, then the switching terms dominate the velocity field direction at the each switching instance. Consequently, all the velocity direction is opposite of the sign of x_i at the instance.

2.4.3. Passing Points on the Hyperplane

The error state of sliding observer with an arbitrary initial condition is desirable to converged to, within finite time of passing, the sliding patch and stays on it. Through a series of switching, designing an asymptotically

stable system is required the notion of passing points. As a notational convenience, the set of passing points is defined by sequences of switching timing $0 \leq \tau_j < \infty$, $\forall \tau_j \in \tau_s = \tau_0, \tau_1, \dots, \tau_{k-1}, \tau_k, \dots$

$$\{s(x_s, \tau_j)\} = s(\tau_0), s(\tau_1), \dots, s(\tau_k), \dots \quad (2.55)$$

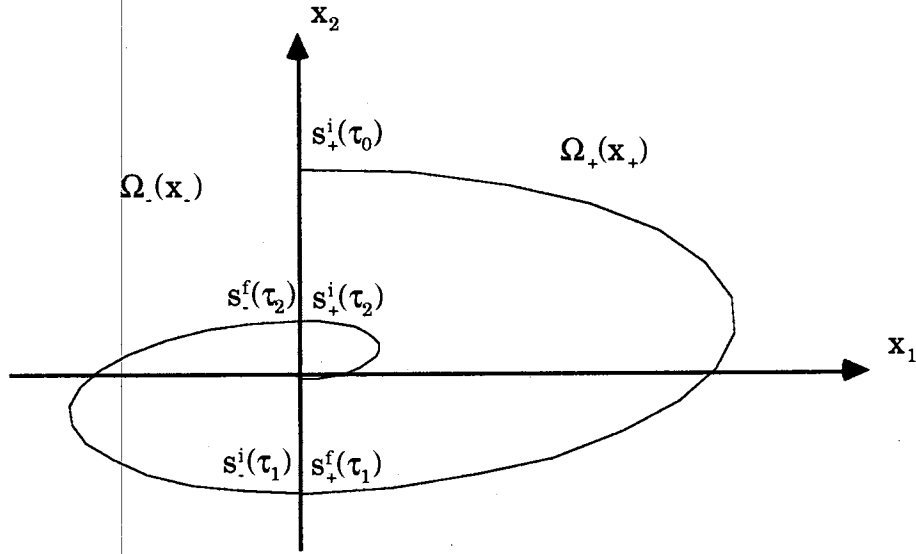


Figure 2.3 Passing points on the hyperplane

At the passing instance τ_j on the hyperplane, the new initial state is reset as the same as the final state of the former reaching dynamics except the changed sign of x_1 ($x_1 \approx 0$). Even though the velocity field of the system is discontinuous as equation (2.42) and (2.46), the trajectory is continuous (see Appendix A.1). The passing point $s(x_s, \tau_j)$ is decomposed into $s_+(\tau_j)$ and $s_-(\tau_j)$ according to the sign of x_1 . Hence, the continuity equation of passing state is

$$\begin{cases} s_s(\tau_j) = s_-^i(\tau_j) = s_+^f(\tau_j) \\ s_s(\tau_j) = s_+^i(\tau_j) = s_-^f(\tau_j) \end{cases} \quad (\text{except changed sign of } x_1, s=-,+) \quad (2.56)$$

$$\text{where } s_+^i(\tau_j) = \begin{bmatrix} 0_+^i \\ s_{2+}^i \\ \vdots \\ s_{n+}^i \end{bmatrix}, \quad s_+^f(\tau_j) = \begin{bmatrix} 0_+^f \\ s_{2+}^f \\ \vdots \\ s_{n+}^f \end{bmatrix}, \quad s_-^i(\tau_j) = \begin{bmatrix} 0_-^i \\ s_{2-}^i \\ \vdots \\ s_{n-}^i \end{bmatrix}, \quad s_-^f(\tau_j) = \begin{bmatrix} 0_-^f \\ s_{2-}^f \\ \vdots \\ s_{n-}^f \end{bmatrix} \quad (2.57)$$

It is convenient to express the initial state and the final state in the shifted-coordinate x_s

$$\sigma_+^i(\tau_j) = \begin{bmatrix} 0_+^i \\ \sigma_{2+}^i \\ \vdots \\ \sigma_{n+}^i \end{bmatrix}, \quad \sigma_+^f(\tau_j) = \begin{bmatrix} 0_+^f \\ \sigma_{2+}^f \\ \vdots \\ \sigma_{n+}^f \end{bmatrix}, \quad \sigma_-^i(\tau_j) = \begin{bmatrix} 0_-^i \\ \sigma_{2-}^i \\ \vdots \\ \sigma_{n-}^i \end{bmatrix}, \quad \sigma_-^f(\tau_j) = \begin{bmatrix} 0_-^f \\ \sigma_{2-}^f \\ \vdots \\ \sigma_{n-}^f \end{bmatrix} \quad (2.58)$$

The relations of the passing state between the original coordinate and the shifted-coordinate are

$$\left\{ \begin{array}{l} \sigma_+^i(\tau_j) = s_+^i(\tau_j) - K_s \\ \sigma_+^f(\tau_j) = s_+^f(\tau_j) - K_s \\ \sigma_-^i(\tau_j) = s_-^i(\tau_j) + K_s \\ \sigma_-^f(\tau_j) = s_-^f(\tau_j) + K_s \end{array} \right. \quad (2.59)$$

By plugging equation (2.59) into the continuity equation (2.53), we have:

i) Passing left (with the passing condition $x_1=0, x_2 < -k_1$)

$$s_-^i(\tau_j) = s_+^f(\tau_j) \Rightarrow \sigma_-^i(\tau_j) = \sigma_+^f(\tau_j) + 2K_s \quad (2.60)$$

ii) Passing right (with the passing condition $x_1=0, x_2 > k_1$)

$$s_+^i(\tau_j) = s_-^f(\tau_j) \Rightarrow \sigma_+^i(\tau_j) = \sigma_-^f(\tau_j) - 2K_s \quad (2.61)$$

In the shifted-coordinate, the initial and final states are different from each other by twice of the shifted-coefficient because the coordinate origin is shifted.

CHAPTER III

STABILITY ANALYSIS

3.1 Worst Case Analysis

3.1.1 Worst Case Analysis of Switching System

The initial condition and the disturbance input of the sliding observer determine a trajectory of system. For the sliding observer, the disturbance input can worsen the error state. If the worst direction is known and the worst case is stable, then the system is obviously stable. The worst-case trajectory is defined as the worst-convergence trajectory that encloses any other trajectory with the same bounded disturbance in the phase plane.

Consider the worst case in a second-order switching system with a passing condition.

$$\begin{cases} \dot{x}_1 = x_2 - k_1 \operatorname{sgn}(x_1) \\ \dot{x}_2 = -k_2 \operatorname{sgn}(x_1) + w \end{cases} \quad (3.1)$$

where $|w| < k_2$ is a disturbance whose bound is known (3.2)

With no loss of generality, we can assume that an initial point starts on a hyperplane, i.e., $x_1=0$, $|x_2| > k_1$. In a second-order phase plane analysis, the plane is divided into 4 regions as Figure 3.1.

Region I) For the region $(x_1 > 0 \cap x_2 > k_1)$, the system is

$$\begin{cases} \dot{x}_1 = x_2 - k_1 \\ \dot{x}_2 = -k_2 + w \end{cases} \quad (3.3)$$

Region II) For the region ($x_1 > 0 \cap x_2 < k_1$), the system is the same as the case of region I. The worst trajectory of solution point is the line CD in Figure, that is by minimum disturbance $w = -\omega$ and the equation is

$$x_1 = \frac{-1}{2(k_2 + \omega)} (x_2 - k_1)^2 + C_2 \quad (3.6)$$

The final solution point D in this region is clearly the worst point because it is the outermost point. If the disturbance has a positive sign, then it will be helpful to converge like the trajectory line C'D' whose equation is

$$x_1 = \frac{-1}{2(k_2 - \omega)} (x_2 - k_1)^2 + C_2' \quad (3.7)$$

If the bound of disturbance is known and if the coefficient k_2 is greater than the bound of disturbance, then the trajectories of solution point are enveloped with the curves, i.e., the worst trajectory ABCD and the best trajectory AB'C'D' as in Figure. According to the equations (3.4) and (3.6), the worst direction of disturbance in right half plane is

$$\begin{aligned} w &= \omega \operatorname{sgn}(x_2 - k_1 \operatorname{sgn}(x_1)) \\ &= \omega \operatorname{sgn}(\dot{x}_1) \end{aligned} \quad (3.8)$$

For a left half plane, the worst direction is the same as the above equation, since it is symmetric about the origin. Let assume the initial states $x_1^i = 0$ and $x_2^i = L2_+^i > k_1$. For the worst case, the constants of equations (3.4) and (3.6) are:

$$C_1 = C_2 = \frac{(L2_+^i - k_1)^2}{2(k_2 - \omega)} \quad (3.9)$$

With the given condition (3.9), solve the equation (3.6), and the final point, $x_{2|x_1=0}$, is obtained for the worst case:

$$x_{2|x_1=0} = -\sqrt{(k_2 + \omega) \frac{(L2_+^i - k_1)^2}{(k_2 - \omega)}} + k_1$$

$$\begin{aligned} L2_-^f &= |x_{2|x_1=0}| \\ &= \sqrt{\frac{(k_2 + \omega)}{(k_2 - \omega)}} (L2_+^i - k_1) - k_1 \end{aligned} \quad \begin{array}{l} \text{(Take positive term)} \\ \end{array} \quad (3.10)$$

If $L2_+^i \geq L2_-^f$, then the system is BIBO stable. If the disturbance is zero ($\omega=0$), then the distance of the final point is closer than the initial condition by twice of k_1 until it reaches sliding patches. The worst case analysis of the left half plane is the same as that of right half plane. This jump approach to origin shows "*shearing effect*" of the sliding observer.

$$L2_+^f = (L2_+^i - 2k_1) \quad (3.11)$$

$$L2_-^f = (L2_-^i - 2k_1) \quad (3.12)$$

With the known bound of ω and $L2_+^i$ (or $L2_-^i$), we need to design k_1 and k_2 . (k_2 is presumed greater than the bound of ω).

The algebraic condition for k_1 is

$$\frac{k_1}{L2_+^i} \geq \left(\frac{k_2}{\omega} - \sqrt{\left(\frac{k_2}{\omega}\right)^2 - 1} \right) \quad (3.13)$$

The above equation is singular for $\omega = 0$: since this analysis is for the worse case, it is reasonable to assume $\omega \neq 0$. From the algebraic stability criterion, if k_2 equals ω then the initial condition x_2 should be on the sliding patch i.e., $x_2^i = k_1$ in order to guarantee stability. Using the stability criterion (3.13), Figure 3.2 is plotted as a function of k_2/ω . We can see that k_2 is not necessarily the same as the bound of disturbance. If k_2 is 2 times of ω , then k_1 can be selected as small as $0.3 \cdot L2_+^i$ as shown in Figure 3.2.

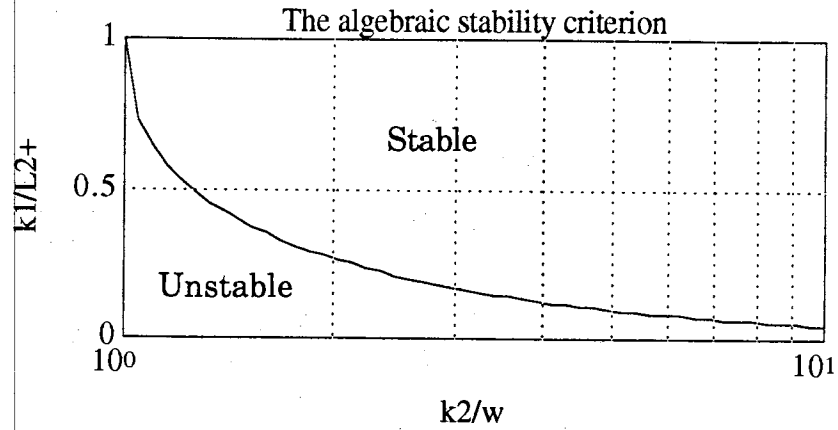


Figure 3.2 Stable region by the stability criterion (3.13)

3.1.2 Example

Let us consider a following second-order switching system

$$\begin{cases} \dot{x}_1 = x_2 - \text{sgn}(x_1) \\ \dot{x}_2 = -2 \text{sgn}(x_1) + w \end{cases} \quad (3.14)$$

where $x_1 = 0$, $x_2^i = L2_+^i = 5$, $w_1 = 0.8 \cdot \text{sign}(x_2)$, $w_2 = 0.5 \cdot \text{sign}(x_2)$

The above initial condition satisfies the passing condition. Therefore, apply the stability criterion (3.13) and we have the necessary condition for stability:

$$k_2=2, L2_+=5 \begin{cases} w_1=0.8 \rightarrow k_1 > 1.044 \\ w_2=0.5 \rightarrow k_1 > 0.635 \end{cases} \quad (3.15)$$

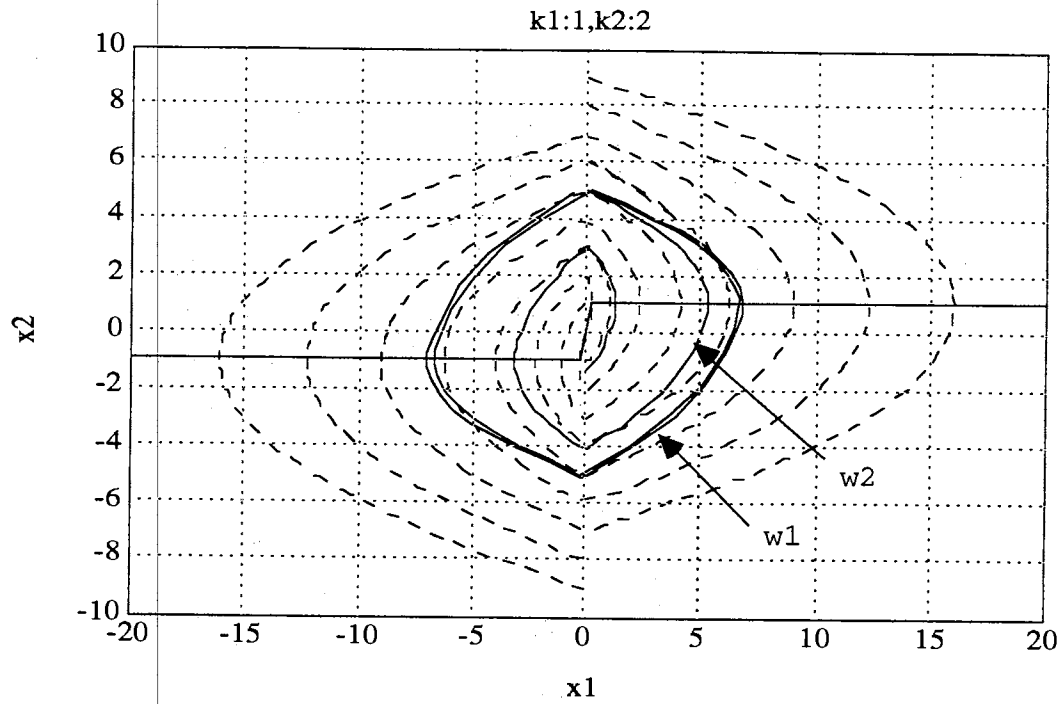


Figure 3.3 The template (dotted lines) and disturbed trajectories

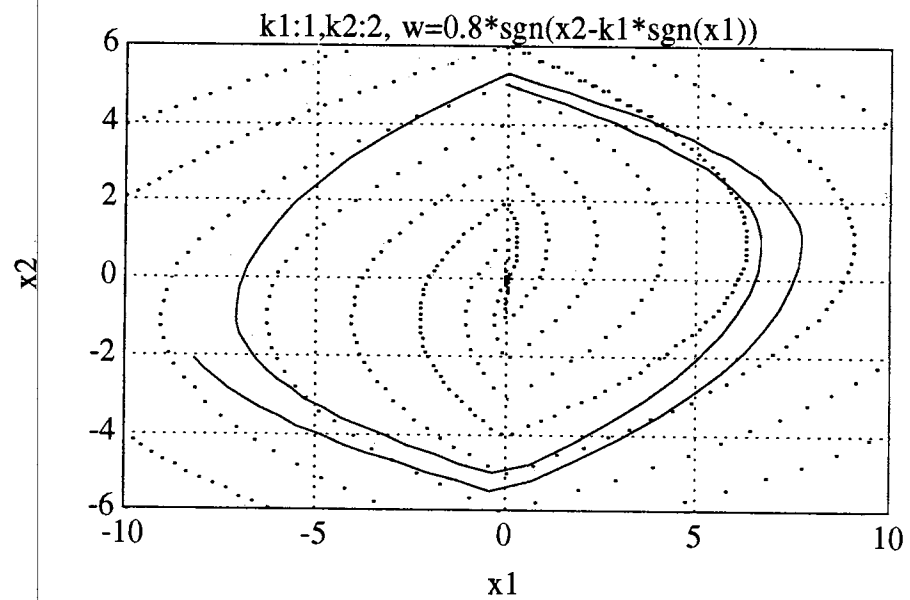


Figure 3.4 The worst case: $w_1=0.8*\text{sign}(x_2 - k_1*\text{sgn}(x_1))$

The template (dotted lines) is made by the system without disturbance, and the disturbances for the trajectories (solid lines) are: $w_1=0.8*\text{sign}(x_2)$, $w_2=0.5*\text{sign}(x_2)$. The system's coefficient $k_1 = 1$ is sufficient for the worst case of $w_2 = 0.5$: for the case of $w_2 = 0.8$, it is not. In Figure 3.3, the disturbance $w_1=0.8*\text{sign}(x_2)$ forces the system to grow slowly. On the contrary, in Figure 3.4, the worst disturbance $w_1=0.8*\text{sign}(x_2 - k_1*\text{sgn}(x_1))$ forces the system to diverge faster than the former one does.

3.2 Worst Direction in the Shifted-coordinate

3.2.1 Second-Order Reaching Dynamics

Rewrite the equation (2.39) in Chapter 2 for a second-order case:

$$\begin{cases} \dot{x}_1 = -h_1 x_1 + x_{2+} \\ \dot{x}_{2+} = -h_2 x_1 + u_d \end{cases} \quad (3.16)$$

$$\text{where } u_d = w - k_2 \text{sgn}(x_1), \quad -k_2 \leq w_{\min} \leq w \leq w_{\max} \leq k_2 \quad (3.17)$$

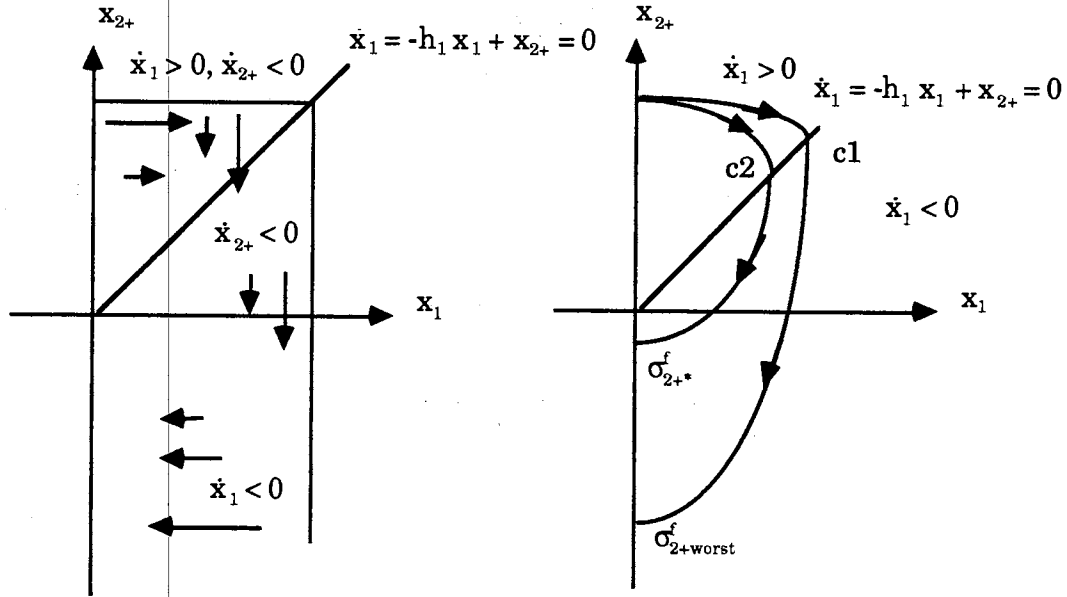


Figure 3.5 Velocity field and the worst trajectory

For the region $(x_1 > 0 \cap \dot{x}_1 > 0)$, the worst direction is

$$\begin{aligned}
 \dot{x}_{2+ \text{worst}} &= \dot{x}_{2+} \big|_{\max(\dot{x}_2)} \\
 &= \dot{x}_{2+} \big|_{\max(w)} \\
 &= \dot{x}_{2+} \big|_{\min(\dot{x}_2)} \quad (\because \dot{x}_{2+} < 0) \\
 &= -h_2 x_1
 \end{aligned} \tag{3.18}$$

With the passing condition, the solution point starts to move right. The maximum outermost point is c_1 which is determined by the slope h_1 and the coefficient h_2 .

For the region $(x_1 > 0 \cap \dot{x}_1 < 0)$, the worst direction is

$$\begin{aligned}
 \dot{x}_{2+ \text{worst}} &= \dot{x}_{2+} \big|_{\min(\dot{x}_2)} \\
 &= \dot{x}_{2+} \big|_{\min(w)} \\
 &= \dot{x}_{2+} \big|_{\max(\dot{x}_2)} \quad (\because \dot{x}_2 < 0) \\
 &= -h_2 x_1 - 2k_2
 \end{aligned} \tag{3.19}$$

It is clear that any other trajectories are bounded by the worst trajectory, that the magnitude of the worst passing point is the bound of any other passing points.

$$|\sigma_{2+ \text{worst}}^f| \geq |\sigma_{2+}^f| \tag{3.20}$$

In the both half space, the worst disturbance is

$$w = \omega \operatorname{sgn}(\dot{x}_1) \tag{3.21}$$

This worst direction is the same as that of the switching system (see equation (3.8)).

3.2.2 Worst Direction in the Velocity Field

Let us consider the velocity field of a 2-dimensional space:

$$\begin{cases} \dot{x}_1 = -h_1 x_1 + x_{2+} \\ \dot{x}_{2+} = -h_2 x_1 + u_d \end{cases}$$

where $u_d = w \cdot k_2 \operatorname{sgn}(x_1)$, $-k_2 \leq w_{\min} \leq w \leq w_{\max} \leq k_2$

In order to specify the coordinate transformation, the subscript + or - are used in the dynamics equations. However, for convenience, the subscript can be ignored without confusion.

At the point P_1 on the trajectory in Figure 3.6 (a), the disturbance input does not change the difference dx_1 but change the difference dx_2 , e.g. dx_2 ① and dx_2 ②. The sign of the velocity direction dx_2 is strictly negative according (3.17). The worst case trajectory is defined as a trajectory that encloses any other trajectory with the same bounded disturbance in the phase plane. If a moving point moves outward always, then it will compose the worst trajectory for a given initial condition.

Even though the finite next point P_2° is outward compared to the point P_2^\oplus , the distance of P_2° from the origin itself is closer than the other point.

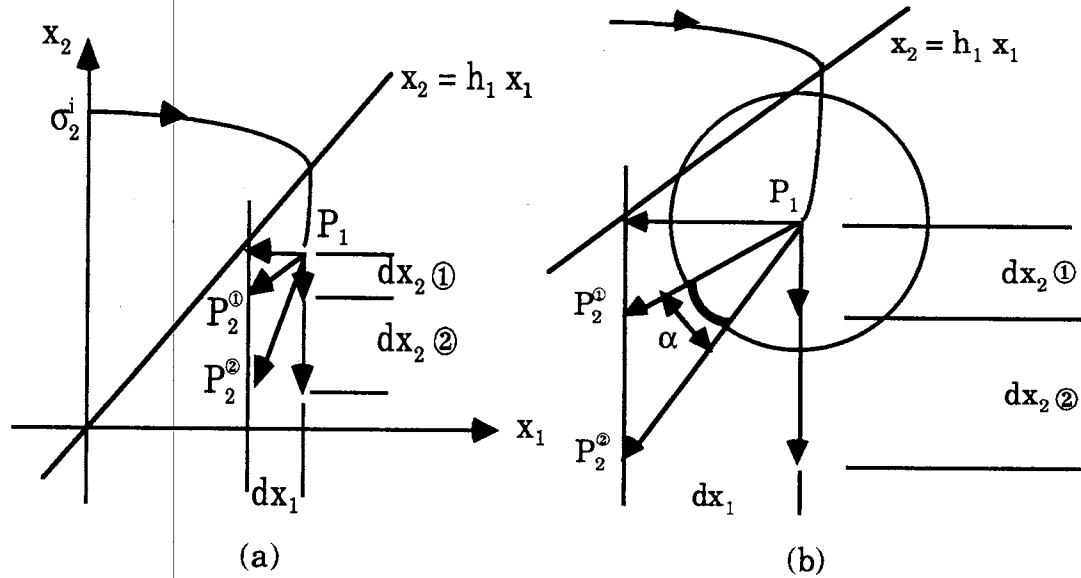


Figure 3.6 (a) Conception of velocity field (b) The fictitious next point

By adding the scaled differences of dx_1 and dx_2 to the point P_1 , fictitious next point P_{2*} is defined as follows:

$$P_{2*} = P_{2*}(x_{1*}(t+dt), x_{2*}(t+dt)) \quad (3.22)$$

$$\text{where } x_{1*}(t+dt) = x_1(t) + \frac{dx_1}{\delta\xi}$$

$$x_{2*}(t+dt) = x_2(t) + \frac{dx_2}{\delta\xi}$$

$$\delta\xi = C_s \sqrt{(dx_1)^2 + (dx_2)^2} \text{ and } C_s \text{ is a constant.}$$

It is clear that the outmost fictitious points compose the worst trajectory. The generalization of the fictitious next point is obvious and the direction of worst fictitious point is the worst direction of disturbance input.

$$\left\{ \begin{array}{l} x_{1*}(t+dt) = x_1(t) + \frac{dx_1}{\delta\xi} \\ x_{2*}(t+dt) = x_2(t) + \frac{dx_2}{\delta\xi} \\ \dots \\ x_{n*}(t+dt) = x_n(t) + \frac{dx_n}{\delta\xi} \end{array} \right. \quad (3.23)$$

$$\text{where } \delta\xi = C_s \sqrt{(dx_1)^2 + (dx_2)^2 + \dots + (dx_n)^2} \text{ and } C_s \text{ is a constant.}$$

For the second-order case, the fictitious next points e.g. $P_2^{\textcircled{1}}, P_2^{\textcircled{2}}$ lie on the arc α in Figure 3.6 (b) which is less than the quarter of the peripheral of the unit circle centered at P_1 because the sign of dx_n is strictly negative and dx_1 is fixed as positive or negative.

For the general n _th-order case, the fictitious next points composes a line on the n _th-order sphere surface since all the different components dx_i except dx_n are determined by only $x(t)$ and dx_n is strictly negative and bounded. In the phase plane of x_n and x_1 , the fictitious next point is less than the

quarter of the peripheral of the unit circle centered at P_1 also. Since the direction of quarter line is function of $\dot{x}_1, \dot{x}_2, \dots, \dot{x}_{n-1}$, it is not easy to visualize the worst direction as the second-order case. Hence, it is proper to search the worst direction by numeric simulation.

3.2.3 Numerical Search

The worst bound by the disturbance input can be interpreted as the problem where the distance (or the Lyapunov-like function) has to be maximized based on the evaluations of the results from several simulations of the bounded disturbance input. The optimization is done by the Golden-section search that does not require the derivatives of the function. It is more reliable but slower method. Suppose that the disturbance input in (3.17) is a real valued function defined on $[-2k_n, 0]$. The distance from the shifted origin or the Lyapunov-like function can be the cost function. It is reasonable to assume that the cost function is unimodal and its graph takes one of the three forms as shown in Figure 3.7. The interval $[0, 2]$ in Figure 3.7 is not essential but convenient to implement the sliding observer. The Golden-section search algorithm is optimal in the sense that it uses the least number of evaluations of the cost function for a desired accuracy.

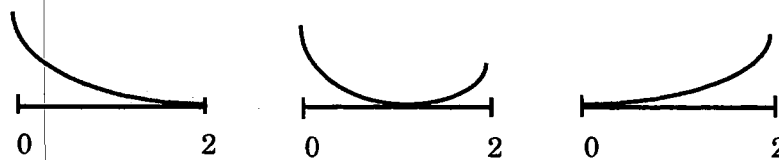


Figure 3.7 Unimodal functions

Structure of the Code. The worst direction of the sliding observer should be evaluated by simulation for each value of the disturbance input. The different simulations are used by the search procedure. The optimization algorithm is written as a discrete time system to control each simulation conveniently. Thus, the many simulations are integrated to one long worst simulation. Three subsystems are connected by the connecting system CONN.T. They are: SYS.T, which contains the sliding observer error dynamics, the search algorithm GOLD.T, and the cost function COST.T. Each step in the search starts with a given value of the disturbance input from the GOLD.T, then the response of the SYS.T is evaluated by COST.T. The value $J(U_d)$ is obtained at the end of the each step GOLD.T, then the value $J(U_d)$ is used to calculate the next value of U_d . The initial values of SYS.T and COST.T are reset by GOLD.T. (See detail Appendix C.5).

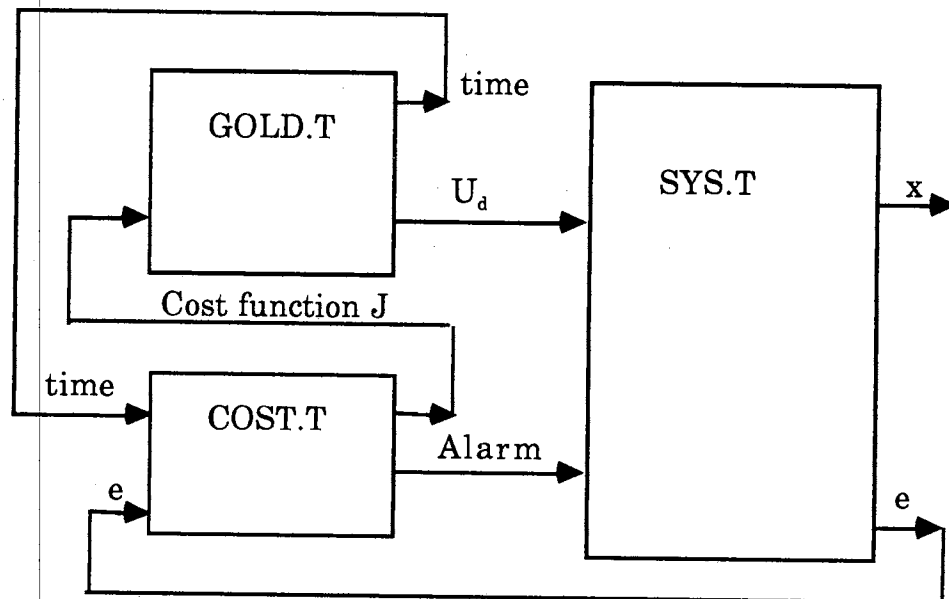


Figure 3.8 Block diagram of the optimization algorithm

Example 3.1 The simulation results of the reaching dynamics with $H=[1.8 \ .95 \ .25]^T$, $k_n = 0.023$.

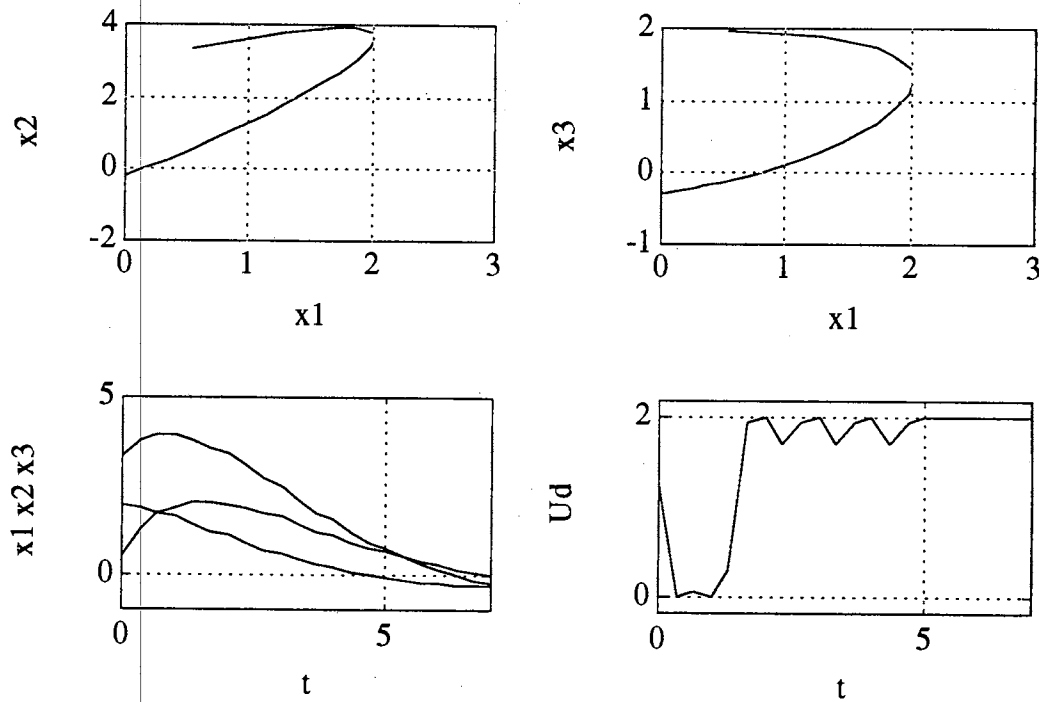


Figure 3.9 The simulation result of the numeric search

The state x_1 is maximum at $x_2 = h_1 x_1$ and in about 1.7 second. The worst direction by the numerical search is approximately $w = \text{sign}(\dot{x}_1)$ which is the same as the 2-order case.

3.2.4 Approximate Worst Direction

For the second-order case, the worst direction is analytically obtained. For the higher dimensional cases, it is difficult to define the outward direction, so that, theoretically, a numerical search is proposed in the previous section.

However, the numeric search for the high dimensional space takes much more computational efforts. Hence, it is reasonable to find an approximate worst direction for a practical design purpose.

Consider a third-order reaching dynamics in the shifted-coordinate. It satisfies the passing condition and it is a linear system until it reaches the hyperplane.

$$\begin{cases} \dot{x}_1 = -h_1 x_1 + x_{2+} \\ \dot{x}_{2+} = -h_2 x_1 + x_{3+} \\ \dot{x}_{3+} = -h_3 x_1 + u_d \end{cases} \quad (3.24)$$

where $u_d = w \cdot k_3 \operatorname{sgn}(x_1)$, $-k_3 \leq w_{\min} \leq w \leq w_{\max} \leq k_3$

From the equation (3.24), even though the velocity \dot{x}_1 and \dot{x}_{2+} are function of the position only, the trajectory of moving point is also a function of the disturbance input.

For the region $(x_1 > 0 \cap \dot{x}_1 > 0)$, in the x_1 - x_2 phase plane, the equation (3.24) is rewritten as:

$$\begin{cases} \dot{x}_1 = -h_1 x_1 + x_{2+} \\ \dot{x}_{2+} = -h_2 x_1 + \sigma_{3+}^i - h_3 \int_0^t x_1 dt + \int_0^t u_d dt \end{cases} \quad (3.25)$$

For the region, the worst direction of \dot{x}_2 is approximately the same as the maximized velocity \dot{x}_2 by the disturbance input. Because the disturbance input is strictly negative, the maximum of time integral of the disturbance input in (3.25) is zero.

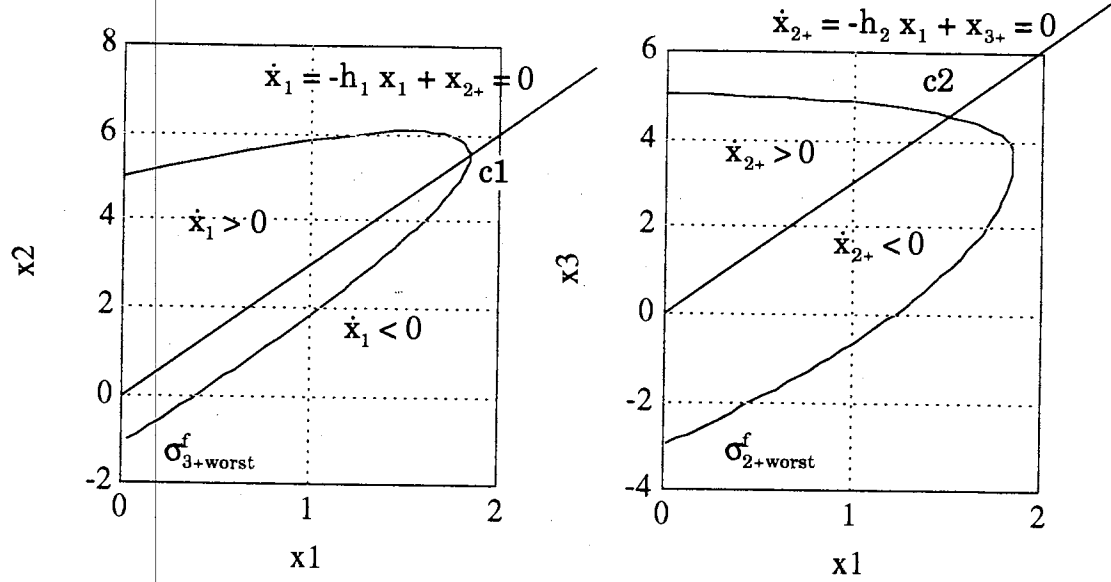


Figure 3.10 The trajectory of solution point and velocity field

Along the worst trajectory, the velocity of moving point is

$$\begin{aligned}\dot{x}_{2+}^{\text{worst}} &= \dot{x}_{2+} \big|_{\max(\dot{x}_{2+})} \\ &= \dot{x}_{2+} \big|_{\max(x_{3+})}\end{aligned}\quad (3.26)$$

When the trajectory pass through the line $\dot{x}_1 = 0$, i.e., at the changing point c1, the velocity direction of \dot{x}_1 changes. The worst direction disturbance pushes the change point c1 off from the origin point. When \dot{x}_3 is maximum i.e. $u_d=0$, the x_3 state is maximized. Since $\dot{x}_1 > 0$, $w = \omega \operatorname{sgn}(\dot{x}_1)$ makes $u_d=0$ by (3.17)

$$\begin{aligned}\dot{x}_{3+}^{\text{worst}} &= \dot{x}_{3+} \big|_{\max(\dot{x}_3)} \quad (\because \dot{x}_{3+} < 0) \\ &= \dot{x}_{3+} \big|_{\max(w)} \\ &= -h_3 x_1\end{aligned}\quad (3.27)$$

For the region $(x_1 > 0 \cap \dot{x}_1 < 0)$, along the worst trajectory in the x_1 - x_2

phase plane, the velocity of moving point is

$$\dot{x}_{2+ \text{worst}} = \dot{x}_{2+} |_{\min(x_3)} \quad (3.28)$$

To minimize x_3 , the worst velocity direction is approximately:

$$\begin{aligned} \dot{x}_{3+ \text{worst}} &= \dot{x}_{3+} |_{\min(x_3)} \quad (\because \dot{x}_{3+} < 0) \\ &= \dot{x}_{3+} |_{\min(w)} \\ &= -h_3 x_1 - 2k_3 \end{aligned} \quad (3.29)$$

Since the velocity of \dot{x}_2 is function of integral of disturbance input as the equation (3.26), the minimum velocity might be obtained by minimum disturbance input. However, the worst changing point $c1$ is obtained already by the maximum disturbance input as the equation (3.27). Hence, the direction is only approximation of the worst case.

In the both half space, the approximate worst disturbance is

$$w = \omega \operatorname{sgn}(\dot{x}_1) \quad (3.30)$$

which is the same as the second-order case. Even though the exact worst direction is function of all states, the disturbance effect in the x_1 - x_{2+} space was considered only in the approximate worst direction method.

Generalization of Approximate Worst Direction. Consider a n -th-order reaching dynamics in the shifted-coordinate. We can assume that it satisfies the passing condition without loss of generality.

$$\begin{cases} \dot{x}_1 = -h_1 x_1 + x_{2+} \\ \dot{x}_{2+} = -h_2 x_1 + x_{3+} \\ \dots \\ \dot{x}_{n+} = -h_n x_1 + u_d \end{cases} \quad (3.31)$$

Since the passing state is not desirable than the sliding state and the

sliding condition(2.9) is a function of the state x_2 only, the state x_2 is more important than the other states except x_1 . Hence, it is reasonable to define the worst direction of disturbance as a disturbance that makes the state x_2 worst or equivalently maximizes $|\sigma_2^f|$.

Each state is obtained as time functions as follows:

$$\begin{aligned}
 x_{2+}(t) &= \sigma_{2+}^i - h_2 \int_0^t x_1 d\tau + \int_0^t x_{3+} d\tau \\
 x_{3+}(t) &= \sigma_{3+}^i - h_3 \int_0^t x_1 d\tau + \int_0^t x_{4+} d\tau \\
 &\dots \\
 x_{n+}(t) &= \sigma_{n+}^i - h_n \int_0^t x_1 d\tau + \int_0^t u_d d\tau
 \end{aligned} \tag{3.32}$$

By plugging the equation (3.32) into the simultaneous differential equation (3.31), we obtains the following equation. According to the notational definition (2.58), the initial states x^i is denoted as σ^i to emphasize that they are constants.

$$\left\{ \begin{aligned}
 \dot{x}_1 &= -h_1 x_1 + x_{2+} \\
 \dot{x}_{2+} &= -h_2 x_1 + \sigma_{3+}^i - h_3 \int_0^t x_1 d\tau \\
 &\quad + \int_0^t \sigma_{4+}^i(d\tau) - h_4 \int_0^t x_1(d\tau)^2 \\
 &\quad \dots \\
 &\quad + \int_0^t \sigma_{n+}^i(d\tau)^{n-3} - h_n \int_0^t x_1(d\tau)^{n-2} + \int_0^t u_d(d\tau)^{n-2}
 \end{aligned} \right. \tag{3.33}$$

where $\int x_1(dt)^n$ is n-multiple integral and $u_d = w - k_n \operatorname{sgn}(x_1)$,
 $-k_n \leq w_{\min} \leq w \leq w_{\max} \leq k_n$.

In the x_1 - x_{2+} phase plane, the solution point of the general dimensional case behaves according to equation (3.33). For the short period ($t \ll 1$), the integral of disturbance input hardly affects the velocity direction of the state x_2 comparing to other terms. Since the disturbance input alters the velocity direction of the lower state via the integrators, for the short period, it changes the velocity direction of x_n only. For the case of positive initial state of x_{n+} , the worst direction in x_1 - x_{n+} phase plane can be obtained as the same way as the case of 2-dimension. However, for the case of negative initial state of x_{n+} , the worst direction in x_1 - x_{n+} phase plane cannot be defined as clearly as the case of 2-dimension.

Let us consider a long period motion of solution point. Since the integrator order of disturbance input is the highest term of the equation (3.33), the velocity direction of the state x_2 will be affected mostly by the disturbance input. For a long period, the approximate worst direction can be obtained as the same method as the 3- dimensional case.

For the region ($x_1 > 0 \cap \dot{x}_1 > 0$), the approximate worst direction is

$$\begin{aligned}\dot{x}_{2+ \text{worst}} &= \dot{x}_{2+} \mid_{\max(\dot{x}_2)} \\ &= \dot{x}_{2+} \mid_{\max(w)}\end{aligned}$$

For the region ($x_1 > 0 \cap \dot{x}_1 < 0$), the approximate worst direction is

$$\begin{aligned}\dot{x}_{2+ \text{worst}} &= \dot{x}_{2+} \mid_{\min(\dot{x}_2)} \\ &= \dot{x}_{2+} \mid_{\min(w)}\end{aligned}$$

For the both cases, the approximate worst disturbance is

$$w = \omega \operatorname{sgn}(\dot{x}_1)$$

which is the same as the second- or third-order cases.

3.2.5 General Remarks

Usually, it was conjectured that the second-order switching system is globally stable with the bounded disturbance condition, i.e., $k_2 > |w|$. In the worst analysis, the algebraic stability condition (3.13) shows that the switching system is not globally stable and it depends on the initial condition and the design constants k_1 and k_2 . The shearing effects (3.11) and (3.12) explain why the sliding observer converges faster than the linear observers do. In the second-order phase plane analysis, it is clear that the shifted-coordinate system brings the shearing effect. By introducing the coordinate transformation, the worst case analysis shows that the switching terms shift the coordinate and bring the shearing effect. However, we should notice that these effects are finite and constant, i.e., k_1 , k_2 , etc. These switching terms are compared to the linear correction terms that have relatively small effect near the origin but have proportional effect to the state x_1 . The necessity of linear correction terms are already showed in the reaching dynamics (see (2.23)). Roughly speaking, the second-order sliding observer stability is: if the state divergence due to the worst disturbance is less than the shearing effect plus the convergence by linear correction, then it is stable. For higher dimensional system, phase plane analysis is not sufficient to explain the "general shearing effect." Therefore, we need another tool to measure the effects and to explain stability.

3.3 Lyapunov-like Function

3.3.1 Introduction

This chapter focuses on the stability analysis of the sliding observer.

The scheme to analyze the stability is as follows: First, when the sliding observer does not satisfy the sliding condition, it passes through the hyperplane until satisfying the sliding condition. By applying the shifted-coordinate system, the sliding observer is transformed to a linear system with disturbance input, i.e., reaching dynamics. Second, after satisfying the sliding condition, it becomes a reduced order linear system, i.e., Filippov's equivalent dynamics. This chapter investigates the stability of the sliding observer by using a Lyapunov-like function which describes a fictitious energy, i.e., so called "pseudo-energy" of a system. The employment of quadratic Lyapunov-like function makes easy the whole domain to separate into regions where, with the passing condition, two reaching dynamics are activated and, with the sliding condition, the reduced order sliding dynamic is turned on. Each coordinate associated with switching has its own a Lyapunov-like function of the form $V_s = x_s^T P_s x_s$ ($s=+,-$) where P_s is a real symmetric positive definite (r.s.p.d) matrix. Roughly speaking, if the pseudo-energy of each dynamics is strictly decreasing along the trajectories in the accompanied successive coordinate systems, then the sliding observer is stable. The shearing effect due to the shifted-coordinate characterizes the sliding observer. The difference of Lyapunov-like functions of successive switching coordinates is due to the shearing effect. Generalization of shearing effect is explained by several intriguing system properties.

3.3.2 Lyapunov-like Function Theorem

A quadratic function of the form, $x^t P x$, are common form of a Lyapunov function used for investigating stability questions of linear autonomous systems, i.e., $\dot{x}(t) = A x(t)$ [Kailath, 1980]. Since the system with $u_d=0$ is

equivalent to the composition of the three linear autonomous systems, i.e., $\dot{x}_s(t) = A_s x_s(t)$ (subscript $s=+,-,0$), it would be natural to use a quadratic function as representing the Lyapunov-like function [Alimov, 1960]. Hence, it is necessary to delineate the composite structure of $V_s(x_s) = x_s^T P x_s$ in the domain of Ω_s (subscript $s=+,-,0$) [Peleties, 1991].

Definition 3.1 A scalar continuous function $V(x)$ is said to be *locally positive definite* if $V(0)=0$ and, in a ball B_{R_0} [Slotine, 1991].

$$x \neq 0 \Rightarrow V(x) > 0 \quad (3.31)$$

If $V(0)=0$ and the above property holds over the whole state space the $V(x)$ is said to be *globally positive definite*. ■

Definition 3.2 The function $V_s(x)$ is said to be *radially unbounded* if

$$\lim_{\|x_s\| \rightarrow \infty} V_s(x_s) \rightarrow \infty \quad (3.32)$$

Definition 3.3 A linear system $\dot{x}(t) = A x(t) + b u(t)$, $y(t) = c x(t)$ is *internally stable* or *stable in the sense of Lyapunov* if the solution of $\dot{x}(t) = A x(t)$, $x(t^i) = x_0$, $t \geq t^i$ tends toward zero as $t \rightarrow \infty$ for arbitrary x_0 . ■

Definition 3.4 A set \mathcal{R} is said to be a *cone* if $\forall x_s \in \mathcal{R}, \alpha x_s \in \mathcal{R}, \forall \alpha > 0$. ■

Definition 3.5 Let us define a domain Ω_+ where $x_1 > 0$ as *right half space* and a domain Ω_- where $x_1 < 0$ as *left half space* in each shifted-coordinate system. A hyperplane domain Ω_0 where $x_1 = 0$ and $|x_2| \leq k_1$ in the original coordinate is said sliding zone. The whole domain is as follow:

$$\Omega = \Omega_+ \cup \Omega_- \cup \Omega_0 \subset \mathcal{R}^n \quad \blacksquare$$

Observe that both Ω_+ and Ω_- are cones. If x_s is a member of Ω_s , then any

positive scalar multiple α of x_s is also a member of Ω_s . Neither right or left reaching dynamics has equilibrium point within the domain of Ω_s .

Corollary 3.1 If $V_s(x_s) = x_s^T P x_s$ then every region x_s is a cone [Peleties, 1991].

□

Proof) Let assume $x'_s \in \Omega_s$. The time derivative of V_s is

$$\dot{V}_s(x'_s) = \frac{\partial V_s(x_s)}{\partial x} A_s x_s \big|_{x_s=x'_s} = \frac{\partial V_s(x_s)}{\partial x} \big|_{x_s=x'_s} A_s x'_s \leq 0.$$

Consider $x'' = \alpha x'$. Then the time derivative of V_s indicates that $x'' \in \Omega_s$ as follows:

$$\dot{V}_s(x''_s) = \frac{\partial V_s(x_s)}{\partial x} A_s x_s \big|_{x_s=x''_s} = \alpha \frac{\partial V_s(x_s)}{\partial x} \big|_{x_s=x'_s} A_s \alpha x'_s = \alpha^2 \frac{\partial V_s(x_s)}{\partial x} \big|_{x_s=x'_s} A_s x'_s \leq 0$$

Note that the above is true for any value of α , therefore the positive values of α satisfy Definition 3.4. □

Corollary 3.2 Let (λ_j, e_j) be an eigenvalue/ eigenvector pair of A_m . Then the derivative of Lyapunov-like function is negative definite ($\dot{V}_s(e_j) < 0$) if and only if $\text{Re}(\lambda_j) < 0$ [Peleties, 1991]. □

Proof) Let assume that $\dot{V}_s(e_j) < 0$. Then it can be rewrite as follows:

$$\begin{aligned} \dot{V}_s(e_j) &= e_j^T (A_m^T P + P A_m) e_j = e_j^T A_m^T P e_j + e_j^T P A_m e_j \\ &= \overline{\lambda_j} e_j^T P e_j + \lambda_j e_j^T P e_j = (\overline{\lambda_j} + \lambda_j) V_s(e_j) = 2 \text{Re}(\lambda_j) V_s(e_j) < 0 \quad (=0) \end{aligned}$$

A quadratic Lyapunov function is positive definite:

$$V_s(x_s) > 0, x_s \neq 0, \forall x_s \in C^n$$

Since $V_s(e_j) > 0$, the other term must be negative ($\text{Re}(\lambda_j) < 0$).

Let assume $\text{Re}(\lambda_j) < 0$. Applying similar procedures, we have the same results: $\dot{V}_s(e_j) = 2 \text{Re}(\lambda_j) V_s(e_j)$. Since $V_s(e_j) > 0$ then $\dot{V}_s(e_j) < 0$. \square

Corollary 3.3 A solution trajectory of system A_m cannot escape to infinity within Ω_s . \square

Proof Assume a solution point of system A_m escape to infinity within Ω_s , i.e., $\lim_{t \rightarrow \infty} x_s(t; x_o, \tau_o) = \infty$, then $\exists t_2 > t_1 \geq \tau_o$ such that $V_s(x_s(t_2)) > V_s(x_s(t_1))$ where $x_s(t) \equiv x_s(t; x_s^i, \tau^i)$. However, $V_s(x_s(t_2)) = V_s(x_s(t_1)) + \int_{t_1}^{t_2} \dot{V}_s(x_s(q)) dq$ implies that $\int_{t_1}^{t_2} \dot{V}_s(x_s(q)) dq > 0$ which is clearly a contradiction of the fact that $\dot{V}_s(x_s(q)) < 0, \forall x_s(t) \in \Omega_s, s=+.-.0$. \square

The definitions and propositions give us the general pictures of the dynamics of system A_m within Ω_s . We have established that there are no equilibrium points within Ω_s and in addition the trajectories will not go to infinity. This implies that the trajectories will either asymptotically approach the shifted origin or they will approach the sliding patch. The trajectories will enter the sliding patch where sliding can take place so that the Filippov's equivalent dynamics will describe the behavior of the error dynamics.

3.3.3 Passing Jump of Lyapunov-like Function

A Lyapunov-like function candidate is a quadratic form, $V_s = x_s^T P x_s$ which is not a continuous function and does not satisfy the usual requirement of Lyapunov function. This function has several interesting features that can be interpreted as a good nature. Whereas the usual Lyapunov function shows continuity, Lyapunov-like function in the shifted-coordinate shows a

discontinuity ("passing jump") between the initial and final states on the hyperplane.

Relations Between the Passing Points.

i) Passing right case (with the passing condition $x_1=0, x_2 > k_1$):

The passing points relations in the shifted-coordinate are

$$s_+^i(\tau_j) = s_-^f(\tau_j) \Rightarrow \sigma_+^i(\tau_j) = \sigma_-^f(\tau_j) - 2K_s \quad (3.33)$$

ii) Passing left case (with the passing condition $x_1=0, x_2 < -k_1$):

The passing points relations in the shifted-coordinate are

$$s_-^i(\tau_j) = s_+^f(\tau_j) \Rightarrow \sigma_-^i(\tau_j) = \sigma_+^f(\tau_j) + 2K_s \quad (3.34)$$

Since the sign unity property for the case of 2- and 3-dimension, the distance of the passing point from the shifted-coordinate origins are decreasing by passing:

$$\begin{cases} \text{Passing Right : } |\sigma_+^i(t_j)| = |\sigma_-^f(t_j)| - 2K_s \\ \text{Passing Left : } |\sigma_-^i(t_j)| = |\sigma_+^f(t_j)| - 2K_s \end{cases} \quad (3.35)$$

Since, Lyapunov-like function is defined in the shifted-coordinate, it shows a "passing jump" between the initial and final functions. Rewrite the Lyapunov-like function in the original coordinate:

$$\begin{aligned} V_s &= x_s^T P x_s \\ &= (x - k_s \operatorname{sgn}(x_1))^T P (x - k_s \operatorname{sgn}(x_1)) \\ &= x^T P x + K_s^T P K_s - 2 K_s^T P x \operatorname{sgn}(x_1) \end{aligned}$$

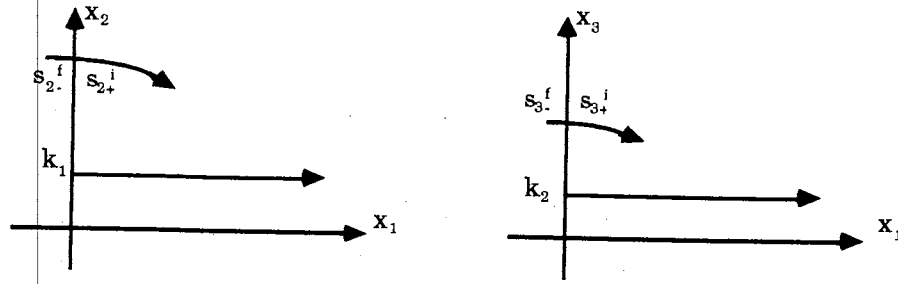


Figure 3.11 A solution point shows passing right through the hyperplane

Passing Jump of Lyapunov-like Function.

i) Passing right case ($x_2 > k_1$): If $x_2 > k_1$, then the solution point passes from the left half space to the right half space, i.e., $\dot{x}_1 > 0$. The difference of Lyapunov-like function between the passing points is

$$\begin{aligned}
 J(\tau_j)_{(x_2 > k_1)} &= V_+^i(\tau_j) - V_-^f(\tau_j) \\
 &= -4 K_s^T P x \\
 &= -4 [0 \ k_1 \ \dots \ k_{n-1}] P \begin{bmatrix} 0 \\ x_2 \\ \vdots \\ x_n \end{bmatrix}
 \end{aligned} \tag{3.36}$$

For the third-order system, as shown in Figure 3.11, all of the final passing states are positive except the first state $x_1 \approx 0$ - (see proof Appendix C.3). Each elements of shifted-coefficient K_s is positive except the first one. We can see that the passing jump $J(t_j)$ is a form of bilinear function, xPy , and the $(n-1) \times (n-1)$ submatrix of P of equation (3.36) is positive definite. The sign unity of the bilinear function do not guarantee that the passing jump J is strictly negative (see Appendix A.2). With the diagonally dominant submatrix P_{n-1} and the sign unity of the bounded states and positive coefficients k 's, the passing jump J is negative. After approximation, the passing

jump J is

$$J = -4 \{k_1 P_{22} x_2 + k_2 P_{33} x_3 + \dots + k_{n-1} P_{nn} x_n\} \quad (3.37)$$

ii) Passing left case: If $x_2 < -k_1$, then the solution point passes from the left half space to the right half space, i.e., $\dot{x}_1 < 0$. The difference of Lyapunov-like function between the passing points is

$$\begin{aligned} J(\tau_j)_{(x_2 < -k_1)} &= V_-(\tau_j) - V_+(\tau_j) \\ &= 4 K_s^T P x \\ &= 4 [0 \ k_1 \ \dots \ k_{n-1}] P \begin{bmatrix} 0 \\ x_2 \\ \vdots \\ x_n \end{bmatrix} \end{aligned} \quad (3.38)$$

Since each domain in the shifted-coordinate is symmetry about the origin, all of the features are the same each other. In this domain, the sign unity is negative and consequently the passing jump J is negative. After approximation, the passing jump J is

$$J = 4 \{k_1 P_{22} x_2 + k_2 P_{33} x_3 + \dots + k_{n-1} P_{nn} x_n\}$$

where x_i is negative ($i=2, \dots, n$).

Hence, with a passing condition, the solution point of sliding observer approaches to the shifted-coordinate origins quickly as shown above passing jump.

3.4 Lyapunov-like Stability Analysis

3.4.1 Lyapunov-like Stability Theorem

The objective is to asymptotically stabilize the system through a series of switching, which is expressed by the set of passing points along with

sequences of switching timing [Peleties, 1991]:

$$0 \leq \tau_j < \infty, \quad \forall \quad \tau_j \in \tau_s = \tau_0, \tau_1, \dots, \tau_{k-1}, \tau_k, \dots$$

$$\{s(x_s, \tau_j)\} = s(\tau_0), s(\tau_1), \dots, s(\tau_k), \dots \quad (3.40)$$

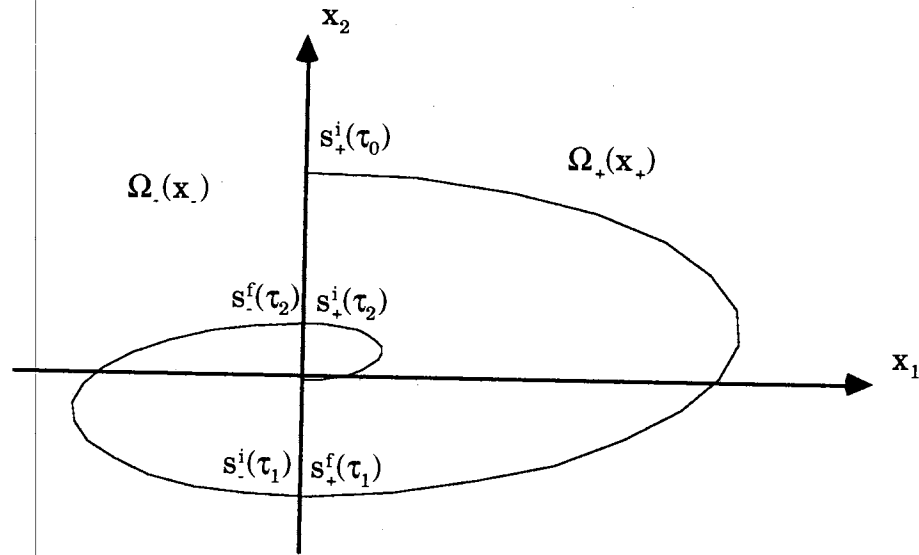


Figure 3.12 Passing points on the hyperplane

Lyapunov-like Function Sets on the Hyperplane. Let us define the initial and final Lyapunov-like function set [Peleties, 1991]:

$$\{V_s(x_s, \tau_j)\} = V_+^i(\tau_0), V_+^f(\tau_1), V_-^i(\tau_1), V_-^f(\tau_2), V_+^i(\tau_2), V_+^f(\tau_3), \dots, V_s^f(\tau_j) \quad (3.41)$$

and the initial and final passing point set:

$$\{s_s(x_s, \tau_j)\} = s_+^i(\tau_0), s_+^f(\tau_1), s_-^i(\tau_1), s_-^f(\tau_2), s_+^i(\tau_2), s_+^f(\tau_3), \dots, s_s^f(\tau_j) \quad (3.42)$$

The sequence of Lyapunov-like functions is identical to that of passing

points. The detailed notion of Lyapunov-like function sequences is follows:

$$\begin{array}{ccccccc}
 & \text{Passing Left} & \text{Passing Right} & & & & \\
 & \underbrace{\hspace{1.5cm}} & \underbrace{\hspace{1.5cm}} & & & & \\
 \underbrace{V_+^i(\tau_0), V_+^f(\tau_1)}_{\text{Right Domain}}, & \underbrace{V_-^i(\tau_1), V_-^f(\tau_2)}_{\text{Left Domain}}, & \underbrace{V_+^i(\tau_2), V_+^f(\tau_3)}_{\text{Right Domain}}, & \dots, & V_s^f(\tau_j) & & \\
 & & & & \text{Until satisfying} & & \\
 & & & & \text{passing condition} & &
 \end{array} \quad (3.43)$$

The set $\{V_+(x_s, \tau_j)\}$ for the right half space can be defined as Lyapunov-like function sequences corresponding to the right passing points sequences $\{s_+(x_s, \tau_j)\}$:

$$\{V_+(x_s, \tau_j)\} = V_+^i(\tau_0), V_+^f(\tau_1), V_+^i(\tau_2), V_+^f(\tau_3), \dots, V_+^f(\tau_j) \quad (3.44)$$

$$\{s_+(x_s, \tau_j)\} = s_+^i(\tau_0), s_+^f(\tau_1), s_+^i(\tau_2), s_+^f(\tau_3), \dots, s_+^f(\tau_j) \quad (3.45)$$

For the left half space, $\{V_-(x_s, \tau_j)\}$, and $\{s_-(x_s, \tau_j)\}$ are

$$\{V_-(x_s, \tau_j)\} = V_-^i(\tau_1), V_-^f(\tau_2), V_-^i(\tau_3), V_-^f(\tau_4), \dots, V_-^f(\tau_j) \quad (3.46)$$

$$\{s_-(x_s, \tau_j)\} = s_-^i(\tau_1), s_-^f(\tau_2), s_-^i(\tau_3), s_-^f(\tau_4), \dots, s_-^f(\tau_j) \quad (3.47)$$

Zero-input Responses of the Reaching Dynamics. For the stability of the sliding observer, it is desirable that any initial state asymptotically converge to the origin. Hence, we need to consider the worst case whose initial state is not on the sliding patch and does not satisfy the sliding condition. For this case, by adapting this coordinate transformation, the well-known linear system theory can be applied to interpret the sliding observer as the reaching dynamics which is a linear system in each shifted-coordinate half space.

The reaching dynamics in the shifted-coordinate is

$$\dot{\mathbf{x}}_s = \mathbf{A}_m \mathbf{x}_s + \begin{pmatrix} 0 \\ \vdots \\ 0 \\ u_d \end{pmatrix} \quad (3.48)$$

where $u_d = w - k_n \text{sgn}(x_1)$

Let us consider first the internal stability of the reaching dynamics by setting the disturbance input zero, $u_d = 0$. The internal system is

$$\dot{\mathbf{x}}_s = \mathbf{A}_m \mathbf{x}_s \quad (3.49)$$

A candidate Lyapunov-like function for this system:

$$V_s = \mathbf{x}_s^T \mathbf{P} \mathbf{x}_s \quad (3.50)$$

Assuming that the Lyapunov-like function is differentiable except switching plane, its derivative with respect to time is

$$\begin{aligned} \dot{V}_s &= \dot{\mathbf{x}}_s^T \mathbf{P} \mathbf{x}_s + \mathbf{x}_s^T \mathbf{P} \dot{\mathbf{x}}_s \\ &= [\mathbf{A}_m \mathbf{x}_s]_s^T \mathbf{P} \mathbf{x}_s + \mathbf{x}_s^T \mathbf{P} [\mathbf{A}_m \mathbf{x}_s] \\ &= \mathbf{x}_s^T \mathbf{A}_m^T \mathbf{P} \mathbf{x}_s + \mathbf{x}_s^T \mathbf{P} \mathbf{A}_m \mathbf{x}_s \\ &= -\mathbf{x}_s^T \mathbf{Q} \mathbf{x}_s \end{aligned} \quad (3.51)$$

We can see that each reaching dynamics is asymptotically attractive to the shifted origin (or to the sliding patch). If, whenever the solution point passes through the hyperplane, the Lyapunov-like function strictly decreases, then the Lyapunov-like function is strictly decreasing along the trajectory over the whole reaching dynamics domain.

Theorem 3.1 Given an reaching dynamics of the form $\dot{\mathbf{x}}_s = \mathbf{A}_m \mathbf{x}_s$ (where \mathbf{A}_m : Hurwitz system matrix, $\mathbf{x}_s = \mathbf{x} - \mathbf{K}_s \text{sgn}(x_1)$, $s = -$ or $+$), let us consider a quadratic Lyapunov-like function candidate:

$$V_s(\mathbf{x}) = \mathbf{x}_s^T \mathbf{P} \mathbf{x}_s, \quad s = -, + \quad (3.52)$$

which is a real positive definite on \mathcal{R}^n and unbounded where $V_s(x)$ is associated with the domain $\Omega_-(x), \Omega_+(x)$. Suppose $|x_2^i| > k_1$ at $x_1=0$, $\forall x_0 \in \mathcal{R}^n$, there exist constants $\gamma > 0$, $\rho > 0$ and a switching sequence

$$\{s_s(x_s, \tau_j)\} = s_+^i(\tau_0), s_+^f(\tau_1), s_-^i(\tau_1), s_-^f(\tau_2), s_+^i(\tau_2), s_+^f(\tau_3), \dots, s_s^f(\tau_j), \dots \quad (3.53)$$

as in the followings:

i) In an reaching domain, the total derivative of Lyapunov-like function is negative definite in the domain $\Omega_s(x_s)$ [Peleties, 1991]:

$$\dot{V}_s(x_s) \leq \gamma |x_s|^2 < 0, \quad \forall x_s \neq 0, \forall s, s=-, + \quad (3.54)$$

ii) While the solution point is passing the hyperplane, the Lyapunov-like function always decreases:

$$V_s^i(\tau_j) - V_{s^*}^f(\tau_j) \leq -\rho \|\sigma_s(\tau_j)\|^2, \quad \forall \sigma_s(\tau_j) \in \sigma_s \quad (3.55)$$

where the subscripts s and s^* are: $\text{sign}(s) \neq \text{sign}(s^*)$, $s=-$ or $+$, $s^*=+$ or $-$.

Then, the system is globally asymptotically attractive to the sliding patch that is defined as $|x_2| \leq k_1$ at the switching plane ($x_1 = 0$). \square

Proof) The above two conditions mean that the sequence $\{V_s(x_s, \tau_j)\}$ strictly decreases along the trajectories up to its limit. This implies that $V_s^f(\sigma(\tau_{j+1})) - V_s^i(\sigma(\tau_j)) = \int_{\tau_j}^{\tau_{j+1}} \dot{V}(x_s, \tau) d\tau < 0$ for each side and $\lim_{j \rightarrow \infty} V_s(\sigma(\tau_j)) = L \geq 0$. This limit exists by virtue of the fact that the sequence $\{V_s(\sigma(\tau_j))\}$ strictly decreases by the passing condition ii) and lower-bounded by zero:

$$\begin{aligned} & \lim_{j \rightarrow \infty} V_s^f(\sigma(\tau_{j+1})) - \lim_{j \rightarrow \infty} V_s^i(\sigma(\tau_j)) = L - L = 0 \\ & = \lim_{j \rightarrow \infty} [V_s^f(\sigma(\tau_{j+1})) - V_s^i(\sigma(\tau_j))] \leq \lim_{j \rightarrow \infty} [-\gamma \|\sigma_s(\tau_j)\|^2] \leq 0. \end{aligned}$$

In other words, $\lim_{j \rightarrow \infty} [-\gamma \|\sigma_s(\tau_j)\|^2] = -\gamma \lim_{j \rightarrow \infty} [\|\sigma_s(\tau_j)\|^2] = 0$, which implies

$\lim_{j \rightarrow \infty} \sigma_s(\tau_j) = 0$, which is a sufficient condition for attractiveness to the sliding patch. □

Example 3.2 Consider following 2-order sliding observer:

$$\begin{cases} \dot{x}_1 = x_2 - h_1 x_1 - k_1 \operatorname{sgn}(x_1) \\ \dot{x}_2 = -h_2 x_1 - k_2 \operatorname{sgn}(x_1) + w \end{cases} \quad (3.56)$$

where $k_1:1, k_2:0, h_1: 0.1, h_2: 0.2, w=0$, initial conditions: $x_1:0, x_2:10$

Rewrite the above equation using the shifted-coordinate transformation then we have a reaching dynamics:

$$\begin{cases} \dot{x}_1 = x_{2s} - h_1 x_1 \\ \dot{x}_{2s} = -h_2 x_1 + u_d \end{cases} \quad (3.57)$$

where $u_d = 0$

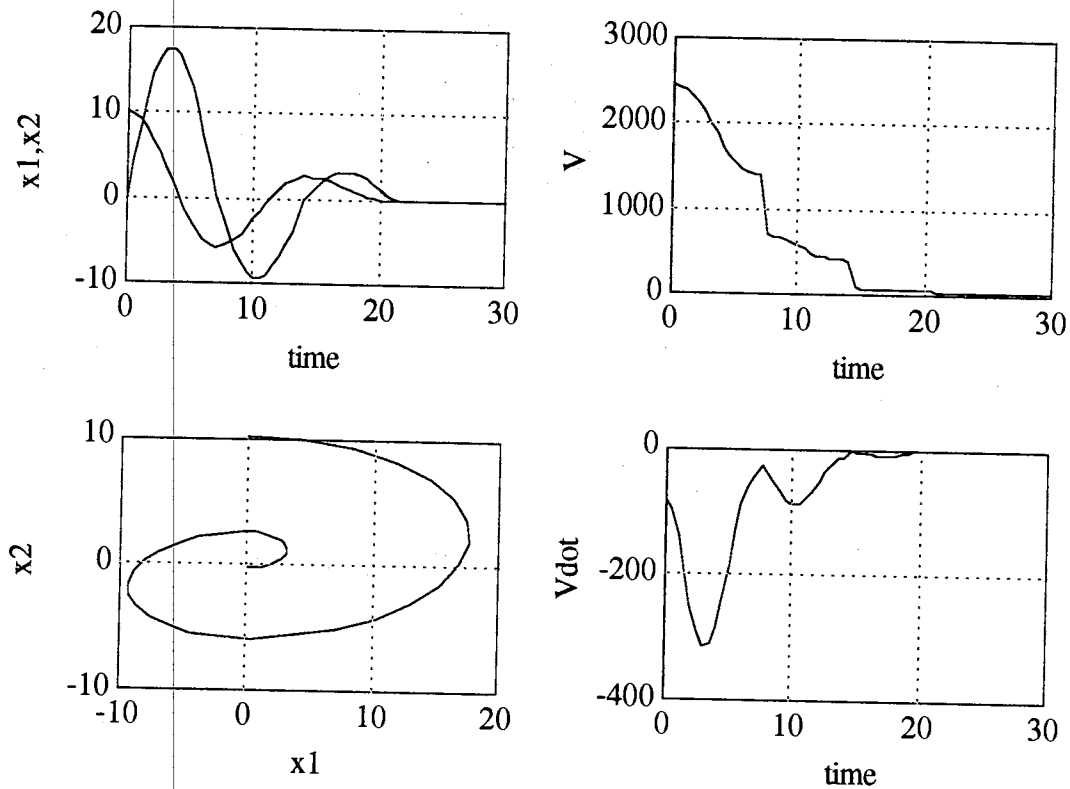


Figure 3.13 Phase plane and Lyapunov-like function

Lyapunov equation $A'^*P + P^*A = Q$

$$A_m = \begin{bmatrix} -.1 & 0 \\ -.2 & 0 \end{bmatrix}, Q = \begin{bmatrix} -1 & 0 \\ 0 & -1 \end{bmatrix}, P = \begin{bmatrix} 6 & -.5 \\ -.5 & 30.25 \end{bmatrix} \quad (3.58)$$

The phase plane Figure 3.13 shows that the solution point is asymptotically approaching to the sliding patch via passing the hyperplane $x_1=0$ twice. The Lyapunov-like function shows two passing jumps around 8 and 14 second. \square

Total Responses of the Reaching Dynamic. Since the disturbance input u_d includes the neglected nonlinearities and disturbances, without considering this term, the sliding observer cannot handle uncertain/nonlinear systems. In a linear stability theory, if the internal system of controllable and observable system is stable then the total stability of LTI system is guaranteed . (see Appendix B.1) On the contrary, we cannot conclude the stability of reaching dynamics only based on the zero-input response of the system.

Assuming that the Lyapunov-like function is differentiable, its derivative with respect to time is

$$\dot{V}_s = \dot{x}_s^T P x_s + x_s^T P \dot{x}_s \quad (3.59)$$

Plug in the reaching dynamics (3.34) with $u_d \neq 0$.

$$\begin{aligned} \dot{V}_s &= \left[A_m x_s + \begin{pmatrix} 0 \\ \vdots \\ 0 \\ u_d \end{pmatrix} \right]^T P x_s + x_s^T P \left[A_m x_s + \begin{pmatrix} 0 \\ \vdots \\ 0 \\ u_d \end{pmatrix} \right] \\ &= x_s^T A_m^T P x_s + x_s^T P A_m x_s + 2 \begin{pmatrix} 0 \\ \vdots \\ 0 \\ u_d \end{pmatrix}^T P x_s \\ &= -x_s^T Q x_s + 2 \begin{pmatrix} 0 \\ \vdots \\ 0 \\ u_d \end{pmatrix}^T P x_s \end{aligned} \quad (3.60)$$

Owing to the 2nd term of right hand side equation, the time derivative of Lyapunov-like function may be not negative definite. At this situation the so-called matching condition could be a solution that guarantees negative definiteness of \dot{V}_s . However, in real situation, the condition usually cannot be satisfied or it is so conservative that it is almost useless. The every conservativeness comes into the system by sticking to the negative definiteness. Hence it is desirable that the negative definite of \dot{V} in Theorem 3.1 is replaced by strictly decreasing Lyapunov-like function of passing states as following theorem:

Theorem 3.2 Given a reaching dynamics of the form $\dot{x}_s = A_m x_s + u_d$ (where A_m : Hurwitz system matrix, $x_s = x - K_s \text{sgn}(x_1)$, u_d : input, $s=-$ or $+$), let us consider a quadratic Lyapunov-like function candidate:

$$V_s(x) = x_s^T P x_s, s = -, + \quad (3.61)$$

which are real positive definite on \mathcal{R}^n and unbounded where $V_s(x)$ is associated with the domain $\Omega_-(x), \Omega_+(x)$. Suppose $|x_2^i| > k_1$ at $x_1=0, \forall x_0 \in \mathcal{R}^n$, there exists constants $\gamma > 0, \rho > 0$ and a switching sequence $\{s_s(x_s, \tau_j)\}$ as in:

i) In an reaching domain, the final Lyapunov-like function $V_s^f(\sigma(\tau_{j+1}))$ is strictly less than the initial Lyapunov-like function $V_s^i(\sigma(\tau_j))$ in the domain $\Omega_s(x_s)$:

$$V_s^f(\sigma(\tau_{j+1})) - V_s^i(\sigma(\tau_j)) < -\gamma \|\sigma_s(\tau_j)\|^2 \quad (3.62)$$

ii) While the solution point passes the hyperplane, the Lyapunov-like function always decreases:

$$V_s^i(\tau_j) - V_{s^*}^f(\tau_j) \leq -\rho \|\sigma_s(\tau_j)\|^2, \forall \sigma_s(\tau_j) \in \sigma_s \quad (3.63)$$

where the subscripts s and s^* are: $\text{sign}(s) \neq \text{sign}(s^*)$, $s=-$ or $+$, $s^*=+$ or $-$.

Then, the system is asymptotically attractive to the sliding patch. \square

Proof) The proof is the same as Theorem 3.1. \square

While Theorem 3.1 requires negative definite of \dot{V}_s , Theorem 3.2 compares the Lyapunov-like function of the initial and the final passing point. In the case of Theorem 3.2, the Lyapunov-like function may not strictly decrease. However, the reaching dynamics is equivalently linear time-invariant system so that the system is *bibo* stable. The shifted coordinate transformation of the sliding observer enables to apply the linear stability theorem to nonlinear system. All the more, the passing jump brings the shearing effect so that the solution point approaches sliding patch fast.

Example 3.3 Consider the same 2-order sliding observer as that of the former example except the disturbance input:

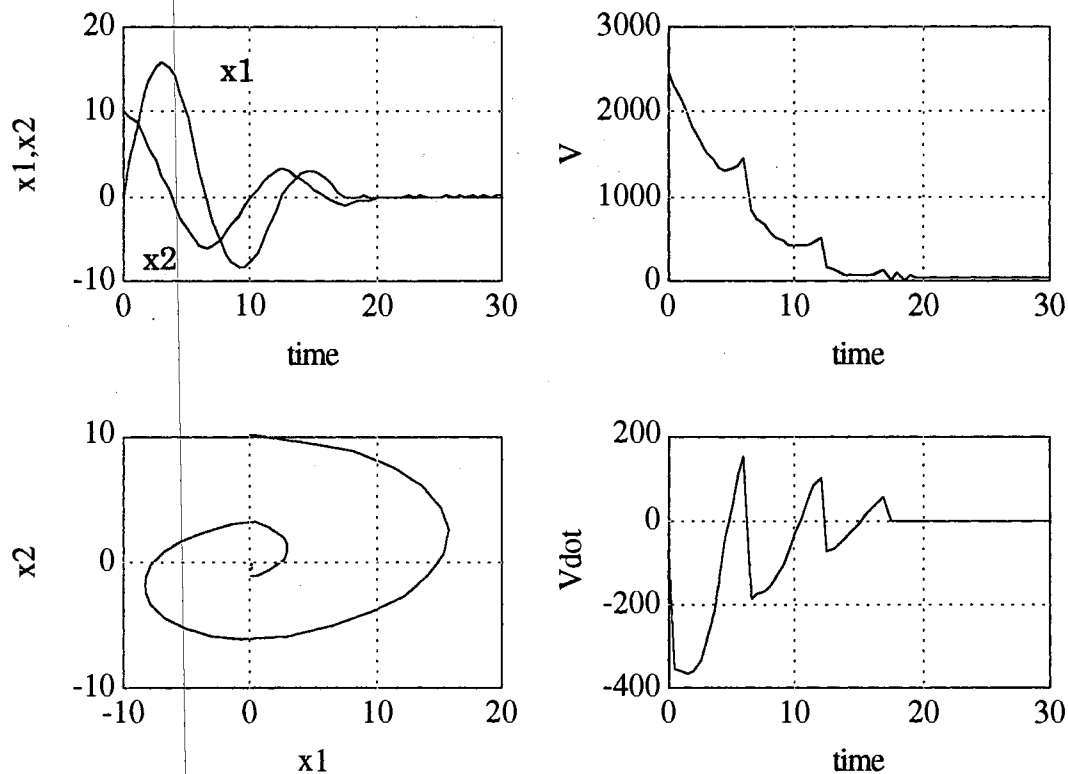


Figure 3.14 Phase plane and Lyapunov-like function

$$\begin{cases} \dot{x}_1 = x_2 - h_1 x_1 - k_1 \operatorname{sgn}(x_1) \\ \dot{x}_2 = -h_2 x_1 - k_2 \operatorname{sgn}(x_1) + w \end{cases} \quad (3.64)$$

where $k_1:1, k_2:0.5, h_1: 0.1, h_2: 0.2, w=0$, initial conditions: $x_1:0, x_2:10$

Rewrite the above equation using the shifted-coordinate transformation then we have a reaching dynamics:

$$\begin{cases} \dot{x}_1 = x_{2s} - h_1 x_1 \\ \dot{x}_{2s} = -h_2 x_1 + u_d \end{cases} \quad (3.65)$$

where $u_d = -0.5 * \operatorname{sgn}(x_1)$

The Lyapunov equation is the same as the former one. The phase plane shows that the solution point with disturbance input approaches to the sliding patch faster than the former example because the sign of disturbance input u_d is opposite sign of x_1 . The Lyapunov-like function shows several passing jumps around 6.5 second and 12 second and so on. Since, \dot{V} is not negative definite, V is not strictly decreasing either. However, this example shows the Theorem 3.3 is valid. The passing jump is proved for 2- and 3- order cases in Appendix B. The other requirement, i.e., decreasing sequences of initial and final Lyapunov-like function set, is assured by the design algorithm "SOON"(see Chapter 4). \square

Finally the next Theorem 3.3 is the generalization of the worst analysis: If the system pseudo-energy decreases as solution trajectory passes from the final point of one domain to the final point of the other domain, then it is possible to stabilize the system.

Theorem 3.3 Given an reaching dynamics of the form $\dot{x}_s = A_m x_s + u_d$ (where A_m : Hurwitz system matrix, $x_s = x - K_s \operatorname{sgn}(x_1)$, u_d : input, $s=-$ or $+$), let us consider a quadratic Lyapunov-like function candidate:

$$V_s(x) = x_s^T P x_s, s = -, + \quad (3.66)$$

which are real positive definite on \mathcal{R}^n and unbounded where $V_s(x)$ is associated with the domain $\Omega_-(x), \Omega_+(x)$. Suppose $|x_2^i| > k_1$ at $x_1=0, \forall x_0 \in \mathcal{R}^n$, there exists a switching sequence $\{\sigma_s(x_s, \tau_j)\}$ and there exists constants $\rho > 0$ such that the final Lyapunov-like function $V_{s^*}^f(\sigma(\tau_{i+1}))$ is strictly less than the precedent final Lyapunov-like function $V_s^f(\sigma(\tau_i))$ of the domain $\Omega_s(x_s)$:

$$V_{s^*}^f(\sigma(\tau_{i+1})) - V_s^f(\sigma(\tau_i)) < -\rho \|\sigma_s(\tau_j)\|^2 \quad (3.67)$$

where the subscripts s and s^* are: $\text{sign}(s) \neq \text{sign}(s^*)$, $s=-$ or $+$, $s^*=+$ or $-$, then the system is asymptotically attractive to the sliding patch. \square

Proof The above condition means that the sequence $\{V_s^f(x_s, \tau_j)\}$ strictly decreases along the switching sequence $\{\sigma_s(x_s, \tau_j)\}$ up to its limit, i.e., $\lim_{j \rightarrow \infty} V_s(x(\tau_j)) = L \geq 0$. This limit exists by virtue of the fact that the sequence $\{V_s^f(\sigma(\tau_j))\}$ is strictly decreasing and lower-bounded by zero:

$$\begin{aligned} & \lim_{j \rightarrow \infty} V_{s^*}^f(\sigma(\tau_{j+1})) - \lim_{j \rightarrow \infty} V_s^f(\sigma(\tau_j)) = L - L = 0 \\ & = \lim_{j \rightarrow \infty} [V_{s^*}^f(\sigma(\tau_{j+1})) - V_s^f(\sigma(\tau_j))] \leq \lim_{j \rightarrow \infty} [-\rho \|\sigma_s(\tau_j)\|^2] \leq 0. \end{aligned}$$

In other words,

$$\lim_{j \rightarrow \infty} [-\rho \|\sigma_s(\tau_j)\|^2] = -\rho \lim_{j \rightarrow \infty} [\|\sigma_s(\tau_j)\|^2] = 0$$

which implies $\lim_{j \rightarrow \infty} \sigma_s(\tau_j) = 0$, which is a sufficient condition for attractiveness to the sliding patch. \square

Since this theorem concerns only the final state sequence $\{V_s^f(\sigma(\tau_j))\}$, one may worry about the possibilities of growing Lyapunov-like function during

the reaching dynamics. But the boundedness of Lyapunov-like function is guaranteed by the well-known linear system theory that a Hurwitz linear system is *BIBO* stable with bounded external input. Since the space is cone about the shifted-coordinate origin, for each reaching domain, decreasing final state sequence $\{V_s^f(\sigma(\tau_j))\}$ provides a *BIBO* stability. Next example shows 3-order case whose eigenvalues are chosen intentionally so small (Figure 3.15) that its solution point approaches slowly to the sliding patch and the attractiveness can be explained by Theorem 3.3.

Example 3.4 Consider a 3-order sliding observer as that of the former example of Chapter 2 except the disturbance input:

$$\begin{cases} \dot{x}_1 = x_2 - h_1 x_1 - k_1 \operatorname{sgn}(x_1) \\ \dot{x}_2 = x_3 - h_2 x_1 - k_2 \operatorname{sgn}(x_1) \\ \dot{x}_3 = -h_3 x_1 - k_3 \operatorname{sgn}(x_1) + w \end{cases} \quad (3.68)$$

where $K=[.8 \ .31 \ .7]^T$, $H=[.8 \ .31 \ .05]^T$, $w=0$, initial states: $x_1:2$, $x_2:-3$, $x_3:-6$

The reaching dynamics is:

$$\begin{cases} \dot{x}_1 = x_{2s} - h_1 x_1 \\ \dot{x}_{2s} = x_{3s} - h_2 x_1 \\ \dot{x}_{3s} = -h_3 x_1 + u_d \end{cases} \quad (3.69)$$

where $u_d = -0.7 * \operatorname{sgn}(x_1)$

Even though the initial state is not on the hyperplane, we can see the sign unity at the first passing. This example shows that after first 3 passings, the final passing Lyapunov-like function is greater than the initial's in each reaching domain until reaching the sliding patch. However, the final Lyapunov-like function sequence is decreasing so that it is attracted to the sliding patch by the Theorem 3.3. \square

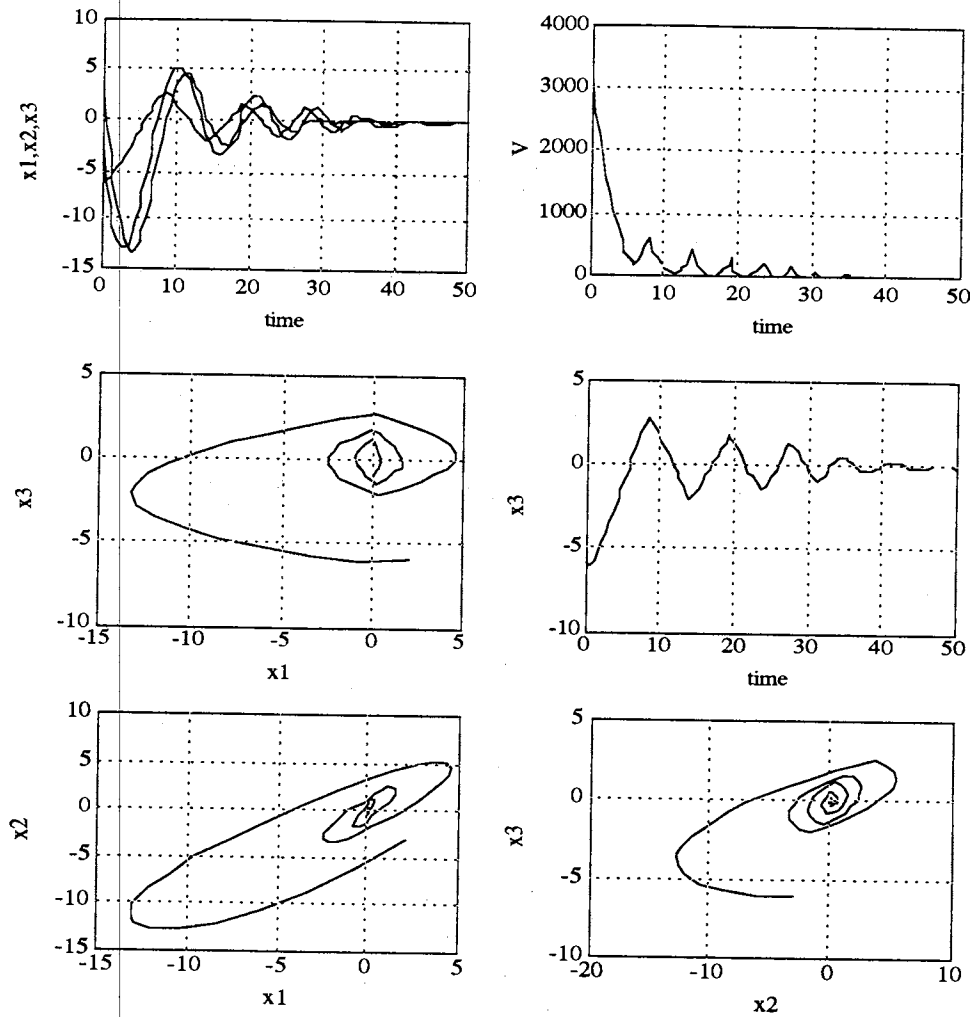


Figure 3.16 Phase plane and Lyapunov-like function

The third mode is the sliding mode that is in the hyperplane $x_1 = 0$ and with the sliding condition $|x_2| < k_1$.

$$\begin{pmatrix} \dot{x}_2 \\ \dot{x}_3 \\ \vdots \\ \dot{x}_n \end{pmatrix} = \begin{bmatrix} -k_2/k_1 & 1 & 0 & \dots & 0 \\ -k_3/k_1 & 0 & 1 & \dots & 0 \\ \vdots & \vdots & \vdots & \ddots & \vdots \\ \vdots & \vdots & \vdots & \vdots & 1 \\ -k_n/k_1 & 0 & 0 & \dots & 0 \end{bmatrix} \begin{pmatrix} x_2 \\ x_3 \\ \vdots \\ x_n \end{pmatrix} + \begin{pmatrix} 0 \\ \vdots \\ 0 \\ w \end{pmatrix} \quad (3.71)$$

After satisfying the sliding condition, the sliding dynamics is, equivalently, a reduced order linear system. For linear system, asymptotic stability requires that the state of system asymptotically approaches the origin, i.e., $\lim_{t \rightarrow \infty} \mathbf{x}(t) = 0 \forall \mathbf{x}(\tau_0) \equiv \mathbf{x}_0$. For the stability of sliding observer, the state of system also should approach the origin, via a series of switching. Since the sliding dynamics has switching terms, Lyapunov-like function at the origin may not be zero.

Definition 3.6 A linear dynamical equation is said to be totally stable if and only if for any initial state and for any bounded input the output as well as all the state variables are bounded. ■

Theorem 3.4 The forced response (zero state) of the sliding equivalent dynamics, i.e., $\dot{\mathbf{x}}_0 = \mathbf{A}_0 \mathbf{x}_0$, is asymptotically stable if and only if all the eigenvalues of \mathbf{A}_0 have negative real parts. □

Proof Let \mathbf{P} be the nonsingular matrix such that $\hat{\mathbf{A}}_0 = \mathbf{P} \mathbf{A}_0 \mathbf{P}^{-1}$ and $\hat{\mathbf{A}}_0$ is in the Jordan form. In order for the zero state to be asymptotically stable, $\|\mathbf{e}^{\mathbf{A}_0 t}\|$ should not only be bounded but also tend to zero ($\|\mathbf{e}^{\hat{\mathbf{A}}_0 t}\| \rightarrow 0$) as $t \rightarrow \infty$. Since every entry of $\mathbf{e}^{\hat{\mathbf{A}}_0 t}$ is of the form $t^k e^{a_j t + i w_j t}$, we conclude that $\|\mathbf{e}^{\hat{\mathbf{A}}_0 t}\| \rightarrow 0$ as $t \rightarrow \infty$ if and only if all the eigenvalues of $\hat{\mathbf{A}}_0$, and consequently of \mathbf{A}_0 have negative real parts. ✱

If a linear time-invariant system is asymptotically stable, its zero-input response will approach zero exponentially; thus it is also said to be exponentially stable. It is clear that total stability implies *BIBO* stability.

3.4.2 Contour of Lyapunov-like Function

Consider a contour of equivalent Lyapunov-like function on the

hyperplane for the previous 3-order instance of Example 3.4. The 2x2 submatrix is $P_{n-1} = \begin{bmatrix} 5 & -5 \\ -5 & 73.5 \end{bmatrix}$.

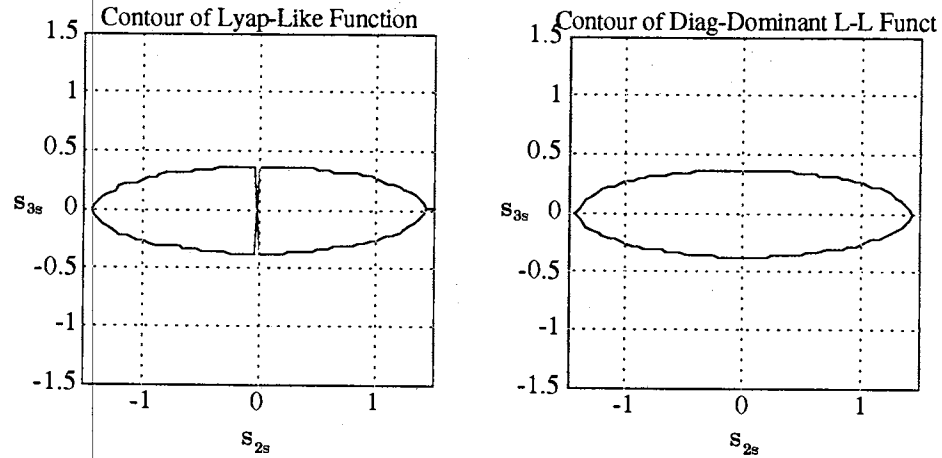


Figure 3.17 Contour of Lyapunov-like functions

The Lyapunov-like function is $V_+ = 5 \sigma_{2+}^2 - \sigma_{2+} \sigma_{3+} + 73.5 \sigma_{3+}^2$ whose contour for $V_+ = 10$ is shown at Figure 3.17(a). The contour of Lyapunov-like function with neglected off-diagonal terms is plotted at Figure 3.17(b). Since the 2x2 submatrix is diagonal dominant, these are almost identical as expected. For the diagonal dominant case, the principal radius are approximately the square root of corresponding diagonal terms.

$$R_{s_j} \cong \sqrt{P_{jj}}, \quad (j=2, \dots, n) \quad (3.72)$$

Consider a initial passing point $\sigma_{2+} > 0, \sigma_{3+} > 0$ which is on the arc $a+b+$ in the hyperplane.

Consider a case of $\dot{V}_s < 0$ or $V_s^f - V_s^i < 0$, the final point in Figure 3.18 will

remain inside the ellipsoid $a_+ b_+ c_+ d_+$ and the sign unity confines the region as $0_+ c_+ d_+$. If $0 > \sigma_{2+} > -2 k_1$, then it satisfies the sliding condition. Otherwise, it will pass again the hyperplane and the Lyapunov-like function V_s decreases by the jump difference.

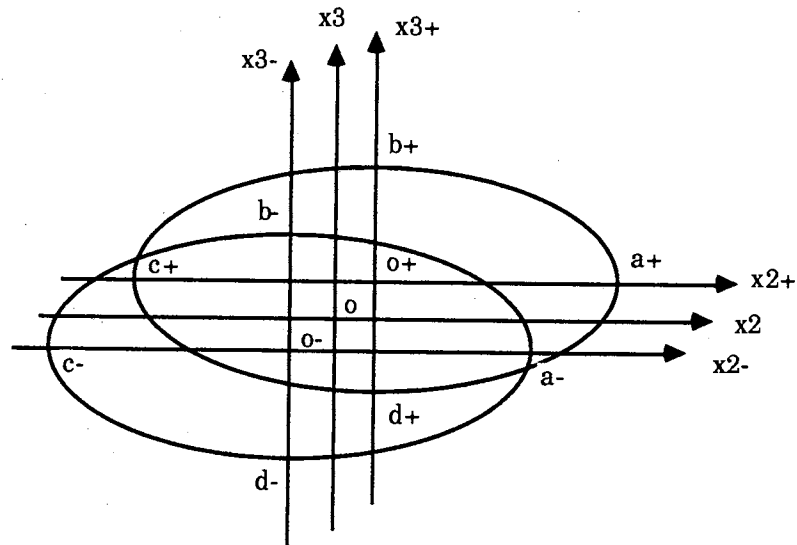


Figure 3.18 Contour of Lyapunov-like function on the hyperplane

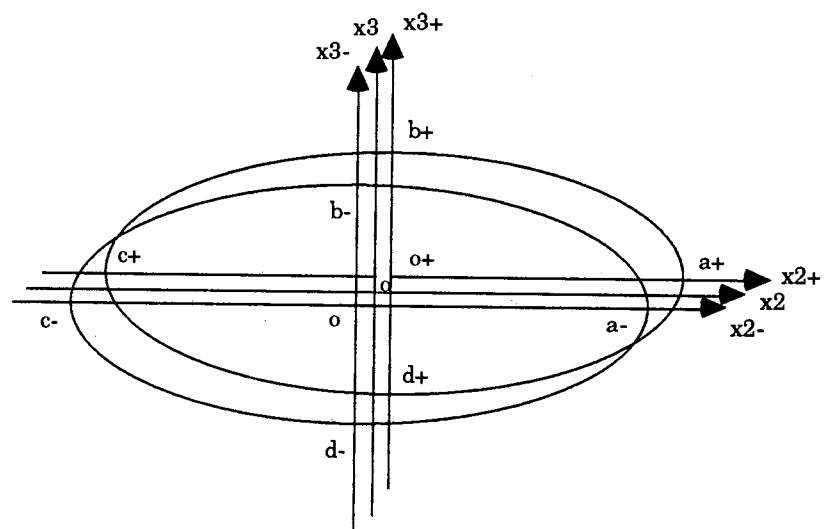


Figure 3.19 Contour of large Lyapunov-like function case

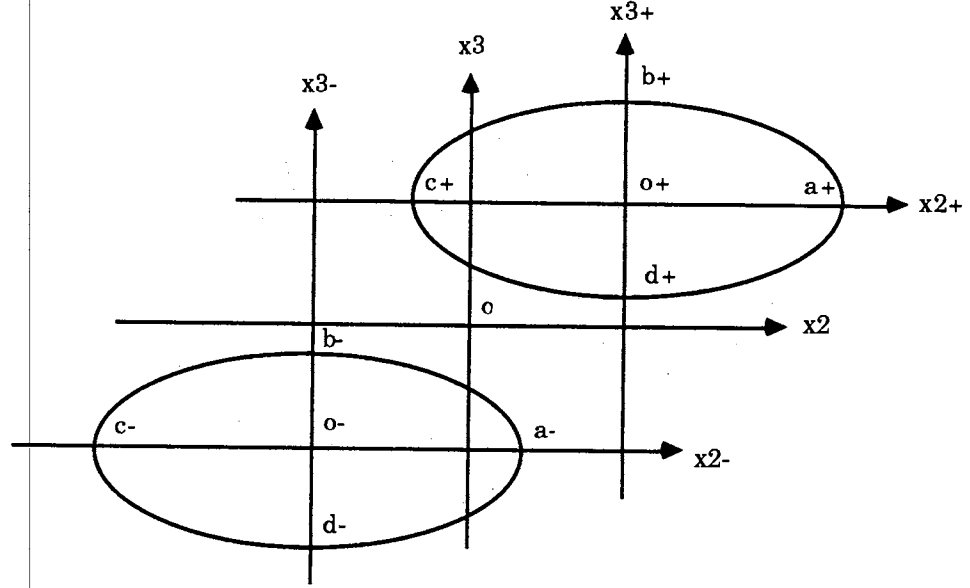


Figure 3.20 Contour of small Lyapunov-like function case

Consider contours of large Lyapunov-like function case as shown in Figure 3.19. It shows that V_+ covers more region of V_- than the previous one as shown in Figure 3.18.

For the case of small Lyapunov-like function, all the final point on the arc $0_+, c_+, d_+$ satisfies the sliding condition as shown in Figure 3.20

The ellipsoidal contour is determined by the positive definite matrix P . Figure 3.20 shows that a contour does not cover the other side contour at all. This case can increase the Lyapunov-like function by switching. Hence the coefficient K which determines shifted-coordinate system should be a function of aspect of contour, i.e., principal radius.

The Lyapunov-like function in Figure 3.22 strictly decreases by switching. Hence, for 3-order case, the suggested design methodology of coefficient K is

$$\frac{\sqrt{P_{22}}}{\sqrt{P_{33}}} \approx \frac{k_1}{k_2} \quad (3.73)$$

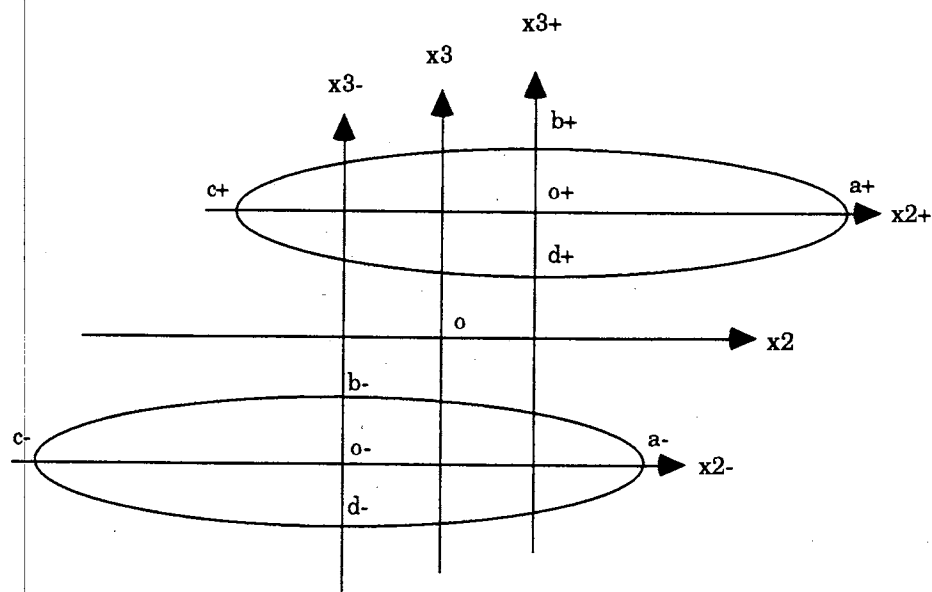


Figure 3.21 Contour of badly designed case

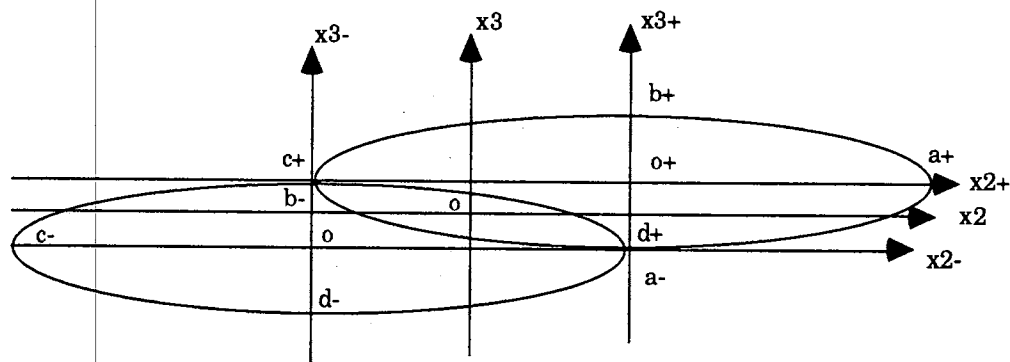


Figure 3.22 Contour of suggested case

Remarks. In Chapter 3.3.3, the general shearing effect was explained by the passing jump of the Lyapunov-like function at the hyperplane. For 3-order system, the sign equalization is proved in Appendix C.3 and the passing jump J is always negative. For the 3-order case, the contour of Lyapunov-like function of the passing point not only explains the general

shearing effect but also suggests how to choose the design coefficient K in relation with the linear coefficient H . The sign unification in n -dimensional space was studied in Appendix C but it is not proved analytically yet. Therefore, the design algorithm based on the Lyapunov-like stability Theorem 3.3 are proposed as a future study.

CHAPTER IV

DESIGN OF SLIDING OBSERVERS

4.1 Development of Design Algorithm

4.1.1 Reaching Dynamics Response

In Chapter 2, it was showed that the dynamics of the sliding observer in each reaching domain is the same as linear system with the shifted-coordinate. At the passing instant, even though the velocity field is discontinuous, the trajectory of solution point in reaching domain is continuous. Consequently the dynamical characteristic for the half domain can be extended to the whole domain directly. Hence let us review reaching dynamics in the view point of linear system theory [Chen, 1970] as follows:

$$\begin{array}{ccc} x(t) = e^{A(t-\tau)} x(\tau) & + & \int_{\tau}^t e^{A(t-\lambda)} B u(\lambda) d\lambda \\ \underbrace{\hspace{10em}} & & \underbrace{\hspace{10em}} \\ \text{Zero-input response} & & \text{zero-state response} \end{array} \quad (4.1)$$

A very important property of any linear system is that the responses of the system can be decomposed into two parts, as follows [Chen, 1970]:

$$\begin{aligned} & \text{Responses due to } \{x(t_0), u(t_0, \infty)\} \\ & = \text{responses due to } \{x(t_0), 0\} + \text{responses due to } \{0, u(t_0, \infty)\} \end{aligned}$$

The responses due to $\{x(t_0), 0\}$ are called zero-input responses or transient term: they are generated exclusively by the nonzero initial state $x(t_0)$. The

responses due to $\{0, u(t_0, \infty)\}$ are called zero-state response or forced term: they are excited exclusively by the input $u(t_0, \infty)$. Hence, for linear systems, we can consider the zero-input responses and zero-state responses independently.

A 2-order reaching dynamics in the shifted-coordinate is [Zhu, 1992]

$$\begin{pmatrix} \dot{x}_1 \\ \dot{x}_2 \end{pmatrix} = \begin{bmatrix} -h_1 & 1 \\ -h_2 & 0 \end{bmatrix} \begin{pmatrix} x_1 \\ x_2 \end{pmatrix} + \begin{pmatrix} 0 \\ u \end{pmatrix} \quad (4.2)$$

where $u = w - k_2 \operatorname{sgn}(x_1) < 0$ for $x_1 > 0$

$$\begin{cases} x_1 = \frac{1}{s^2 + h_1 s + h_2} u \\ x_2 = \frac{s + h_1}{s^2 + h_1 s + h_2} u \end{cases} \quad (4.3)$$

With zero initial values, the steady state is obtained by applying the final value theorem. For critical damping, e.g., $h_1^2 = 4 h_2$, the states by the forcing term are bounded:

$$\begin{aligned} |x_1| &= \left| \frac{1}{\left(s + \frac{h_1}{2}\right)^2} u \right| \\ &\leq \frac{4}{h_1^2} \max_{0 \leq t < t_f} |u| \leq \frac{8k_2}{h_1^2} \end{aligned} \quad (4.4)$$

$$\begin{aligned} |x_2| &= \left| \left[\frac{1}{\left(s + \frac{h_1}{2}\right)} + \frac{h_1/2}{\left(s + \frac{h_1}{2}\right)^2} \right] u \right| \\ &\leq \frac{4}{h_1} \max_{0 \leq t < t_f} |u| \leq \frac{8k_2}{h_1} \end{aligned} \quad (4.5)$$

These bounds are only due to the forcing term. The transient term by the initial conditions cannot be considered in an analytic manner except for

some special cases. The reaching dynamics is valid only to the next passing point, i.e., $x_1 = 0$. Usually, the steady states bounds are too conservative as compared to the actual passing state values. Even though these bounds are big enough, it is hard to verify that the transient overshoot can be considered in the same manner. The Kalman-Yakubovich lemma is an usual approach to this problem. With the so-called "matching condition", the Lyapunov function of this kind of system is perfect in mathematics but too conservative to find the real applications. The conservativeness is mainly due to the strict negative definiteness of \dot{V} . This conservativeness can be overcome by considering the system's properties, i.e., "shearing effect" etc. Hence, a design algorithm "Sliding Observer design by the wOrst reaching dynamics for Nonlinear/uncertain system" (SOON) is developed to consider all the phenomena--that is the overshoot by initial conditions, the transient by forcing term and shifted-coordinate.

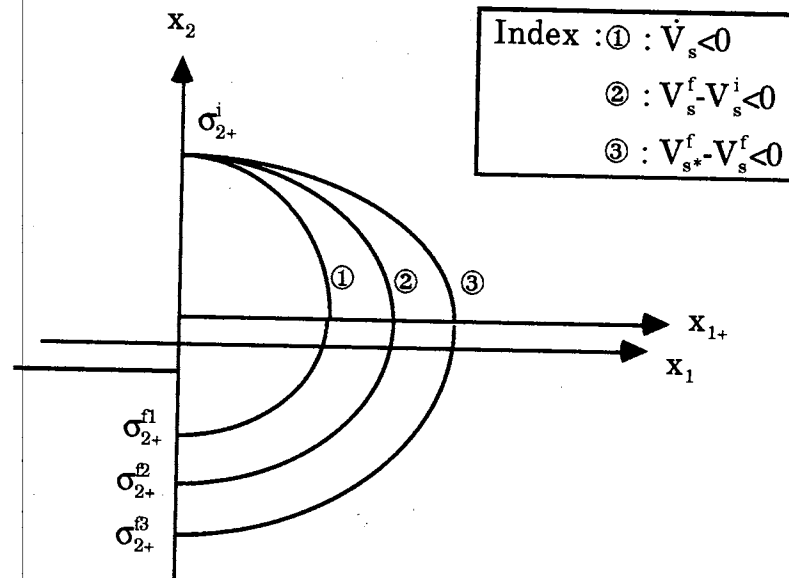


Figure 4.1 Conceptual comparison of stability theorems

4.1.2 Conceptual Comparisons of Stability Theorems

Let us compare the sliding observer stability theorems in Chapter 3 for the case of 2-order reaching dynamics.

2-order Case. Theorem 3.1 requires $\dot{V}_s < 0$. The Lyapunov-like function strictly decreases along the line ① in Figure 4.1 so that $\sigma_{2+}^{f1} > -\sigma_{2+}^i$ ($s_{2+}^{f1} > -s_{2+}^i + 2k_1$)

Along the line ② the Lyapunov-like function V_s of the final point strictly less than that of initial point: $V_s^f - V_s^i < 0$, $\sigma_{2+}^{f2} > -\sigma_{2+}^i$ ($s_{2+}^{f2} > -s_{2+}^i + 2k_1$)

Theorem 3.3 requires $V^f - V^i < 0$ (V is the same quadratic function as V_s except that it is expressed in the original coordinate) The Lyapunov-like function V of the final point strictly less than that of initial point, i.e., line ③: $\sigma_{2+}^{f3} > -\sigma_{2+}^i - 2k_1$ ($s_{2+}^{f3} > -s_{2+}^i$). This condition is exactly the same as the worst case analysis.

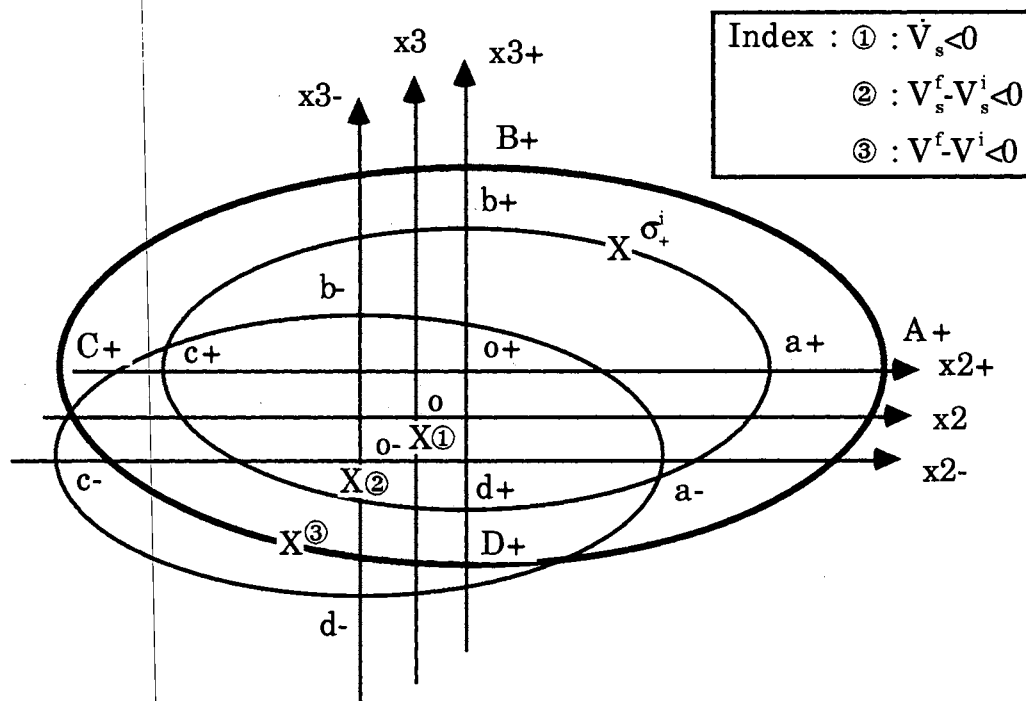


Figure 4.2 Lyapunov-like function contour on the hyperplane

3-order Case. Let us compare the sliding observer stability theorems in Chapter 3 for the case of 3-order reaching dynamics. Figure 4.2 is only a conceptual diagram to compare the theorems.

The ellipse $a_+b_+c_+d_+$ is the Lyapunov-like function contour of initial passing point σ_+^i . If $\dot{V}_s < 0$ then a final passing point will fall inside of the ellipse $a_+b_+c_+d_+$. If the final passing point $X①$ is $-2k_1 < \sigma_{2+}^f < 0$ then it satisfies the sliding condition. If a final passing point, e.g. $X②$, is inside the ellipse $a_+b_+c_+d_+$ then $V_s^f - V_s^i < 0$. Hence the stability of this case is guaranteed by Theorem 3.2. If a final passing point is the point $X③$ then its contour $A_+B_+C_+D_+$ is larger than the contour $a_+b_+c_+d_+$. However, the Lyapunov-like function of the sequenced initial passing point σ_+^i is less than the initial passing point σ_+^i . In Figure 4.2 the ellipse $a_+b_+c_+d_+$ encloses the final passing point $X③$.

4.1.3 Sliding Observer Design Algorithm

It is hard to obtain an analytic solution of the forced response of reaching dynamics except some special cases. The analytic bounds of the forcing term like equations (4.5) and (4.6) are not only conservative but also hard to get for higher order system. The transient term by the initial conditions cannot be considered in an analytic manner also. Since the Lyapunov-like stability Theorem 3.2 and Theorem 3.3 require the Lyapunov-like function of the final passing point only, it is reasonable to obtain the worst bound of final passing point via a simulation. According to the observer requirements, the design criteria can be adjusted iteratively. However, the goal of the design procedure is to make a stable observer. Hence, the first design procedure is suggested to make the initially bounded error dynamics converge

to the sliding patch directly as follows:

Design Procedures for Direct Converging to the Sliding Patch. (SOON)

1. Determine the system order
2. Determine the maximum bound of the disturbance w
3. Determine the bound of the initial states
4. Choose proper linear correction coefficients
 - According to the desirable converging speed
5. Simulate SIMNON program Reaching I
 - Worst reaching dynamics
6. Designing the switching constant K
 - The switching constant k_{n-1} is determined by half $\text{Max } \sigma_n^f$
 - For convergence purpose only, the coefficient k_{n-1} does not need to be half of $\text{Max } \sigma_n^f$
 - For n _th order case, the suggested coefficient K is

$$\frac{\sqrt{P_{22}}}{\sqrt{P_{33}}} \approx \frac{k_1}{k_2}, \frac{\sqrt{P_{33}}}{\sqrt{P_{44}}} \approx \frac{k_2}{k_3}, \dots, \frac{\sqrt{P_{n-1}}}{\sqrt{P_n}} \approx \frac{k_n}{k_{n-1}} \quad (4.6)$$

where P_{ii} is obtained from the Lyapunov equation with the proper matrix Q .

7. Tuning the design constants:
 - If the switching constant k 's are big compared to the desired precisions then h_i 's are need to be increased
 - The characteristic equation (2.24) of the sliding equivalent dynamics:

$$\det \left(sI_{n-1} - \begin{bmatrix} -k_2/k_1 & 1 & 0 & \dots & 0 \\ -k_3/k_1 & 0 & 1 & \dots & 0 \\ \vdots & \vdots & \vdots & \ddots & \vdots \\ \vdots & \vdots & \vdots & \vdots & 1 \\ -k_n/k_1 & 0 & 0 & \dots & 0 \end{bmatrix} \right) = 0 \quad (4.7)$$

- Steady state error equation (2.54) in sliding region

Remark. If the characteristic equation has some positive eigen value, then the sliding observer error dynamics will form a "limit" cycle near the sliding patch. Equation (4.6) is based on the contour analysis (3.73). The linear correction coefficient H is also related to the matrix Q and P by the Lyapunov equation (3.58). However, for the second and the third order system, (4.6) has only one term or not. Hence, the tuning procedure between the design constant H and K is actually important. For more general design procedure based on the Lyapunov-like stability theorem is suggested as a future study.

4.2 Comparative Example with VSS Observer

As a comparative example for the sliding observer and VSS observer, consider a nonlinear system as follows:

$$\begin{aligned}\dot{z}_1 &= z_2 \\ \dot{z}_2 &= g(z,w)\end{aligned}\tag{4.8}$$

where $g(z,w) = -\sin(z_1)$

4.2.1 Sliding Observer

For this system, the sliding observer can be written:

$$\begin{aligned}\hat{\dot{z}}_1 &= \hat{z}_2 + h_1 x_1 + k_1 x_1 \\ \hat{\dot{z}}_2 &= \hat{g}(z,w) + h_2 x_1 + k_2 x_1\end{aligned}\tag{4.9}$$

where $\hat{g}(z,w) = -\sin(\hat{z}_1)$

For the sliding observer, it needs only one measurement case and the output equations are

$$\begin{aligned}y_1 &= z_1 \\ y &= \hat{z}_1\end{aligned}\tag{4.10}$$

The sliding observer error dynamics is

$$\begin{cases} \dot{x}_1 = x_2 - h_1 x_1 - k_1 \operatorname{sgn}(x_1) \\ \dot{x}_2 = -h_2 x_1 - k_2 \operatorname{sgn}(x_1) + u_d \end{cases} \quad (4.11)$$

where $x_1 = z_1 - \hat{z}_1$, $x_2 = z_2 - \hat{z}_2$, $u_d = g(z, w) - \hat{g}(\hat{z}, w)$ and $\hat{g}(\hat{z}, w) = -\sin(\hat{z}_1)$.

The numerical data for the system are

$$x_1^i = 0.57, x_2^i = -1; \text{ initial error states}$$

The linear correction coefficients choosed as $h_1 = 2$ and $h_2 = 1.2$ to place poles around -1 and to make the system underdamped. With the given bound of initial state, the bound of disturbance input is evaluated as $u_d = 1$. Hence $k_2 = 1$ may be a reasonable starting value. For the design algorithm SOON, the initial states are assumed as $x_1^i = 0$, $x_2^i = 1.5$. The simulated results are shown in Figure 4.3. The worst final passing point is $\sigma_{2+}^f = -0.95$ whose absolute value is less the initial value. According to Theorem 3.2, this system is stable. If the shifting coordinate constant k_1 is assigned as half of the worst final passing point, then it will make the error state converge to sliding patch directly. Finally the tested design constant are

$$k_1 = 0.5, k_2 = 1, h_1 = 2, h_2 = 1.2$$

The simulation results of the sliding observer as shown in Figure 4.4 is compared with the VSS (Variable Structure Systems) observer which is designed by [Walcott et al.].

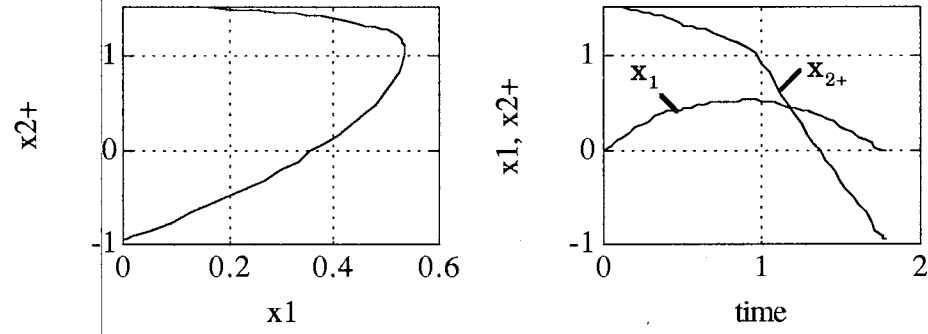


Figure 4.3 Simulation results of SOON

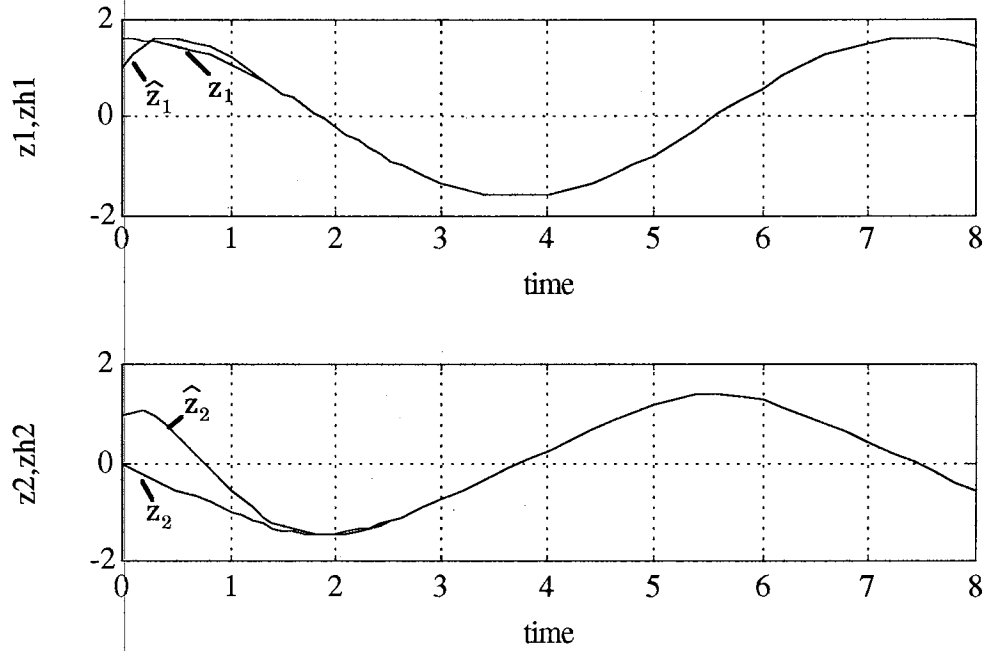


Figure 4.4 Sliding observer simulation results

4.2.2 VSS Observer

The suggested VSS observer (see detail [Walcott, 1987]) is

$$\begin{aligned}\hat{\dot{z}}_1 &= -\hat{z}_1 \\ \hat{\dot{z}}_2 &= -\hat{z}_1 - \hat{z}_2 + \hat{g}(\hat{z}, w)\end{aligned}\tag{4.12}$$

where $\hat{g}(\hat{z}, w) = -2 \operatorname{sgn}(\hat{z}_1 + \hat{z}_2 - y_2)$

To design VSS observer, so-called matching condition should be satisfied. It has the form as follows:

$$P B = C^T \quad (4.13)$$

where P is the unique positive-definite solution to the Lyapunov equation.

To satisfy this condition two measurement are necessary and the output equation is

$$y_2 = z_1 + z_2 \quad (4.14)$$

For the same initial condition as previous one, the VSS observer is simulated.

Compared to VSS observer, the sliding observer can be designed without satisfying the so-called matching condition as shown above. Another superiority in favor of the sliding observer design methodology is that, according to design requirements, its characteristic may be easily adjusted by tuning the design coefficient H and K .

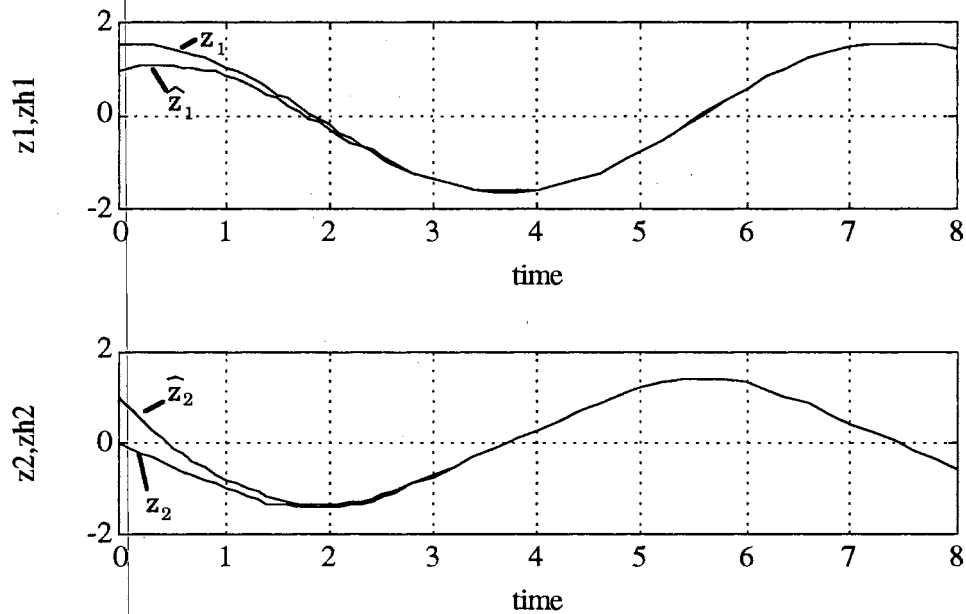


Figure 4.5 VSS observer simulation results

4.3 Inverted pendulum with a moving support

Since Stephenson [Stephenson, 1908] predicted the possibility of inverting the unstable equilibrium of a pendulum on an end by applying a vertical periodic force at the bottom, parametric excitations of an inverted pendulum have been studied by many investigators [Nayfeh, 1979]. Sethna [Sethna, 1973] proved that an inverted pendulum can be stable near the upright position for arbitrary vertical excitations with the condition that they are fast and the time average of the square of the velocity of the vertical excitations is greater than the square of the time average of the velocity of these motions by a constant that depends on the system parameters.

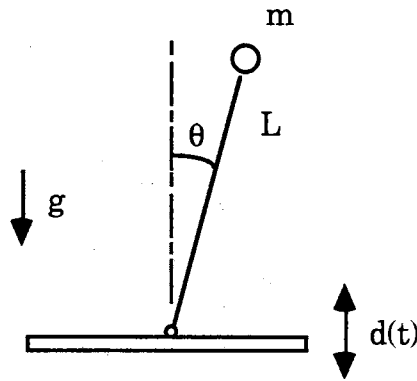


Figure 4.6 Inverted pendulum with a moving support

The equation of motion is derived as follows:

$$\ddot{\theta} + \frac{g}{L} \sin(\theta) = \frac{1}{L} (\cos(\theta) \dot{\theta} \dot{d} + \sin(\theta) \ddot{d}) \quad (4.15)$$

where $g=9.8 \text{ m/sec}^2$, $L = 0.5 \text{ m}$, $d(t) = 0.001 \sin(100 t)$

Rewrite equation (1) in the state space form:

$$\begin{cases} \dot{z}_1 = z_2 \\ \dot{z}_2 = -\frac{g}{L} \sin(z_1) + \frac{\dot{d}}{L} \cos(z_1) z_2 + \frac{\ddot{d}}{L} \sin(z_1) \end{cases} \quad (4.16)$$

The system model for the sliding observer design is

$$\begin{cases} \dot{z}_1 = z_2 \\ \dot{z}_2 = w \end{cases} \quad (4.17)$$

where w is the neglected nonlinearities and model uncertainties.

Let us assume each initial state is bounded by 0.01 then the disturbance input bound is obtained as follows:

$$\begin{aligned} |w| &\leq \left| -\frac{g}{L} \sin(z_1) \right| + \left| \frac{\dot{d}}{L} \cos(z_1) z_2 \right| + \left| \frac{\ddot{d}}{L} \sin(z_1) \right| \\ \left| -\frac{g}{L} \sin(z_1) \right| &\leq 0.2, \quad \left| \frac{\dot{d}}{L} \cos(z_1) z_2 \right| \leq 0.01, \quad \left| \frac{\ddot{d}}{L} \sin(z_1) \right| \leq 0.2 \end{aligned}$$

The suggested sliding observer is

$$\begin{cases} \hat{\dot{z}}_1 = \hat{z}_2 + h_1 x_1 + k_1 \text{sign}(x_1) \\ \hat{\dot{z}}_2 = \hat{w} + h_2 x_1 + k_2 \text{sign}(x_1) \end{cases} \quad (4.18)$$

The linear correction coefficients were chosen as $h_1 = 10$ and $h_2 = 30$ to place poles around -5 and to make the system underdamped. Simply assign the function $\hat{w} = 0$ to the sliding observer. When the bound of initial state is known as 0.01, the bound of disturbance input is evaluated as $u_d = 0.5$. Hence $k_2 = 0.5$ may be a reasonable starting value. With the data, the design algorithm SOON was simulated and the simulated results are as follows:

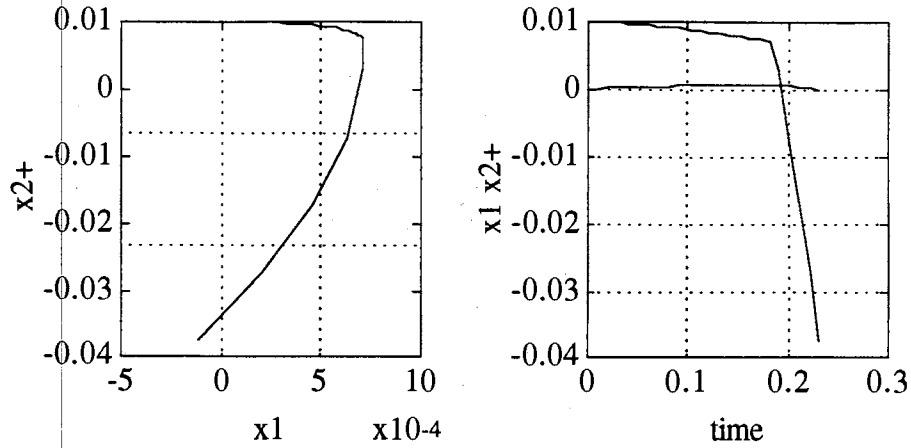


Figure 4.7 Simulation results of SOON

For the design algorithm SOON, the initial states are assumed as $x_1^i = 0$, $x_2^i = 0.01$. The simulated results are shown in Figure 4.7. The worst final passing point is $\sigma_{2+}^f = -0.035$ whose absolute value is greater the initial value. If the shifted coordinate constant k_1 is assigned as half of the worst final passing point, then it will make the error state converge to sliding patch directly according to Theorem 3.3. Since the neglected nonlinearities are sinusoidal functions only, the constant k_1 can be chosen small as according to the desired observing accuracy. Finally the tested design constants are

$$k_1 = 0.005, k_2 = 0.5, h_1 = 10, h_2 = 30$$

Even though the initial error of the simulation is as big as twice of the initial error of the design algorithm, the simulation shows that the solution point converges to sliding patch directly as shown in Figure 4.8. This is not a surprising result because the design algorithm by worst case is conservative as expected.

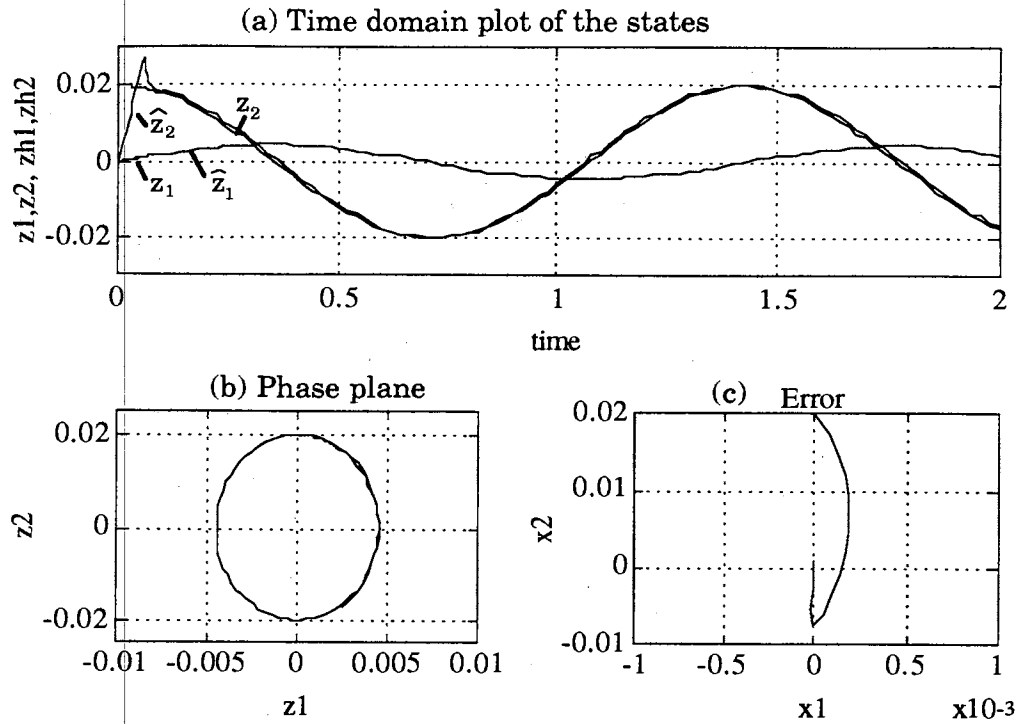


Figure 4.8 Sliding observer simulation results

- (a) Time domain plot of the actual and estimated states
- (b) Phase plane of the actual states
- (c) Phase plane of the error states of the sliding observer

Hence, if the nonlinear model of system is exactly known and if it is composed with sinusoidal functions whose means are zero, then the smaller constant k_1 can be chosen safely.

4.4 Nonlinear Mass-Spring System with Friction

Consider a 2-order nonlinear system, consisting of a mass connected to a nonlinear spring in the presence of dry friction and stiction, in canonical form:

$$\begin{aligned}\dot{z}_1 &= z_2 \\ \dot{z}_2 &= g(z,w) \\ y &= z_1\end{aligned}\tag{4.19}$$

where $g(z,w) = -\kappa z_1^3 - f_s(z_2) + \dot{w}$, κ is a constant nonlinear spring coefficient, and $f_s(z_2)$ represents dry friction with stiction.

For this system, the sliding mode observer can be written:

$$\begin{aligned}\dot{\hat{z}}_1 &= \hat{z}_2 + h_1 x_1 + k_1 x_1 \\ \dot{\hat{z}}_2 &= \hat{g}(z,w) + h_2 x_1 + k_2 x_1 \\ y &= \hat{z}_1\end{aligned}\tag{4.20}$$

The sliding observer error dynamics is

$$\begin{cases} \dot{x}_1 = x_2 - h_1 x_1 - k_1 \operatorname{sgn}(x_1) \\ \dot{x}_2 = -h_2 x_1 - k_2 \operatorname{sgn}(x_1) + u_d \end{cases}\tag{4.21}$$

where $x_1 = z_1 - \hat{z}_1$, $x_2 = z_2 - \hat{z}_2$, $u_d = g(z,w) - \hat{g}(\hat{z},w)$.

The numerical data for the system are

$$\begin{aligned}\kappa &= 1.0, F_s = 1.0; \text{ static friction, } F_d = 0.75; \text{ dynamic friction} \\ x_1^i &= 0, x_2^i = 0.5; \text{ initial values}\end{aligned}$$

The linear correction coefficients was chosen as $h_1 = 8$ and $h_2 = 16$ according to pole placement of linear system theory. Simply assign the function $\hat{g}(z,w) = 0$. With the given bound of initial state, the bound of disturbance input is evaluated as $u_d = 2$. Hence $k_2 = 2$ may be a reasonable starting value.

With the data simulate the design algorithm SOON and the results are as follows:

The worst final passing point is $\sigma_{2+}^f = -0.44$ whose absolute value is less the initial value. According to Theorem 3.2, this system is stable. Hence, we can freely assign the coordinate shifting constant k_1 . Consider the

desirable accuracy x_1 , take $k_1 = 0.01$. Finally the tested design constant are

$$k_1 = 0.01, k_2 = 2, h_1 = 8, h_2 = 16$$

The simulation results by SOON is compared with the sliding observer which is designed by the absolute stability theorem and whose switching function is saturation functions instead of signum function (see Appendix B.2). The numerical data for the saturation sliding observer is the same as new sliding observer except the design coefficients:

$$k_1 = 0, k_2 = 2, h_1 = 44, h_2 = 400$$

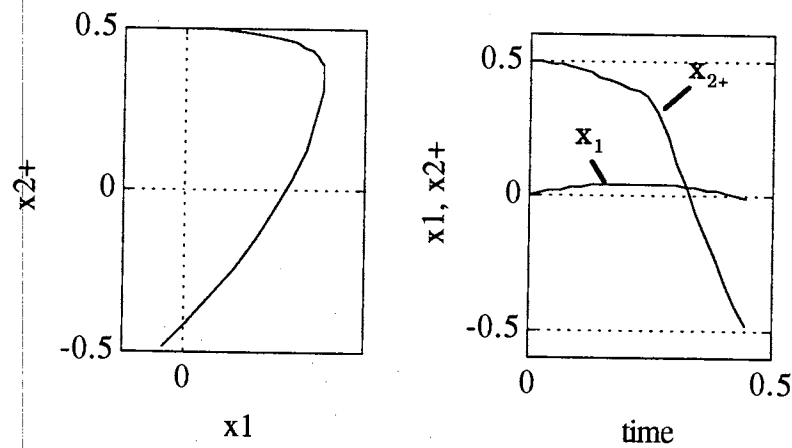


Figure 4.9 Simulation results of SOON

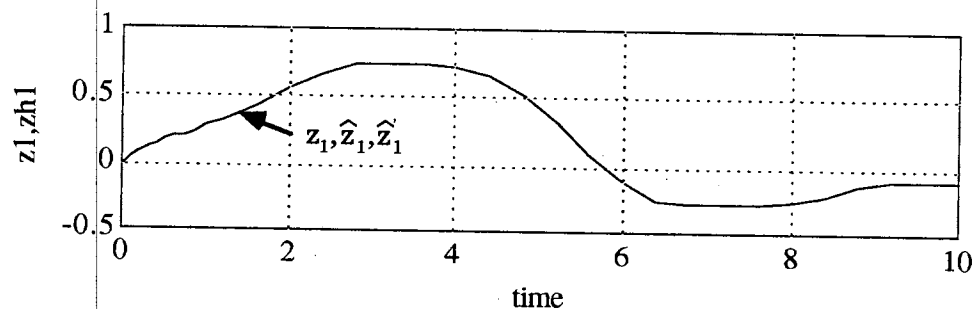


Figure 4.10 Simulation results: time domain plot of 1st states

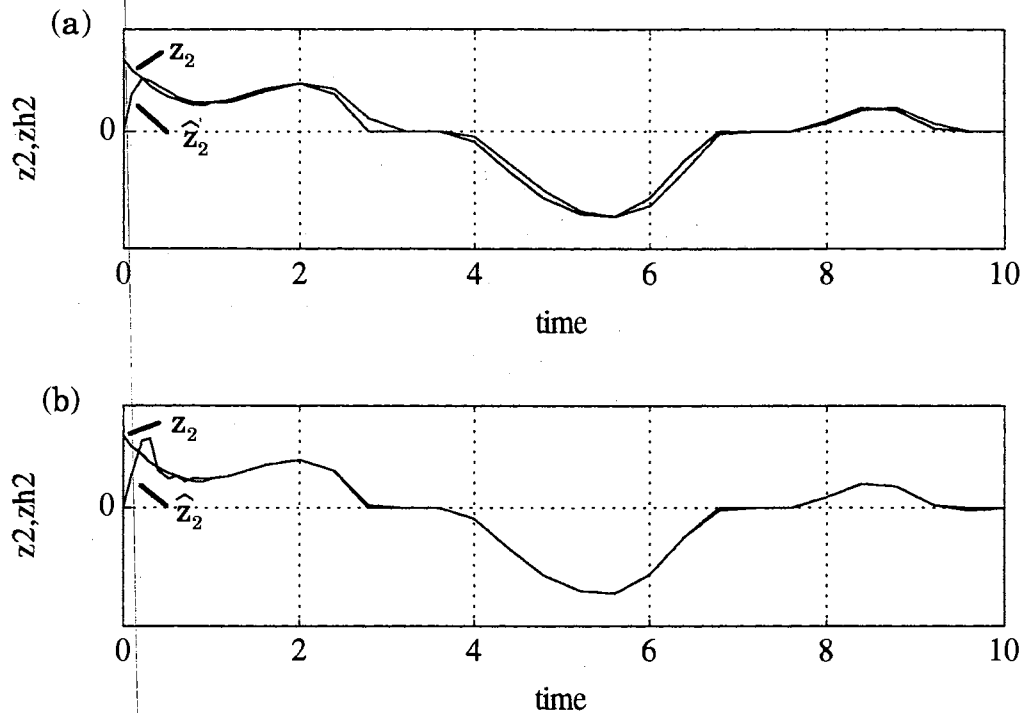


Figure 4.11 Simulation results: time domain plot of 2nd states

- a) The sliding observer by absolute stability theorem
- b) The sliding observer by SOON

Even though the both of simulation results satisfy the design goal, we can see the difference between them. Both of the first estimated state are so close to that of actual system, we cannot see the difference in Figure 4.10. The saturation sliding observer is equivalently high gain system within the boundary layer. On the contrary, if the signum sliding observer is arrived at sliding patch, its dynamics is equivalently reduced order system and its steady state error bounds are limited by the shifted-coefficient as shown in the equation (2.43).

4.5 Super-tanker Lateral Dynamics

For the 3-order example, the sliding observer is used to estimate the angular velocity (yaw rate) and the angular acceleration of a super-tanker from the measurement of the "heading", i.e., the yaw angle. The equation of motion is originally derived by Frimm [1983]. The plant is described as follows:

$$\begin{cases} \dot{z}_1 = z_2 \\ \dot{z}_2 = z_3 \\ \dot{z}_3 = -\frac{\kappa}{T_1 T_2} H(z_2) - \left(\frac{1}{T_1} + \frac{1}{T_2}\right) z_3 + \frac{\kappa}{T_1 T_2} (\delta + T_3 \dot{\delta}) \end{cases} \quad (4.22)$$

where

- $z_1 = \psi$ is the yaw angle (degree)
- $z_2 = \dot{\psi}$ is the yaw rate (degree/sec)
- z_3 is the derivative of yaw rate
- δ is the rudder angle (degree)

The function $H(z_2) = H(\dot{\psi})$ and the constants were identified from the actual ship as:

$$H(\dot{\psi}) = 1.8419 - 21.294 \dot{\psi} - 8.0534 \dot{\psi}^2 + 96.5283 \dot{\psi}^3 - 24.9247 \dot{\psi}^5$$

- $T_1 = -60.26$
- $T_2 = 7.77$
- $T_3 = 17.5$
- $\kappa = -0.04696$

The goal of this example is to design a sliding observer which estimates the second and third states with the only available measurement of yaw angle. A linear model by Arie will be used and the rudder inputs will be

lumped with the nonlinearities and regarded as an uncertainty.

The model used for the observer design is

$$\begin{cases} \dot{z}_1 = z_2 \\ \dot{z}_2 = z_3 \\ \dot{z}_3 = -\frac{1}{T_1 T_2} z_2 - \left(\frac{1}{T_1} + \frac{1}{T_2}\right) z_3 + w \end{cases} \quad (4.23)$$

where $|w| \leq \gamma$

The uncertainty bound γ will be determined based on the knowledge of the actual system. The suggested sliding observer is

$$\begin{cases} \hat{\dot{z}}_1 = \hat{z}_2 + h_1 x_1 + k_1 \operatorname{sgn}(x_1) \\ \hat{\dot{z}}_2 = \hat{z}_3 + h_2 x_1 + k_2 \operatorname{sgn}(x_1) \\ \hat{\dot{z}}_3 = -\frac{1}{T_1 T_2} \hat{z}_2 - \left(\frac{1}{T_1} + \frac{1}{T_2}\right) \hat{z}_3 + h_3 x_1 + k_3 \operatorname{sgn}(x_1) \end{cases} \quad (4.24)$$

where $x_1 = z_1 - \hat{z}_1$

To follow the design procedure, the uncertainty bound needs to be evaluated first. Since modeling errors of this example are mathematically unbounded, it is necessary to use the physical knowledge to determine the bounds for modeling errors. The experimental data are as follows:

- $|z_1| < 1$ (degree)
- $|z_2| < 0.2$ (degree/sec)
- $|\delta| \leq 10$ (degree)

Using the physical bounds given above, the uncertainty bound is obtained via the Schwarz inequalities.

$$|w| = \left| \frac{1}{T_1 T_2} (z_2 - \kappa H(z_2)) + \frac{\kappa}{T_1 T_2} (\delta + T_3 \dot{\delta}) \right| < .023 \quad (4.25)$$

With $\kappa = 0.1$, take the bound as $\gamma = 0.023$. The next step is to determine

the bounds on the initial error states. Let assume the bounds as follows:

- $x_1 \approx 0$
- $|x_2|_{\max} \leq 1.5$
- $|x_3|_{\max} \leq 0.5$

The next step is choosing the linear correction coefficient. Simply pole place all at -2 and make it slightly underdamped to be captured in the sliding patch fast. The chosen coefficient is

$$H = [6 \ 12.2 \ 8.4]^T$$

With this design constant, simulate the reaching dynamics to get the worst final passing point. Considering the bound of initial state, 2 different initial conditions are simulate and the results are shown in following Figures.

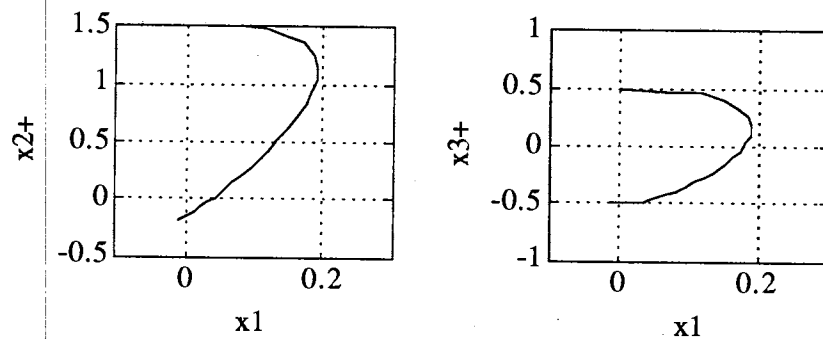


Figure 4.12 Worst reaching dynamics with $x^i = [0 \ 1.5 \ 0.5]$

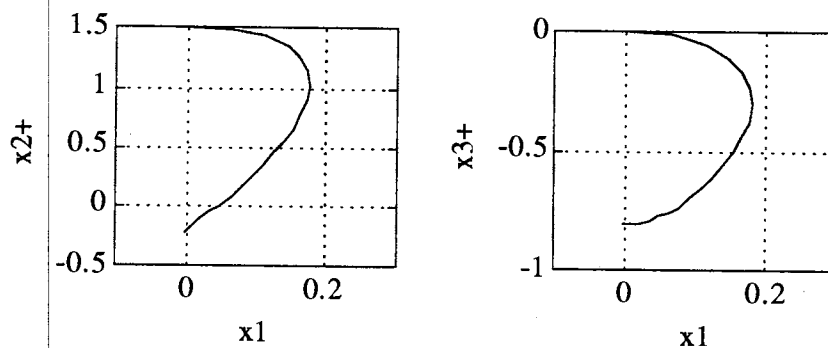


Figure 4.13 Worst reaching dynamics with $x^i = [0 \ 1.5 \ 0]$

The simulation shows that the later one is worse than the first one whose initial Lyapunov-like function is greater than that of later one. The final passing point are $\sigma_+^f = [0 \ -0.18 \ -0.49]^T$ and $\sigma_+^f = [0 \ -0.24 \ -0.8]^T$. However, the both results satisfy the requirement of stability Theorem 3.2. Assigning the shifted-coefficient K_s as half of the worst final passing state will guarantee one cycle convergence. Considering the equivalent sliding dynamics eigenvalues, the switching coefficient is chosen as:

$$K = [0.1 \ 0.2 \ 0.023]^T$$

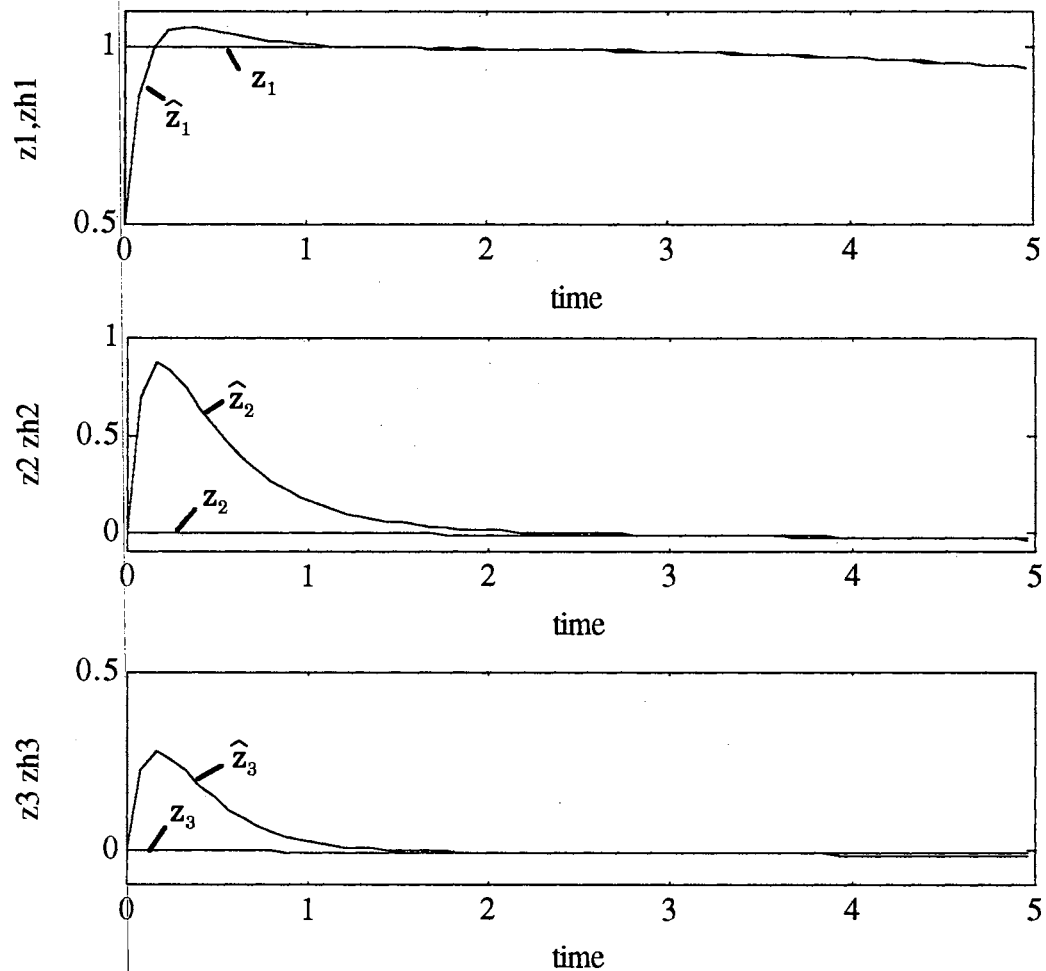


Figure 4.14 The actual and estimated states of super-tanker

Even the bound of the rudder angle is 10° , the simulation is done for $\delta = 30^\circ$ to demonstrate "robustness" of the designed sliding observer as shown in Figure 4.14 in time domain. It shows that the solution point is captured by the sliding patch within one cycle as expected.

CHAPTER V

ROBOT CONTROL BASED ON SLIDING OBSERVERS

5.1 Sliding Observer for Multiple Measurements

In the state estimation problem, the need to handle model uncertainty due to nonlinearities or disturbance leads to the development of a sliding observer. A sliding observer is one of the simple robust estimations. Despite the presence of uncertainty and disturbances whose bound is known it is easy to show that the performance of the sliding observer is theoretically perfect.

The sliding observer with multiple measurement in phase variable canonical form can be designed as far as the disturbance input bound of the error dynamics is known. The system with double measurements is assumed as:

$$\begin{cases} \dot{z}_1 = z_2 \\ \dot{z}_2 = g_1(z, u_1, t, w_1, \theta) \\ \dot{z}_3 = z_4 \\ \dot{z}_4 = g_2(z, u_2, t, w_2, \theta) \end{cases} \quad (5.1)$$

The suggested sliding observer is:

$$\begin{cases} \hat{\dot{z}}_1 = \hat{z}_2 + h_1(y_1 - C_1 \hat{z}) + k_1 \operatorname{sgn}(x_1) \\ \hat{\dot{z}}_2 = \hat{g}_1 + h_2(y_1 - C_1 \hat{z}) + k_2 \operatorname{sgn}(x_1) \\ \hat{\dot{z}}_3 = \hat{z}_4 + h_3(y_2 - C_2 \hat{z}) + k_3 \operatorname{sgn}(x_3) \\ \hat{\dot{z}}_4 = \hat{g}_2 + h_4(y_2 - C_2 \hat{z}) + k_4 \operatorname{sgn}(x_3) \end{cases} \quad (5.2)$$

where $x_1 = y_1 - C_1 \hat{z}$ and $x_3 = y_2 - C_2 \hat{z}$

The error dynamics:

$$\begin{cases} \dot{x}_1 = x_2 - h_1 x_1 - k_1 \text{sgn}(x_1) \\ \dot{x}_2 = w_1 - h_2 x_1 - k_2 \text{sgn}(x_1) \\ \dot{x}_3 = x_4 - h_3 x_3 - k_3 \text{sgn}(x_3) \\ \dot{x}_4 = w_2 - h_4 x_3 - k_4 \text{sgn}(x_3) \end{cases} \quad (5.3)$$

where $w_1 = g_1(z, u_1, t, w_1, \theta) - \hat{g}_1(\hat{z}, u_1, t, \hat{\theta})$ and $w_2 = g_2(z, u_2, t, w_2, \theta) - \hat{g}_2(\hat{z}, u_2, t, \hat{\theta})$

For the sliding observer error dynamics, w_1 and w_2 are the disturbance inputs which include neglected nonlinearities, parametric uncertainties, modeling errors and noises. The bound of the disturbance input w_1 and w_2 are assumed to be known. If the error dynamics of multiple measurements system can be decoupled, then the sliding observer can be designed exactly the same method as the single measurement case. Compared to the single measurements sliding observer, the multiple measurements sliding observer has multiple hyperplanes. This is one of the main difference between the sliding observer and sliding control problem.

In this chapter, the sliding observer is used to estimate the states of a two-link manipulator for multiple measurement example. Since every observer is considered to be a part of a closed-loop feedback system, as a practical example, a sliding observer for a two-link robot system was designed and simulated to compose a closed-loop feedback system with several control method. If the model of robot is known exactly, the nonlinear term of the equations of motion can be included in the sliding observer for an accurate estimation. For this case, the Feedback Linearization method can be applied to control the nonlinear system. And also the SOFL (Feedback Linearization control based on Sliding Observer) is composed and simulated. If the

dynamics is not known exactly, the Feedback Linearization control does not work properly. Also, for the sliding observer, the simplified model may be preferred. For the system control, the adaptive control and the sliding control were designed.

5.2 Robots Dynamics

5.2.1 Dynamics of Rigid Robots

The mathematical model for a n-link robot is derived via the Euler-Laglangian equations (see Spong and Vidyasagar for details [Spong, 1989]):

$$\sum_j d_{kj}(q) \ddot{q}_j + \sum_{i,j} C_{ijk}(q) \dot{q}_i \dot{q}_j + \phi_k(q) = \tau_k \quad (5.4)$$

where d_{kj} ; The coefficient of inertia matrix $D(q)$

ϕ_k ; The gravitational forces and torques

c_{ijk} ; The coriolis and centrifugal terms

$$C_{ijk} = \frac{1}{2} \left\{ \frac{\partial d_{kj}}{\partial q_i} + \frac{\partial d_{ki}}{\partial q_j} - \frac{\partial d_{ij}}{\partial q_k} \right\}$$

Equation (5.4) can be rewritten in the matrix form :

$$D(q) \ddot{q} + C(q, \dot{q}) \dot{q} + g(q) = \tau \quad (5.5)$$

where the k, j _th element of the matrix $C(q, \dot{q})$ is defined as:

$$\begin{aligned} C_{kj} &= \sum_{i=1}^n C_{ijk}(q) \dot{q}_i \\ &= \sum_{i=1}^n \frac{1}{2} \left\{ \frac{\partial d_{kj}}{\partial q_i} + \frac{\partial d_{ki}}{\partial q_j} - \frac{\partial d_{ij}}{\partial q_k} \right\} \dot{q}_i \end{aligned}$$

and the k _th component of g is ϕ_k

For a general n-link manipulator, the equations of motion (5.4) are

nonlinear and coupled, but for the simplest robots, they have several properties [Spong, 1990] that are useful for designing control system.

Property

1) The inertia matrix $D(q)$ is symmetric, positive definite, and both $D(q)$ and $D(q)^{-1}$ are uniformly bounded as a function of $q \in \mathbb{R}^n$

2) There is an independent control input for each degree of freedom.

3) Link masses, moments of inertias etc., appear as coefficients of known functions of the generalized coordinates.

4) The Coriolis and centrifugal forces are quadratic in the terms of \dot{q}_i

$$\|C(q, \dot{q})\dot{q}\| \leq \sigma_1 \|\dot{q}\|^2$$

5) The vector $C(q, \dot{q})\dot{q}$ has elements $\dot{q}^T N_i(q) \dot{q}$ where the N_i 's matrices are symmetric and composed of bounded periodic elements.

Each term of the matrices of dynamic equation (5.4) can be defined as a separate parameter, so that the dynamic equation (5.5) is rewritten in a linear regression form:

$$D(q)\ddot{q} + C(q, \dot{q})\dot{q} + g(q) = Y(q, \dot{q}, \ddot{q})\theta = \tau$$

where $Y(q, \dot{q}, \ddot{q})$ is an $n \times r$ matrix of known functions, known as the regressor, and q is an r -order vector of parameters.

5.2.2 Two Link Manipulator

Fig. 5.1 is a planar type model of two-link robot with a motor at each joint for control input. The dynamic equation (5.3) for a two-link robot in matrix form is:

$$\begin{aligned} d_{11}\ddot{q}_1 + d_{12}\ddot{q}_2 + C_{121}\dot{q}_1\dot{q}_2 + C_{211}\dot{q}_2\dot{q}_1 + C_{211}\dot{q}_2^2 + \phi_1 &= \tau_1 \\ d_{21}\ddot{q}_1 + d_{22}\ddot{q}_2 + C_{112}\dot{q}_1^2 + \phi_2 &= \tau_2 \end{aligned} \quad (5.6)$$

where $i = 1, 2$

τ_i ; The control inputs

q_i ; A generalized coordinate that is the joint angle

$$d_{11} = m_1 l_{c1}^2 + m_2 (l_1^2 + l_{c2}^2 + 2 l_1 l_{c2} \cos(q_2)) + I_1 + I_2$$

$$d_{12} = d_{21} = m_2 (l_{c2}^2 + l_1 l_{c2} \cos(q_2)) + I_2$$

$$d_{22} = m_2 l_{c2}^2 + I_2$$

$$c_{121} = c_{211} = c_{221} = -c_{112} = m_2 l_1 l_{c2} \sin(q_2) := h$$

$$\phi_1 = (m_1 l_{c1} + m_2 l_1) g \cos(q_1) + m_2 l_{c2} g \cos(q_1 + q_2)$$

$$\phi_2 = m_2 l_{c2} g \cos(q_1 + q_2) \text{ where } I_i; \text{ The moment of inertia of link } i$$

is at the center of mass of link i

l_{ci} ; The distance from the previous joint to the center of mass link i

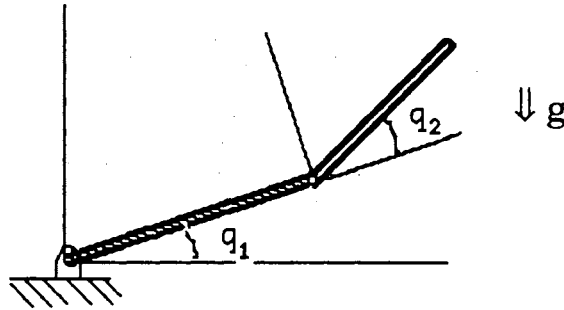


Figure 5.1. Two link Manipulator

Let us define parameters $\theta_1, \dots, \theta_9$ to get a linear regression equation:

$$\theta_1 = m_1 l_{c1}^2, \quad \theta_4 = m_2 l_1 l_{c2}, \quad \theta_7 = m_1 l_{c1} g$$

$$\theta_2 = m_2 l_1^2, \quad \theta_5 = I_1, \quad \theta_8 = m_2 l_1 g$$

$$\theta_3 = m_2 l_{c2}^2, \quad \theta_6 = I_2, \quad \theta_9 = m_2 l_{c2} g$$

$$\text{where } \theta = [\theta_1, \dots, \theta_9]^T \quad (5.7)$$

Using the parameter (5.7), rewrite the equation (5.6) in a linear regression

form:

$$Y(q, \dot{q}, \ddot{q}) \theta = \tau \quad (5.8)$$

$$Y_1(q, \dot{q}, \ddot{q}) \theta_n + Y_2(q, \dot{q}, \ddot{q}) \theta = \tau \quad (5.9)$$

where θ_n : known parameter, θ : to be estimated

Assuming that m_1 is known exactly and does not change, load and disturbances are included in m_2 , so that m_2 is unknown. If the equation (5.9) is applied to a SCARA (for Selective Compliant Articulated Robot for Assembly) type robot, the gravitational terms $\theta_7, \theta_8, \theta_9$ will not appear.

The equations of motion (5.6) is rewritten in a state space form. First, the equation (5.6) is multiplied by the inverse of inertia matrix and we have:

$$\begin{aligned} \dot{z}_1 &= z_2 \\ \dot{z}_2 &= \bar{c}_{11} z_2 + \bar{c}_{12} z_4 + \bar{\phi}_1 + \bar{\tau}_1 \\ \dot{z}_3 &= z_4 \\ \dot{z}_4 &= \bar{c}_{21} z_2 + \bar{c}_{22} z_4 + \bar{\phi}_2 + \bar{\tau}_2 \end{aligned} \quad (5.10)$$

where $z_1 = q_1, z_2 = \dot{q}_1, z_3 = q_2, \text{ and } z_4 = \dot{q}_2$

$$\begin{aligned} \Delta &= d_{11} d_{22} - d_{12} d_{21} ; \text{ determinant of inertia matrix } D(q) \\ \bar{c}_{11} &= - (d_{22} c_{11} - d_{12} c_{21}) / \Delta \\ \bar{c}_{12} &= - (d_{22} c_{12} - d_{12} c_{22}) / \Delta \\ \bar{c}_{21} &= - (d_{11} c_{21} - d_{12} c_{11}) / \Delta \\ \bar{c}_{22} &= - (d_{11} c_{22} - d_{12} c_{12}) / \Delta \\ \bar{\phi}_1 &= - (d_{22} \phi_1 - d_{12} \phi_2) / \Delta \\ \bar{\phi}_2 &= - (-d_{12} \phi_1 + d_{11} \phi_2) / \Delta \\ \bar{\tau}_1 &= (d_{22} \tau_1 - d_{12} \tau_2) / \Delta \\ \bar{\tau}_2 &= (-d_{12} \tau_1 + d_{11} \tau_2) / \Delta \end{aligned} \quad (5.11)$$

where q_1 and q_2 are the two joint angles, τ_1 and τ_2 are the joint inputs, and

$$d_{11} = m_1 l_{c1}^2 + m_2 (l_1^2 + l_{c2}^2 + 2 l_1 l_{c2} \cos(z_3)) + I_1 + I_2$$

$$d_{12} = d_{21} = m_2 (l_{c2}^2 + l_1 l_{c2} \cos(z_3)) + I_2$$

$$d_{22} = m_2 l_{c2}^2 + I_2$$

$$h := m_2 l_1 l_{c2} \sin(z_3)$$

$$c_{11} = -h z_4$$

$$c_{12} = -h z_2 - h z_4$$

$$c_{21} = h z_2$$

$$c_{22} = 0$$

$$\phi_1 = (m_1 l_{c1} + m_2 l_1) g \cos(z_1) + m_2 l_{c2} g \cos(z_1 + z_2)$$

$$\phi_2 = m_2 l_{c2} g \cos(z_1 + z_2)$$

The specification of a two-link manipulator for the computational simulation is $m_1 = 20$, $m_2 = 10$, $l_1 = 1$, $l_{c1} = 0.5$, $l_2 = 0.8$, $l_{c2} = 0.5$, $I_1 = 5$, $I_2 = 2.5$, $g = 9.8$, with the SI unit.

5.3 The Case with No Parameter Uncertainty

5.3.1 The Design of the Sliding Observer

Even though we know the system exactly, the estimated parameters may be different from the actual value, since the parameters are function of estimated states. In this section, the nonlinear term is considered to design a sliding observer. The observer is obtained by replacing the parameters in (5.10) with estimated parameters.

$$\hat{z}_1 = \hat{z}_2 + h_1 \tilde{y}_1 + k_1 1_s(\tilde{y}_1)$$

$$\hat{z}_2 = h_2 \tilde{y}_1 + k_2 1_s(\tilde{y}_1) + \hat{c}_{11} \hat{z}_2 + \hat{c}_{12} \hat{z}_4 + \hat{\phi}_1 + \hat{\tau}_1$$

$$\hat{z}_3 = \hat{z}_4 + h_3 \tilde{y}_2 + k_3 1_s(\tilde{y}_2)$$

$$\hat{z}_4 = h_4 \tilde{y}_2 + k_4 1_s(\tilde{y}_2) + \hat{c}_{21} \hat{z}_2 + \hat{c}_{22} \hat{z}_4 + \hat{\phi}_2 + \hat{\tau}_2 \quad (5.12)$$

where $\tilde{y}_1 = x_1 = z_1 - \hat{z}_1$ and $\tilde{y}_2 = x_3 = z_3 - \hat{z}_3$

The error dynamics equations are

$$\begin{aligned} \dot{x}_1 &= x_2 - h_1 x_1 - k_1 1_s(x_1) \\ \dot{x}_2 &= -h_2 x_1 - k_2 1_s(x_1) + w_1 \\ \dot{x}_3 &= x_4 - h_3 x_3 - k_3 1_s(x_3) \\ \dot{x}_4 &= -h_4 x_3 - k_4 1_s(x_3) + w_2 \end{aligned}$$

where $x_1 = z_1 - \hat{z}_1$, $x_3 = z_3 - \hat{z}_3$ and

$$\begin{aligned} w_1 &= \bar{c}_{11} x_2 + (\bar{c}_{11} - \hat{c}_{11}) \hat{z}_2 + \bar{c}_{12} x_4 + (\bar{c}_{12} - \hat{c}_{12}) \hat{z}_4 + \bar{\phi}_1 - \hat{\phi}_1 + \bar{\tau}_1 - \hat{\tau}_1 \\ w_2 &= \bar{c}_{21} x_2 + (\bar{c}_{21} - \hat{c}_{21}) \hat{z}_2 + \bar{c}_{22} x_4 + (\bar{c}_{22} - \hat{c}_{22}) \hat{z}_4 + \bar{\phi}_2 - \hat{\phi}_2 + \bar{\tau}_2 - \hat{\tau}_2 \end{aligned}$$

By using the properties 4) and 5), it can be proved that the error of estimated parameter w_1 and w_2 are bounded.

The switching gain k_1 , k_2 is chosen as a bound on the steady state estimation error on x_1 , x_3 , and k_3, k_4 is chosen to be larger than the error of estimated parameter w_1 and w_2 . The chosen constants are:

$$k_1 = 0.1, k_2 = 0.1, k_3 = 1, k_4 = 1$$

The true system is tracking the desired trajectories by feedback linearization control law. The simulations were run using SIMNON, on two different initial conditions. The first set of initial conditions of the states and the states of estimation are all zeros. The simulation results for this set of initial conditions are shown in Fig. 5. It is clear that the sliding observer is working properly.

The initial condition of the sliding observer is $\hat{z} = [1 \ 3 \ 1 \ 3]^T$. The chosen

linear correction coefficient is $H=[4 \ 4 \ 12 \ 40]$. The bound of disturbance is known as $k_1: .5$ and $k_3: 1$. The simulated results of the design algorithm SOON is $-.46$ and $-.48$ so that the chosen switching coefficients are $K=[.2 \ 1 \ .25 \ 2]$.

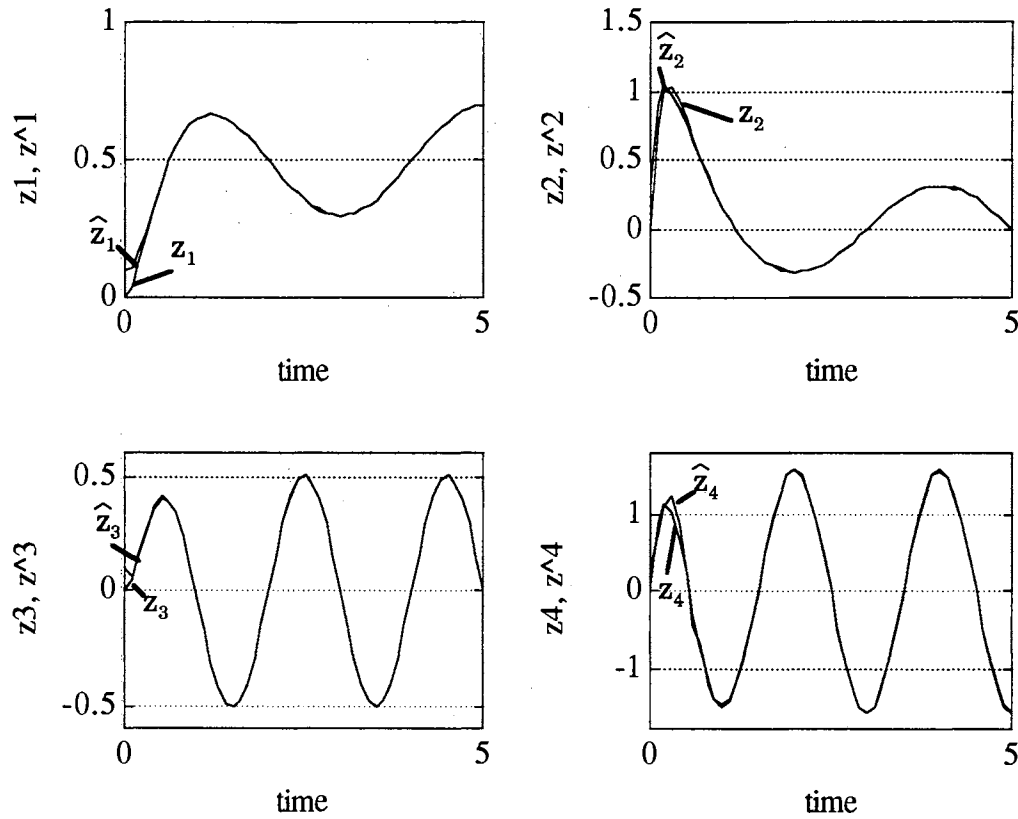


Figure 5.2 The simulated results of the sliding observer

5.3.2 Feedback Linearization Control

If the parameters are known exactly, the inverse dynamics control law (i.e. the Computed Torque control law) cancels exactly all of the nonlinear terms in (5.3) so that the closed loop system is linear and decoupled

$$D(q) \ddot{q} + C(q, \dot{q}) \dot{q} + g(q) = \tau \quad (5.13)$$

$$\text{If the torque is } \tau = D(q) \dot{v} + C(q, \dot{q}) \dot{q} + g(q) \quad (5.14)$$

Then, from (5.14) and (5.3), the equation of motion is

$$D(q) (\ddot{q} - v) = 0 \quad (5.15)$$

$$\text{By property 1, } \ddot{q} = v \quad (5.16)$$

We now consider the case when the manipulator is actually required to follow a desired trajectory, rather than merely reach a desired position. Note that a trajectory control problem may arise even when the task is merely to move a load from its initial position to a final position. The simple P.D. controller cannot be expected to handle the dynamic demands of trajectory tracking effectively. We consider first the use of feedback linearization. We then discuss the extension of adaptive control and sliding control based on the sliding observer.

The term v is the interpretation of an outer loop control law with units of acceleration, which is typically chosen as:

$$v = \ddot{q}_d - K_v \dot{\tilde{q}} - K_p \tilde{q} \quad (5.17)$$

with $\tilde{q} = q - q_d$, where $q_d(t)$; n -order vector of desired joint trajectories.

By plugging (5.17) into (5.16), we get a linear error dynamics

$$\ddot{\tilde{q}} + K_v \dot{\tilde{q}} + K_p \tilde{q} = 0 \quad (5.18)$$

If the gain matrices K_v and K_p are chosen as diagonal matrices with positive diagonal elements, then the closed-loop system is linear, decoupled, and exponentially stable. The global stability for this scheme is thus obvious. In fact, the closed-loop damping ratio and natural frequency may be arbitrarily assigned.

The Feedback Linearization Control based on Sliding Observer. The only difference between previous simulations and this section FL-SO is the

control law in which the actual states are replaced by the sliding observer estimated states. The first set of initial conditions of the states and the states of the sliding observer are all zeros. The simulation for this set of initial conditions are shown in Fig. 5.9. It is clear that the FL-SO closed loop is stable. The initial condition of the sliding observer is $\hat{z} = [.1 \ .3 \ .1 \ .3]^T$. The chosen linear correction coefficient is $H=[6 \ 9 \ 16 \ 60]$. The bound of disturbance is known as $k_1 \ .5$ and $k_3: 1$. The simulated results of the design algorithm SOON is $-.58$ and $-.56$ so that the chosen switching coefficients are $K=[.3 \ 2 \ .3 \ 3]$.

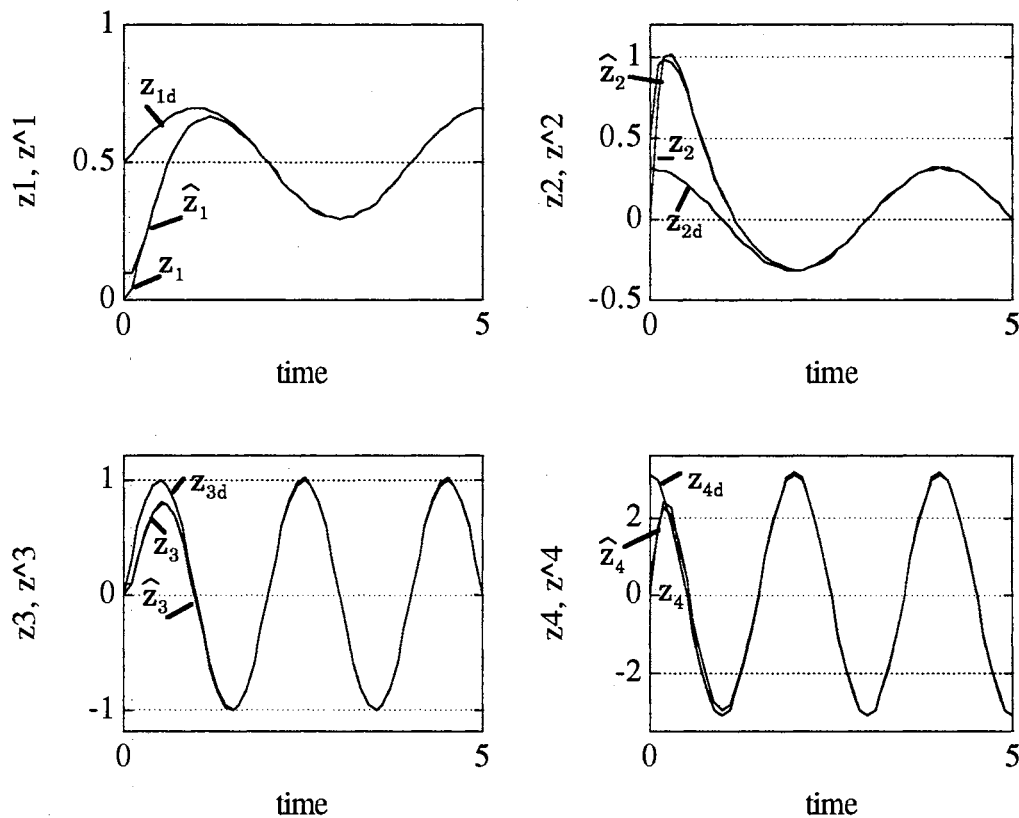


Figure 5.3 The simulated results of feedback linearization control based on the sliding observer

5.4 The Case with Parameter Uncertainty

5.4.1 The Design of the Sliding Observer

Each angular position in a two-link manipulator is measured and both the velocity as well as the position are estimated. For an estimation scheme, we can intuitively include available nonlinear model to make estimation error small. On the contrary, however, it will take more time to compute and it is not desirable for our purpose. Therefore, although the nonlinear model with no uncertainty is available, we may adopt only linear terms for a fast estimation.

The simplified model for a sliding observer design is obtained by taking only linear terms. We need to notice that the input torque is not used and not measured.

$$\begin{aligned}\dot{z}_1 &= z_2 \\ \dot{z}_2 &= w_1 \\ \dot{z}_3 &= z_4 \\ \dot{z}_4 &= w_2\end{aligned}\tag{5.19}$$

The equation (5.19) is really simple compared to the original equation. By comparing equations (5.10) and (5.13), one can identify the disturbance terms w_1 and w_2 , as in (5.12), and try to find the bound for them. The bound of w_1 and w_2 are function of states and cannot be computed explicitly.

Therefore, the bounds can be assumed as the simulated maximum value of \dot{x}_2 and \dot{x}_4 of the operating range and the initial condition. Possibly, the bound can be violated during the transient for the different initial condition. The initial condition of the sliding observer is $\hat{z} = [.1 \ .5 \ .1 \ .5]^T$. The chosen linear correction coefficient is $H = [20 \ 100 \ 40 \ 400]$. The bound of disturbance

is known as $k_1: .5$ and $k_3: 1$. The simulated results of the design algorithm SOON is $-.65$ and $-.9$ so that the chosen switching coefficients are $K=[.32 \ 5 \ .45 \ 10]$.

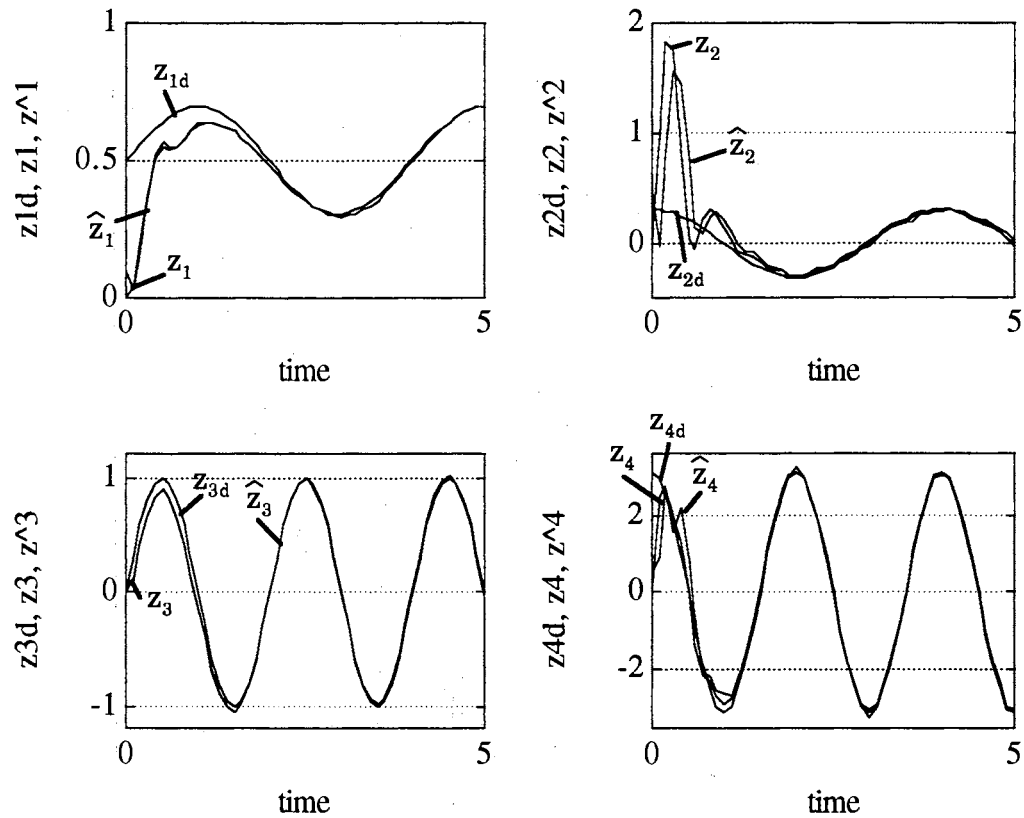


Figure 5.4 The simulated results of feedback linearization control based on the sliding observer with uncertain parameter

5.4.2 Adaptive Control

The Adaptive implementation of the inverse dynamics control law [Astrom, 1989; Slotine, 1991] is obtained by replacing D , C , and g by their estimates, i.e.,

$$\tau = \widehat{D}(q) (\ddot{q}^d - K_v \dot{\tilde{q}} - K_p \tilde{q}) + \widehat{C}(q, \dot{q}) \dot{q} + \widehat{g}(q)$$

$\widehat{D}, \widehat{C}, \widehat{g}$ have the same function form as D, C, g with estimated parameter $\theta_1, \dots, \theta_9$

$$\widehat{D} \ddot{q} + \widehat{C} \dot{q} + \widehat{g} = Y(q, \dot{q}, \ddot{q}) \widehat{\theta}$$

substitute (5.19) into (5.3), we got

$$D \ddot{q} + C \dot{q} + g = \widehat{D} (\ddot{q}^d - K_v \dot{\tilde{q}} - K_p \tilde{q}) + \widehat{C} \dot{q} + \widehat{g} \quad (5.20)$$

Rearrange the terms as:

$$\begin{aligned} D \ddot{q} - \widehat{D} \ddot{q}^d + \widehat{D} (K_v \dot{\tilde{q}} + K_p \tilde{q}) &= (\widehat{C} - C) \dot{q} + \widehat{g} - g \\ (\widehat{D} \ddot{q} - \widehat{D} \ddot{q}^d) - (\widehat{D} \ddot{q} - D \ddot{q}) + \widehat{D} (K_v \dot{\tilde{q}} + K_p \tilde{q}) &= (\widehat{C} - C) \dot{q} + (\widehat{g} - g) \end{aligned}$$

Let $(\tilde{\cdot}) := (\widehat{\cdot}) - (\cdot)$

$$\widehat{D} (\ddot{\tilde{q}} + K_v \dot{\tilde{q}} + K_p \tilde{q}) = \widetilde{D} \ddot{q} + \widetilde{C} \dot{q} + \widetilde{g} = Y(q, \dot{q}, \ddot{q}) \widetilde{\theta} \quad (5.21)$$

$$\ddot{\tilde{q}} + K_v \dot{\tilde{q}} + K_p \tilde{q} = \widehat{D}^{-1} Y \widetilde{\theta} := \Phi \widetilde{\theta} \quad (5.22)$$

Rewrite (5.22) in state space form:

$$\dot{z} = A z + B \Phi \widetilde{\theta} \quad (5.23)$$

A ; Hurwitz matrix:

$$A = \begin{bmatrix} 0 & I \\ -K_p & -K_v \end{bmatrix}; \text{ and } B = \begin{bmatrix} 0 \\ I \end{bmatrix}; z = \begin{bmatrix} \tilde{q} \\ \dot{\tilde{q}} \end{bmatrix} \quad (5.24)$$

$\ddot{\tilde{q}}$; measurable, \widehat{D}^{-1} ; bounded.

The Update Law

$$\dot{\widetilde{\theta}} = -\Gamma^{-1} \Phi^T B^T P z \quad (5.25)$$

where $\Gamma = \Gamma^T > 0$ and P is the unique symmetric positive definite solution to the Lyapunov equation:

$$A^T P + P A + Q = 0 \quad (5.26)$$

for a given symmetric, positive definite Q . Under these conditions then, the solution x of (5.23) satisfies:

$$z \Rightarrow 0 \text{ as } T \Rightarrow \infty$$

with all signals remaining bounded.

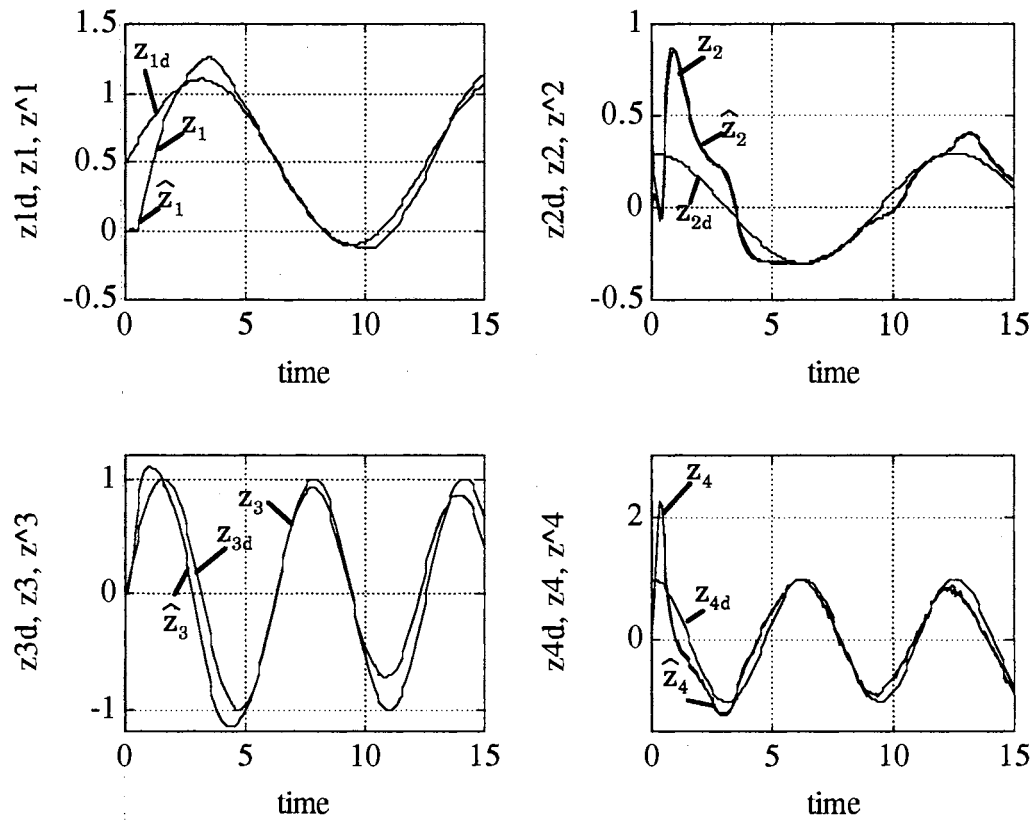


Figure 5.5 The simulated results of adaptive control based on the sliding observer with uncertain parameter

Proof) Choose the Lyapunov function candidate [Astrom, 1989]:

$$V = z^T P z + \tilde{\theta}^T \Gamma \tilde{\theta}$$

$$\dot{V} = -z^T Q z + 2 \tilde{\theta}^T [\Phi^T B^T P z + \Gamma \tilde{\theta}]$$

Using (5.25)

$$\dot{V} = -z^T Q z \leq 0$$

■

The initial condition of the sliding observer is $\hat{z} = [.0 \ .5 \ .0 \ .5]^T$. The chosen linear correction coefficient is $H=[40 \ 400 \ 60 \ 900]$. The bound of disturbance is known as $k_1 \ .5$ and $k_3: 1$. The simulated results of the design algorithm SOON is $-.62$ and $-.9$ so that the chosen switching coefficients are $K=[.31 \ 5 \ .45 \ 10]$.

5.4.3 Sliding Control

We need to handle the model uncertainty or disturbance that leads to develop a sliding control and an adaptive control etc. The sliding control is one of the simple approaches to a robust control. It is easy to show that a perfect performance can be achieved theoretically in the presence of arbitrary uncertainty and disturbances.

Let the tracking error vector $\tilde{q} = q - q^d$.

The sliding condition is:

$$\frac{1}{2} \frac{d}{dt} s_i^2 \leq -\eta_i |s_i| \quad (\eta_i > 0)$$

where $\dot{s}_i = \ddot{q}_i + \lambda_i \tilde{q}_i$

One may extend the sliding observer in a multi-variable case .

$$s = \ddot{q} + \Lambda \tilde{q} = \dot{q} - \dot{q}_r$$

where $\dot{q}_r = \dot{q}_d - \Lambda \tilde{q}$ (q_r : Reference velocity)

The detail derivation of a sliding control law for a multi-variable case is shown by Slotine (1991).

Let us define a Lyapunov function candidate as:

$$V(t) = \frac{1}{2} [s^T H s]$$

Differentiating

$$\dot{V}(t) = s^T (H \ddot{q} - \dot{H} \dot{q}_r) + \frac{1}{2} s^T \dot{H} s$$

From the system dynamics,

$$H \ddot{q} = \tau - C \dot{q} - g = \tau - C (s + \dot{q}_r) - g$$

plug in and get

$$\dot{V}(t) = s^T (\tau - H \ddot{q}_r - C \dot{q}_r - g)$$

The control input has the form as:

$$\tau = \hat{\tau} - k \operatorname{sgn}(s)$$

$\hat{\tau}$ is computed as:

$$\hat{\tau} = \hat{H} \ddot{q}_r + \hat{C} \dot{q}_r + \hat{g}$$

The components of the vector k will be chosen as:

$$k_i \geq \left| [\hat{H}(q) \ddot{q}_r + \hat{C}(q, \dot{q}) \dot{q}_r + \hat{g}(q)]_i \right| + \eta_i$$

so that

$$\dot{V} \leq - \sum_{i=1}^n \eta_i |s_i|$$

As in the single-input case, this sliding condition makes the state reach within a finite time and remain on the surface.

The initial condition of the sliding observer is $\hat{z} = [.5 \ .5 \ .5 \ .5]^T$. The chosen

linear correction coefficient is $H=[40 \ 400 \ 60 \ 900]$. The bound of disturbance is known as $k_1: .5$ and $k_3: 1$. The simulated results of the design algorithm SOON is $-.62$ and $-.9$ so that the chosen switching coefficients are $K=[.31 \ 5 \ .45 \ 10]$.

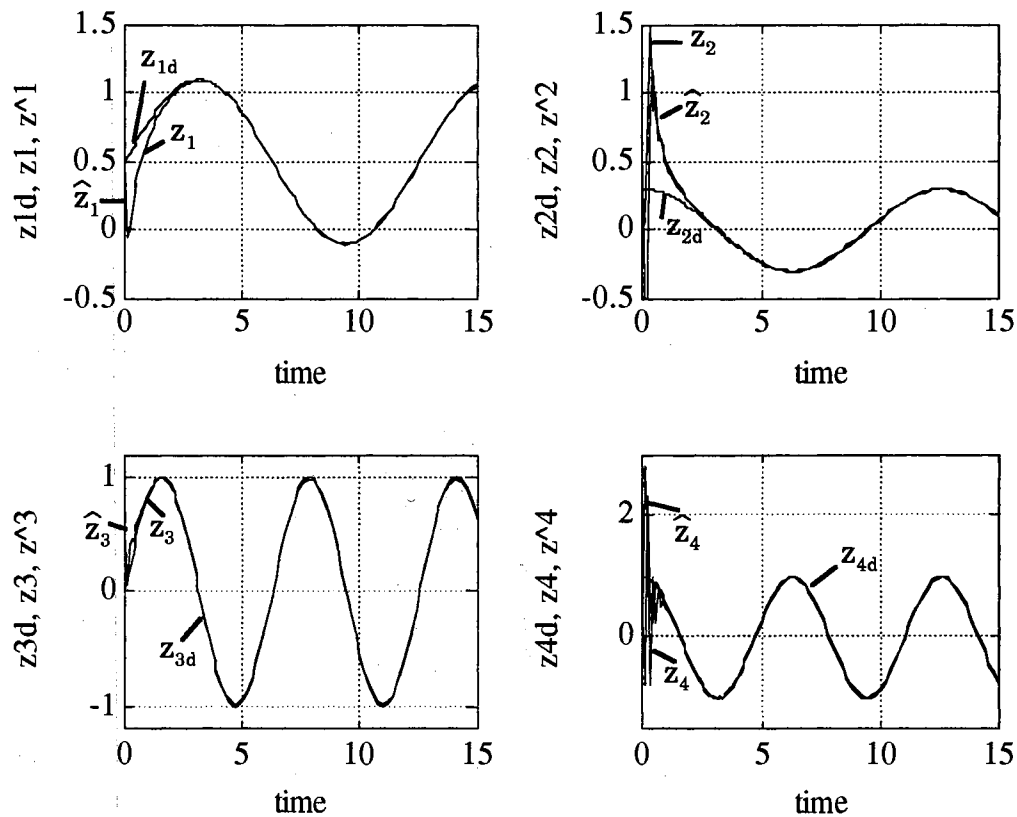


Figure 5.6 The simulated results of sliding control based on the sliding observer with uncertain parameter

CHAPTER VI

STOCHASTIC SLIDING OBSERVER DESIGN

6.1 Introduction

Optimal estimators that minimize the estimation error in a well-defined statistical sense, are of particular interest. For the linear filtering problem, under the assumption that the process noise and the nonsingular measurement noise are white, the Kalman-Bucy filter [Kalman, 1961; Kalman, 1960] is optimal in the sense of the mean-square estimation error criterion. For realizing the filter, we should know the exact intensities of noise which compose the state error covariance matrix, i.e. the Riccati equation. Practically, however, the noises are not measurable and the noise intensities may change according to variation of the operating condition.

To avoid difficulty in adapting a filter in accordance with variation of noise characteristics, Drakunov, in 1983, suggested an Adaptive Quasi-optimal Filter [Drakunov, 1986] which is insensitive to inexact knowledge of the noise intensity. By using the averaging theory his paper shows that the Adaptive Quasioptimal filter, which is actually a sliding observer, can be robust against the changed measurement noise characteristics. With the known statistical properties of the sensor noises, Misawa applied the methods of statistical linearization (the describing function technique [Gelb, 1968]) in designing the stochastic sliding observer.

If all the uncertainties in the input noise can be modeled as white noises,

then one can use the Random Input Describing Function (RIDF) in the design process. Compared to the Drakunov's analysis, Misawa [Misawa, 1988] included the linear gain "H C z" in his analysis for a first order system.

In this preliminary study, the robustness analysis for a second order system was studied about the effect of changing in noise characteristics and parameter mismatch. The theoretical prediction of a steady state estimation error covariance of the sliding observer using RIDF shows good agreements with the simulation, as well as with the first order case of Misawa [1988].

6.2 Sliding Observer Design for Noisy Measurements

Misawa's method [1988] for the sliding observer design procedure for noisy measurement is utilized. System and measurement equations are

$$\begin{aligned}\dot{z} &= A z + w \\ y &= C z + v\end{aligned}\tag{6.1}$$

where w and v are assumed to be stationary and independent white noise.

The sliding observer structure:

$$\hat{\dot{z}} = A \hat{z} + H (y - C \hat{z}) + K 1_s(\tilde{y})\tag{6.2}$$

where $\tilde{y} = y - \hat{y}$

The estimation error dynamics for the sliding observer:

$$\begin{aligned}\dot{x} &= (A - H C) x - K 1_s(\tilde{y}) + w - H v \\ 1_s^T(\tilde{y}) &= [\text{sign}(\tilde{y}_1), \text{sign}(\tilde{y}_2), \dots, \text{sign}(\tilde{y}_m)]\end{aligned}\tag{6.3}$$

The switching function can be approximated by the RIDF function [Gelb, 1974]:

$$1_s(\tilde{y}) \cong N_1 \tilde{y} = N_1 (C x + v) \quad (6.4)$$

where N_1 is the $m \times m$ matrix of RIDF of 1_s and the function of statistics of \tilde{y} . By assuming \tilde{y} is a zero mean Gaussian Process, N_1 is determined by covariance matrix of \tilde{y} . The estimation error dynamics can be rewritten as:

$$\begin{aligned} \dot{\hat{x}} &= (A - H C) \hat{x} - K N_1 (C \hat{x} + v) + w - H v \\ &= A \hat{x} - (H + K N_1) C \hat{x} - (H + K N_1) v + w \end{aligned}$$

Let $H^* = H + K N_1$

$$\begin{aligned} \dot{\hat{x}} &= A \hat{x} - (H + K N_1) (C \hat{x} + v) + w \\ &= A \hat{x} - H^* (y - C \hat{z}) + w \end{aligned} \quad (6.5)$$

The lumped gain matrix H^* is also a function of the covariance matrix of \tilde{y} .

$$\begin{aligned} \tilde{y} &= C x + v \\ E[\tilde{y}(t) \tilde{y}^T(t)] &= C E[x x^T] C^T + E[v v^T] \\ &= C P C^T + R \end{aligned} \quad (6.6)$$

Considering the measurement noise is correlated, the gain matrix H^* should be determined by an iterative optimization method.

The plant is assumed to be described as

$$\begin{aligned} \dot{z} &= A z + w \\ y &= C z + v \end{aligned}$$

where $E[w(t) w(t+\tau)^T] = Q \delta(\tau)$ and w is a n -order column vector that

includes all nonlinearities and uncertainties. Suppose that the measurement noise is colored, i.e. it is correlated. It is assumed that the measurement noise can be modeled through the use of a "shaping filter":

$$\dot{\mathbf{v}} = \mathbf{E} \mathbf{v} + \mathbf{F} \mathbf{v}_1 \quad (6.7)$$

where the matrix \mathbf{E} and \mathbf{F} are chosen properly and \mathbf{v}_1 is a white noise process:

$$\mathbf{E} [\mathbf{v}_1(t) \mathbf{v}_1(t+\tau)^T] = \mathbf{R} \delta(\tau)$$

The augmented system including the noise model is:

$$\dot{\mathbf{z}} = \begin{bmatrix} \dot{\mathbf{z}} \\ \dot{\mathbf{v}} \end{bmatrix} = \begin{bmatrix} \mathbf{A} & \mathbf{0} \\ \mathbf{0} & \mathbf{E} \end{bmatrix} \begin{bmatrix} \mathbf{z} \\ \mathbf{v} \end{bmatrix} + \begin{bmatrix} \mathbf{D} & \mathbf{0} \\ \mathbf{0} & \mathbf{F} \end{bmatrix} \begin{bmatrix} \boldsymbol{\eta} \\ \mathbf{v}_1 \end{bmatrix} \quad (6.8)$$

where $\mathbf{w} = \mathbf{D} \boldsymbol{\eta}$.

Using the lumped gain matrix in the RIDF method, the sliding observer can be written as:

$$\dot{\hat{\mathbf{z}}} = \mathbf{A} \hat{\mathbf{z}} + \mathbf{H}^* (\mathbf{y} - \mathbf{C} \hat{\mathbf{z}}) \quad (6.9)$$

The augmented estimation error dynamics is:

$$\dot{\mathbf{x}} = \begin{bmatrix} \dot{\mathbf{x}} \\ \dot{\mathbf{v}} \end{bmatrix} = \begin{bmatrix} \mathbf{A} - \mathbf{H}^* \mathbf{C} & -\mathbf{H}^* \\ \mathbf{0} & \mathbf{E} \end{bmatrix} \begin{bmatrix} \mathbf{x} \\ \mathbf{v} \end{bmatrix} + \begin{bmatrix} \mathbf{D} & \mathbf{0} \\ \mathbf{0} & \mathbf{F} \end{bmatrix} \begin{bmatrix} \boldsymbol{\eta} \\ \mathbf{v}_1 \end{bmatrix} = \mathbf{A}_m \mathbf{x} + \mathbf{G}_m \mathbf{w} \quad (6.10)$$

The covariance matrix of estimation error:

$$\mathbf{P} = \begin{bmatrix} \mathbf{E} [\tilde{\mathbf{x}} \tilde{\mathbf{x}}^T] & \mathbf{E} [\tilde{\mathbf{x}} \mathbf{v}^T] \\ \mathbf{E} [\mathbf{v} \tilde{\mathbf{x}}^T] & \mathbf{E} [\mathbf{v} \mathbf{v}^T] \end{bmatrix} \quad (6.11)$$

The covariance propagation equation:

$$\dot{\mathbf{P}} = \mathbf{A}_m \mathbf{P} + \mathbf{P} \mathbf{A}_m^T + \mathbf{G}_m \boldsymbol{\Phi} \mathbf{G}_m^T \quad (6.12)$$

where $\Phi = \text{diag}(Q, R)$.

Assuming that the original process is ergodic, the steady state Lyapunov equation can be solved for a fixed matrix H^* .

Let the cost function:

$$J = \text{trace} (E [x x^T]) = \text{trace} (M P M^T) \quad (6.13)$$

where M is the $n \times (n+m)$ matrix with $n \times n$ identity matrix and the remain is zero. To get the optimal gain H^* that minimizes the chosen cost function, the solution of Lyapunov equation should be obtained iteratively.

6.3 1st Order System Example

In this section, the former example of Misawa [Misawa, 1988] is summarized. Let us consider the first-order system with the correlated measurement noise that can be modeled as a first-order Gauss-Markov Process:

$$\dot{z} = -az + w$$

$$y = z + v$$

$$\tau \dot{v} = -v + v_1$$

where $Q = q^2 = E [w w^T] = 1.0$, $R = r^2 = E [v_1 v_1^T] = 0.01$, $a = 1$, $\tau = 0.05$

The Kalman filter is optimal in the least-square sense:

$$\hat{z} = -a \hat{z} + h (y - \hat{z})$$

Assuming the measurement noise v is white, we get the constant Kalman filter gain by using a standard CACSD software.

$$h = 9.05 \Rightarrow \text{KF1}$$

For the colored noise case, the covariance error propagation equation (6.12) should be solved to get the optimal gain H^* . The first step in the

design process would be to get the statistical steady state variance of estimation error. For the 1st order system, it can be solved explicitly.

$$P_x = E[x^2] = \frac{q^2 [(a+h)\tau + 1] + h^2 r^2}{2(a+h)[(a+h)\tau + 1]}$$

To find the gain h that will minimize P_x :

$$\begin{aligned} \frac{\partial P_x}{\partial h} &= 0 \\ \Rightarrow h^* &= \frac{(1+at)(tq^2 - a^2 r^2 \pm \sqrt{a^2 r^4 + q^2 r^2})}{r^2(2at+1) - q^2 r^2} = 17.356 \end{aligned}$$

For a first-order system, the sliding observer is

$$\hat{z} = -a\hat{z} + k \text{sign}(y - \hat{z})$$

where the linear gain term of equation (6.2) is already stable so that no more terms need to guarantee the stability. Because the optimal gain h^* is known, we can proceed to compute the gain for the sliding observer. For this case, the covariance of estimation error and noise are

$$P_x = E[x^2] = 0.07$$

$$P_v = \frac{r^2}{2t} = 0.1$$

The covariance of $E[\tilde{y}^2]$ is

$$\begin{aligned} \sigma_y^2 &= E[\tilde{y}^2] = E[(x + v)^2] \\ &= E[x^2] + 2E[xv] + E[v^2] \\ &= 0.07 - 0.0904 + 0.1 = 0.0796 \\ \sigma_y &= 0.282 \end{aligned}$$

With this input statistics, the gain k for the sliding observer is

$$h^* = \sqrt{\frac{2}{\pi}} \frac{k}{\sigma_y}$$

$$k_{so} = h^* \sigma_y \sqrt{\frac{\pi}{2}} = 6.13$$

Using RIDF, the steady state covariance of the sliding observer for the 1st order example is

$$\sigma_y^2 = \frac{1}{2 \left(a + \sqrt{\frac{2}{\pi}} \frac{k}{\sigma_y} \right)} \left[\frac{\left(a^2 - \frac{1}{\tau^2} \right) \frac{r^2}{\tau}}{a + \frac{1}{\tau} + \sqrt{\frac{2}{\pi}} \frac{k}{\sigma_y}} + q^2 + \frac{r^2}{\tau^2} \right]$$

$$P_{so} = E[x^2] = \sigma_y^2 + \left(1 - 2 \frac{a + \frac{1}{\tau}}{a + \frac{1}{\tau} + \sqrt{\frac{2}{\pi}} \frac{k}{\sigma_y}} \right) \frac{r^2}{2\tau}$$

The above implicit equation for the output error covariance can be solved numerically.

6.4 2nd Order System Example

To extend the first order system to the second order system, consider a simple second-order system, with correlated measurement noise that can be modeled as a second-order Gauss-Markov Process:

$$\begin{aligned} \dot{z}_1 &= z_2 \\ \dot{z}_2 &= -a_1 z_1 - a_2 z_2 + w \\ y &= z_1 + v \\ \tau \dot{v} &= -v + v_1 \end{aligned}$$

where $Q = q^2 = E[w w^T] = 1.0$, $R = r^2 = E[v_1 v_1^T] = 0.01$, $a = 1$, $\tau = 0.05$

The Kalman filter is optimal in the least-square sense and has the form:

$$\hat{\dot{z}} = -a \hat{z} + h (y - \hat{z})$$

where $z = [z_1 \ z_2]^T$. Assuming the measurement noise v is white, we get the constant Kalman filter gain by using a standard CACSD software.

$$H = \begin{bmatrix} 2.7010 \\ 3.6478 \end{bmatrix} \Rightarrow \text{KF1}$$

For the colored noise case, the covariance error propagation equation (6.12) should be solved to get the optimal gain H^* . The first step in the design process would be to get the statistical steady state variance of estimation error. For the 2nd order system, it may be convenient to solve numerically. To find the optimal gain matrix H^* that will minimize the trace of estimation error covariance matrix, the Lyapunov equation is solved iteratively. The covariance equation (6.12) is solved for the steady state by using MATLAB with the matrices:

$$A_m = \begin{bmatrix} -h_1 & 1 & -h_1 \\ a_1 - h_2 & a_2 & -h_2 \\ 0 & 0 & E \end{bmatrix}$$

$$G_m = \begin{bmatrix} D & 0 \\ 0 & F \end{bmatrix} = \begin{bmatrix} 0 & 0 \\ 1 & 0 \\ 0 & F \end{bmatrix} \text{ and } \Phi = \begin{bmatrix} Q & 0 \\ 0 & R \end{bmatrix}$$

One can see the matrix A_m is a function of h_1 and h_2 that is to be solved. The Gain matrix H^* is

$$H^* = \begin{bmatrix} 3.1790 \\ 4.5289 \end{bmatrix} \Rightarrow \text{KF2}$$

For a second-order system, the sliding observer is

$$\hat{\dot{z}} = -a \hat{z} + k \text{sign}(y - \hat{z})$$

where $z = [z_1 \ z_2]^T$ and the linear gain term of equation (6.2) is not need to

guarantee the stability. Because the optimal gain H^* is known, we proceed to compute the gain for the sliding observer. For this case, the covariance of $E[\tilde{y}^2]$ is calculated from the solution of the steady state Lyapunov equation. With this input statistics, $\sigma_y = 0.3102$, the gain K for the sliding observer is

$$K = \begin{bmatrix} 1.2360 \\ 1.7609 \end{bmatrix} \Rightarrow \text{SO}$$

6.5 Prediction and Simulation

6.5.1 Effect of Measurement Noise

In order to test the performance robustness of the sliding observer, the effect of deviation of measurement noise intensity from the nominal value is investigated. When the noise intensities are the ones considered in the design process, the Kalman filter should be the optimal one for a linear system. In this case, the noise is assumed to be colored noise as the equation (6.7) so that the Kalman filter KF1 is not the optimal one and the Kalman filter KF2 is the optimal one at the nominal point.

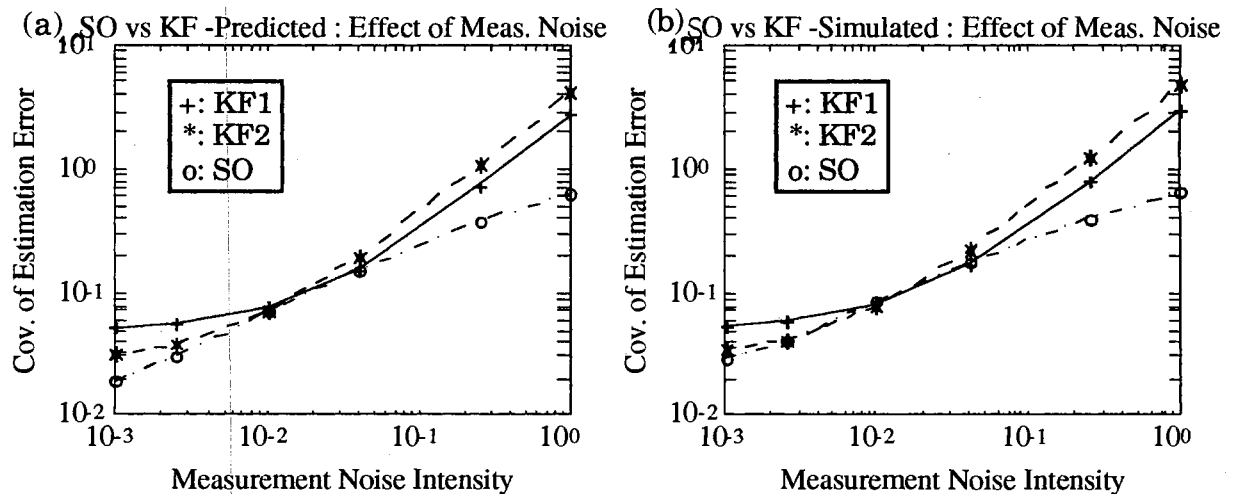


Figure 6.1 Effect of measurement noise: SO vs. KF (for the 1st order system)

a) Prediction

b) Simulated results

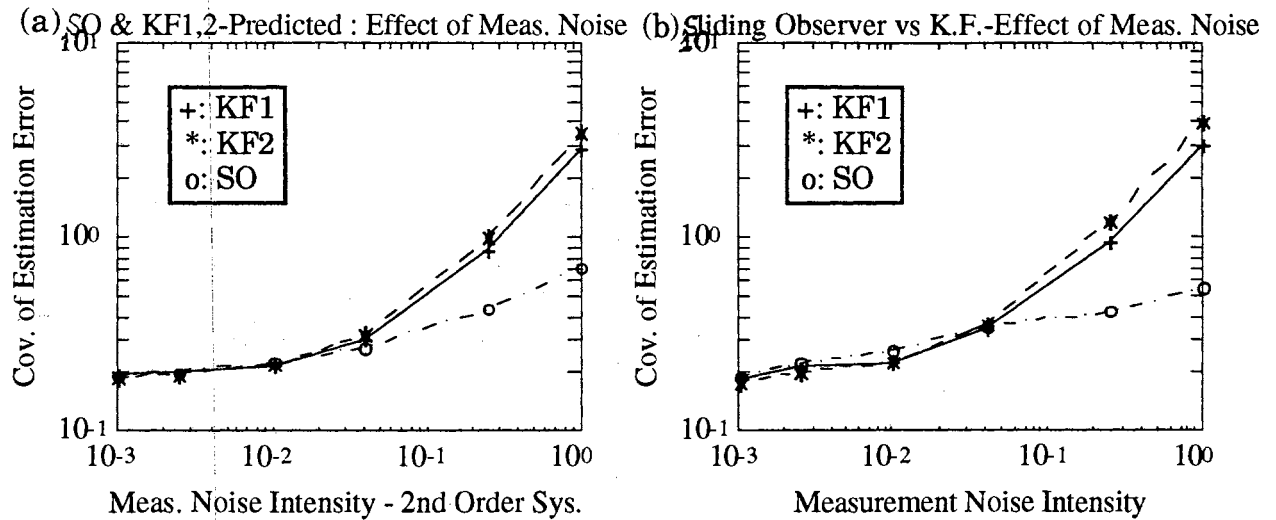


Figure 6.2 Effect of measurement noise: SO vs. KF (for the 2nd order system)

a) Prediction b) Simulated results

The predictions for 1st and 2nd order case are plotted in Figure 6.1 (a) and Figure 6.2 (a) and the Monte Carlo simulation that is the mean of the time averages over 100 simulations are shown in Figure 6.1 (b) and Figure 6.2 (b). Clearly, at the nominal point, the KF2 is the optimal one, seen both from the predicted values and from the values of simulation. The prediction of the SO at nominal point coincides with the KF2 for both cases. When the measurement noise intensity deviates from the nominal condition, the inherent robustness of the SO with respect to changes in the measurement noise becomes evident for both cases. In prediction results, for all values of measurement noise intensities are different from the nominal value, the sliding observer is the best one. On the contrary, the simulation shows the 1st order SO is best for all values, but the 2nd order SO is not best. Even though the 2nd order SO is not best for all values, it apparently shows robustness against the variation of measurement noise.

This result is due to the fact that the sign function has an inherent adaptive-type of behavior with respect to changes in the measurement noise. This fact can be clearly observed if one recalls the definition of RIDF for the sign function:

$$\text{sign}(\tilde{y}) = \sqrt{\frac{2}{\pi}} \frac{1}{\sigma_{\tilde{y}}}$$

Since $\sigma_{\tilde{y}}$ is directly affected by the changes in the measurement noise, one can see that the increased noise reflects as a virtual decrease in the measurement noise intensity is reflected as virtual increase in the filter gain. This behavior is exactly the desired from an adaptive filter in order to maintain a good performance for a wide range of changes in the measurement noise intensity.

6.5.2 Effect of Process Noise

The robustness about the change of process noise was investigated. The predicted results for 1st and 2nd order systems are shown in Figure 6.3 (a) and Figure 6.4 (a). The Monte Carlo simulation that is the averaging the time averages of 10 seconds over 100 simulations are shown in Figure 6.3 (b) and Figure 6.4 (b).

In this case, the sliding observer is not profitable. For both prediction and simulation, the KF1 shows good robustness for smaller intensities and the KF2 shows a good robustness for larger intensities; it is probably due to the fact that for large process noise intensity a larger filter gain is required so that suitable corrections are provided to the filter.

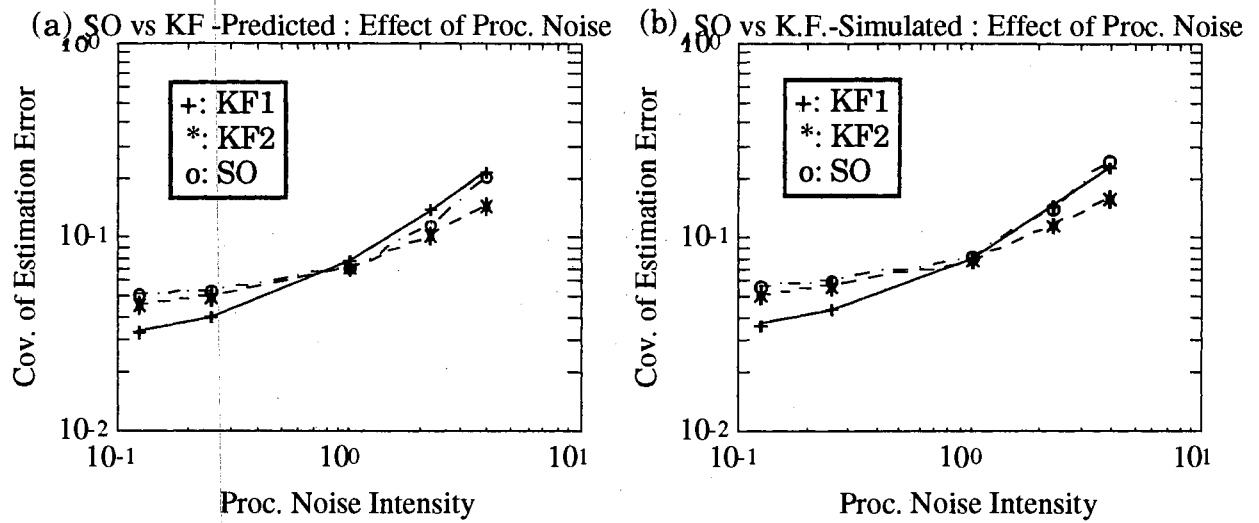


Figure 6.3 Effect of process noise: SO vs. KF (for the 1st order system)

a) Prediction b) Simulated results

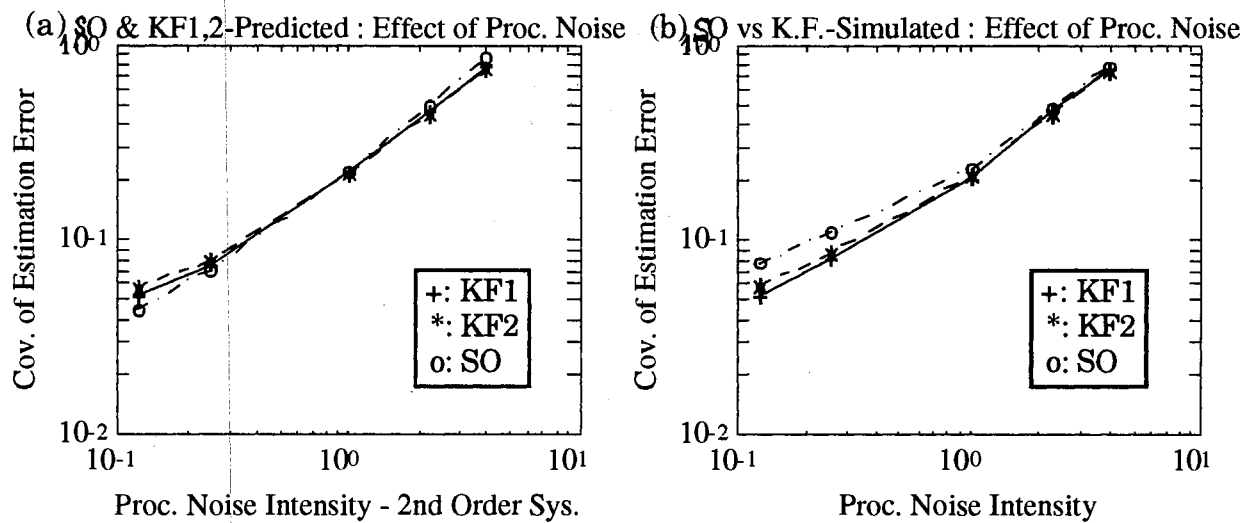


Figure 6.4 Effect of process noise: SO vs. KF (for the 2nd order system)

a) Prediction b) Simulated results

6.5.3 Effect of Parametric Mismatch

System Equations:

$$\dot{z} = A z + w$$

$$y = C x + v$$

$$\hat{\dot{z}} = A^\circ \hat{z} + H (y - C \hat{z})$$

$$= A^\circ \hat{z} + H (C (z - \hat{z}) + v)$$

The error dynamics:

$$\dot{\tilde{x}} = (A - H C) \tilde{x} - H v + \tilde{A} \hat{z} + w$$

where $\tilde{A} = A - A^\circ$, A° is nominal value and A is a actual value.

The estimation error covariance matrix is

$$P = \begin{bmatrix} E[x x^T] & E[x v^T] & E[x \hat{z}^T] \\ E[v x^T] & E[v v^T] & E[v \hat{z}^T] \\ E[\hat{z} x^T] & E[\hat{z} v^T] & E[\hat{z} \hat{z}^T] \end{bmatrix}$$

It can be propagated as:

$$\dot{P} = A_p P + P A_p^T + G_p \Phi G_p^T$$

$$\text{where } A_p = \begin{bmatrix} A - H C & -H & \tilde{A} \\ 0 & E & 0 \\ H C & H & A^\circ \end{bmatrix} \quad \text{and } G_p = \begin{bmatrix} D & 0 \\ 0 & F \\ 0 & 0 \end{bmatrix}$$

The steady state error covariance P is obtained by solving the Lyapunov equation with \dot{P} set to zero. For 2nd order system, the matrix A_p is a 5 x 5 matrix and a function of H with given parameter A . The optimal solution of Lyapunov equation can be solved numerically, for example, by the steep decent method. The remain procedure for prediction is the same as the previous cases.

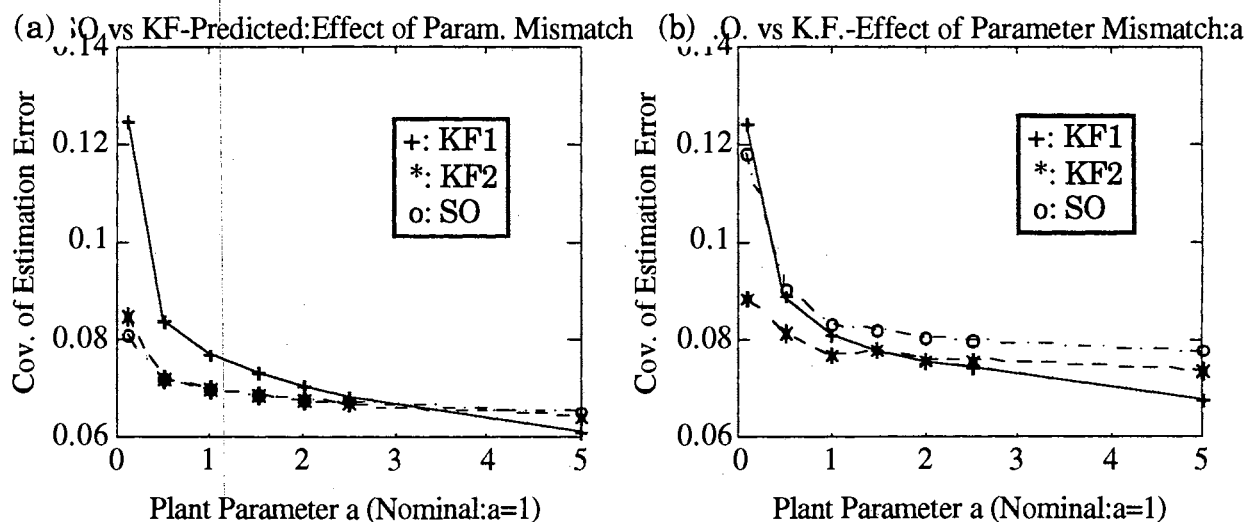


Figure 6.5 Effect of parameter mismatch: SO vs. KF

(for the 1st order system)

a) Prediction b) Simulated results

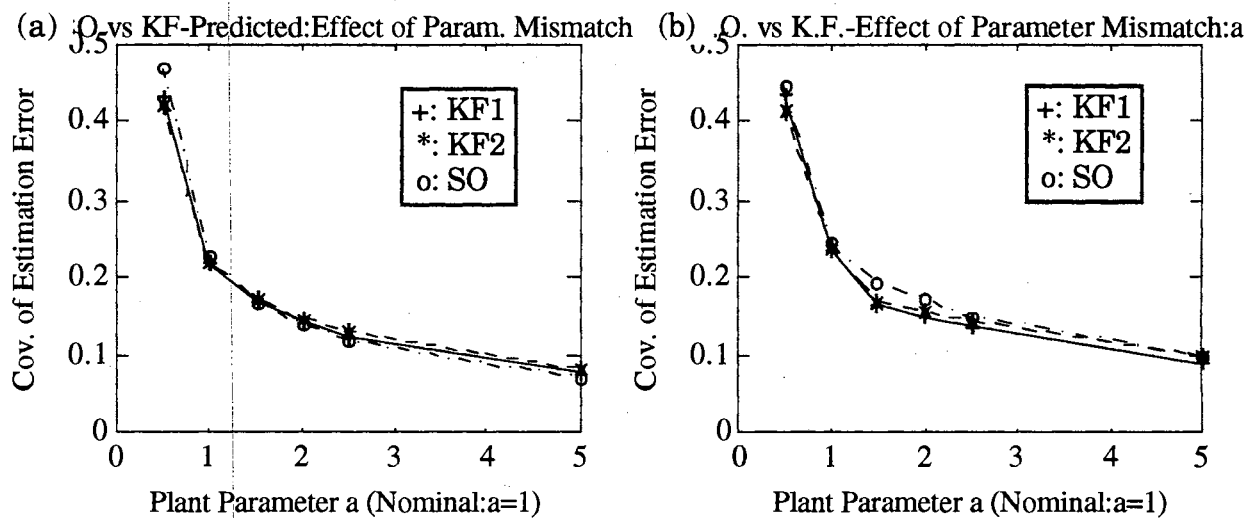


Figure 6.6 Effect of parameter mismatch: SO vs. KF

(for the 2-order system)

a) Prediction b) Simulated results

The results are shown in Figure 6.5 (a) and Figure 6.6 (a) for prediction and in Figure 6.5 (b) and Figure 6.6 (b) for simulation. Theoretically, the sliding observer shows good robustness for larger parameter mismatch but the actual simulation is not the best one. For values if actual A much smaller than the nominal value, the KF2 is the best one and for values if actual A much larger than the nominal value, the KF1 is the best one. This can be explained as the same way as the previous analysis. For small parameter one wants to increase filter gain in order to have a suitable filter, and for large parameter case vice versa.

CHAPTER VII

CONCLUSION AND FUTURE RESEARCH

7.1 Summary and Conclusion

7.1.1 Thesis Summary

The thesis has approached to the stability of the sliding observer based on the differential geometry of the problem. The coordinate transformation enabled to apply the linear system theorem to the stability Theorem of the sliding observer. A semi-analytic design algorithm was suggested according to the stability theorem. The designed sliding observer was compared with other nonlinear observers for several applications.

In Chapter 1, the robust feature and the solution definition of switching system was introduced. A literature survey on robust and practical nonlinear observers were performed.

In Chapter 2, fundamentals of the sliding observer was investigated and explained systematically on the robust features. The analysis includes the solutions and dynamics of switching system. Emphasis are on the derivation of the coordinate transformation.

In Chapter 3, a algebraic stability condition was derived by the worst case analysis for the 2nd order switching system. It is shown that the worst direction of general order of system can be searched by numerical search method. For practical purposes, an approximate worst direction

method is suggested. The worst case analysis is generalized for the stability analysis of the sliding observer by introducing the Lyapunov-like function. The general shearing effect is explained by the contour of Lyapunov-like function.

In Chapter 4, a design algorithm "Sliding Observer design by worst reaching dynamics for Nonlinear/uncertain system" (SOON) was proposed based on the stability theorems. The sliding observer was designed for 4 practical applications and compared with other current nonlinear observers. The advantages and superior performance of the new design methodology was demonstrated via a simulation. Besides utilizing the linear system theory via the coordinate transformation, the new design algorithm also guarantees stability with known bound of uncertainty and the initial states.

In Chapter 5, the sliding observer for multiple measurement, as a practical example, has been designed and combined with a controller for a two-link robot system. The cases with and without parameter uncertainty were implemented and simulated in the digital computer. In this case the sliding observer and controller were designed independently without examining the separation principle.

In Chapter 6, the performance robustness of the sliding observer, with noises and parameter uncertainty, was analyzed by theoretical prediction and numerical simulation as an extension of Misawa's method. To quasi-linearize the error dynamics, a Random Input Describing Function was used as a statistical linearization method. The measurement noise was assumed colored and the process noise was assumed as white gaussian noise. As the results, the sliding observer was designed and analyzed for the 1st and 2nd order Gauss-Markov process.

7.1.2 Conclusion

Most nonlinear observer methods have their own positive aspects, either as extensions of linear techniques or as novel nonlinear techniques, a dual technique of the variable structure control, for instance. A common drawback to the previous nonlinear observer is that the exact nonlinearities of the system must be modeled, either directly or indirectly, into the dynamics of the observer. On the contrary, the sliding observer requires only bounds of uncertainties and nonlinearities of the system in the phase variable canonical form. Furthermore, it guarantees stability with the bounded initial condition, and it can be easily implemented using a microprocessor.

The recent adaptive robust observer of Walcott et al. requires necessarily the matching condition which is difficult to be satisfied practically. On the contrary, the sliding observer can be designed without satisfying the matching condition. The same matching condition was derived by an entirely different way, i.e., the Alimov's transformation (see Appendix B.4 [Alimov, 1960]). One should notice that the design method by passivity theorem (see Appendix B.3 [Misawa, 1988]) also arrived at the same condition. On the contrary, the new stability analysis adopted the linear system theory (i.e., reaching dynamics) so that the conservativeness of the matching condition or strictly negative definite of Lyapunov theorem can be replaced by the strictly decreasing Lyapunov-like function sequence of the passing points. Even though a system has multiple measurements and its states are coupled in the canonical form, the sliding observer can be designed. In this case, the sliding observer error dynamics are decoupled for each measurement.

A new design algorithm "SOON" is proposed according to the stability theorems. Usually by following the design procedure SOON, one can design

the sliding observer converge directly to the sliding patch. If the observer requirement is not satisfied by the above design procedure SOON, then it can be improved by allowing the solution point pass through the hyperplane in the worst case.

In the numerical examples, it was shown that the new sliding observer effectively adopted to the bounded parameter uncertainty, such as the dry friction and inaccuracies of the system model.

7.2 Future Research

7.2.1 Design Algorithm by Lyapunov-like Stability

If the observer requirement is not satisfied by the direct converging design procedures (SOON) then it can be improved by allowing the solution point pass through the hyperplane in the worst case. According to Theorem 3.3, if the final Lyapunov-like function $V_{s^*}^f(\sigma(\tau_{i+1}))$ is strictly less than the precedent final Lyapunov-like function $V_s^f(\sigma(\tau_i))$, then the sliding observer is stable. The equation (3.67) is

$$V_{s^*}^f(\sigma(\tau_{i+1})) - V_s^f(\sigma(\tau_i)) < -\rho \|\sigma(\tau_i)\|^2 \quad (7.1)$$

where the subscripts s and s^* have different signs: $\text{sign}(s) \neq \text{sign}(s^*)$.

If there is no passing at the hyperplane by the direct converge design procedure then we do not need to consider the passing jump. On the contrary, if the solution point passes through the sliding patch then not only should the equation (3.67) be satisfied but also the passing jump of the worst trajectory should be negative in the design procedure based on Theorem 3.3.

In Figure 7.1, even though the passing jump J_1 was already considered in the equation (3.67), the next passing jump J_2 should be negative because

the positive jump by the worst passing point can make the error dynamics unstable.

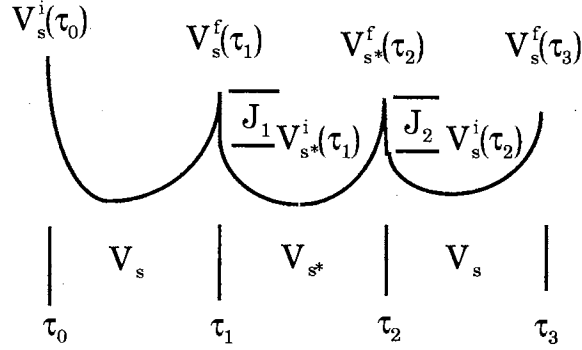


Figure 7.1 Lyapunov-like function and the passing jump

The difference of Lyapunov-like function between the passing points is

$$\begin{aligned}
 J(\tau_j)_{(x_2 > k_1)} &= V_+^i(\tau_j) - V_-^f(\tau_j) \\
 &= -4 K_s^T P x \\
 &= -4 [0 \ k_1 \ \dots \ k_{n-1}] P \begin{bmatrix} 0 \\ x_2 \\ \vdots \\ x_n \end{bmatrix}
 \end{aligned}$$

In Figure 7.1, even though the passing jump J_1 was already considered in the equation (3.67), the next passing jump J_2 should be negative because the positive jump by the worst passing point can make the error dynamics unstable.

If the sign of the passing state is unity then the passing jump is always negative as shown in Appendix A. However, the sign equalization property is hard to prove analytically as is shown in Appendix C. Hence it is reasonable to search the worst case numerically.

will be computed. In the first design procedure, one might tune the design constants K and H already. However, since the available linear correction constant H is practically limited by noise, the available accuracy by the first design method is also limited. With this proper constant H , one can increase the accuracy by allowing the solution point pass through the hyperplane. The suggested design procedure based on the Lyapunov-like stability Theorem is as follows:

7.2.3 Design procedure Based on the Lyapunov-like Stability Theorem

1. Data:

- The maximum bound of the disturbance w
- The worst bound of the initial states
- The linear correction constant H

2. Choose the switching constant K according to the desired observer accuracy.

- For a n _th order case, the suggested coefficient K is

$$\frac{\sqrt{P_{22}}}{\sqrt{P_{33}}} \approx \frac{k_1}{k_2}, \frac{\sqrt{P_{33}}}{\sqrt{P_{44}}} \approx \frac{k_2}{k_3}, \dots, \frac{\sqrt{P_{n-1}}}{\sqrt{P_n}} \approx \frac{k_n}{k_{n-1}}$$

- Check sliding dynamics eigenvalues equation (2.24)
- Check steady state error equation (2.54) in the sliding region

3. Simulate SIMNON program Reaching

- Searching the worst Lyapunov-like function

4. Tuning the design constants K

- If equation (4.7) is satisfied and the jump is negative

then one can increase accuracy by choosing smaller K

- If equation (4.7) is not satisfied or the jump is positive
then one should decrease accuracy by choosing larger K

7.2.4 Design Algorithm for Noisy Measurement

The performance robustness of the sliding observer, with noises and parameter uncertainty, was analyzed by the theoretical prediction and the numerical simulation in Chapter 6. In order to quasi-linearize the error dynamics, a Random Input Describing Function was used as a statistical linearization method. However, the noise characteristics may change according to the variation of the operating condition. In this case, it is necessary to adjust the filter according to the varying noise characteristics: the solution of this problem is usually sought in a class of adaptive systems in which the noise intensities are estimated in one way or another. However, such adaptive systems may be complicated and require more computational power. Furthermore, in a situation in which over long time intervals, the system do not need any adjustment, and the adaptive part of the filter will be idle.

For the practical purpose, it is interesting to design a filter which would obtain a suboptimal estimation error, but it is insensitive to inexact noise intensity.

7.2.5 Using Nonlinear Terms in the Observer

As shown in Chapter 4 and Chapter 5, the nonlinear model sliding observer improves the accuracy of estimation. Therefore, as far as the computational power is allowed, it is preferred to include the proper nonlinear terms in the observer structure. But, if the state estimation error is large,

for example, the initial condition is mismatched, the nonlinear term possibly induces a negative effect [Misawa, 1988].

It is difficult to set up a general rule in using the nonlinear terms. Hence, for the practical purpose, it can be studied as case studies, the estimators for the robot systems in the chapter 5, for instance.

A comparative study between nonlinear models and simple linear models is needed:

- Convergence speed and computational load
- Develop a computational index to compare computational burdens of different nonlinear observers.

This study should be useful as a design criteria.

BIBLIOGRAPHY

- Alimov, Y. I., "Lyapunov Functions for Relay Control Systems", *Automation and Remote Control*, Vol. 21, No. 6, pp. 500-506, Dec. 1960.
- Alimov, Y. I., "On the Application of Lyapunov's Direct Method to Differential Equations with Ambiguous Right Sides", *Automation and Remote Control*, Vol. 22, No. 7, pp. 713-725, Dec. 1961.
- Ambrosino, G., Celentano, G. and Garofalo, F., "Variable Structure Model Reference Adaptive Control Systems", *Int. J. of Control*, Vol. 39, No. 6, pp. 1339-1349, 1984.
- Anderson, B. D. O., Bitmead, R. R., Johnson, C. R. J., Kokotovic, P. V. and Kosut, R. L., *Stability of Adaptive Systems: Passivity and Averaging Analysis*, MIT Press, Cambridge, Mass, 1986.
- Anulova, S. V., "Random Disturbances of the Operation of Control Systems in the Sliding Mode", *Automation and Remote Control*, Vol. pp. April 1986.
- Arie, T., "An Adaptive Steering System for a Ship", *IEEE Control System Magazine*, Vol. 6, pp. 3-8, Oct. 1986.
- Asada, H. and Slotine, J. J. E., *Robust Analysis and Control*, John Wiley and Sons, 1986.
- Astrom, K. J., *Introduction to Stochastic Control Theory*, Academic Press, 1970.
- Athans, M., Kapasouris, P., Kappos, E. and III, H. A. S., "Linear-Quadratic Gaussian with Loop-Transfer Recovery Methodology for the F-100 Engine", *J. Guidance*, Vol. 9, No. 1, pp. 45-52, Jan.-Feb. 1986.
- Banks, S. P., "A note on Non-linear Observers", *Int. J. Control*, Vol. 34, No. 1, pp. 185-190, 1981.
- Baumann, W. T. and Rugh, W. J., "Feedback Control of Nonlinear Systems by Extended Linearization", *IEEE Trans. Automatic Control*, Vol. AC-31, No. 1, pp. Jan. 1986.
- Beaman, J. J., "Non-linear Quadratic Gaussian Control", *Int. J. of Control*, Vol. 39, No. 2, pp. 343-361, 1984.

- Bellgardt, K., Kuhlmann, W. and Meyer, H., "Application of an Extended Kalman Filter for State Estimation of a Yeast Fermentation", *Control Theory and Application*, Vol. 133, pp. 226-34, Sept. 1986.
- Bestle, D. and Zeitz, M., "Canonical form Observer Design for Nonlinear Time-variable Systems", *Int. J. Control*, Vol. 38, No. 2, pp. 419-431, 1983.
- Bockman, S. F., "Lyapunov Exponents for Systems Described by Differential Equations with Discontinuous Right-Hand Sides", *ACC*, Boston, MA, pp. 1673-1678, 1991.
- Brockett, R. W. and Byrnes, C. I., "Multivariable Nyquist Criteria, Root Loci, And Pole Placement: A Geometric Viewpoint", *IEEE Trans. on Autom. Contr.*, Vol. AC-26, No. 1, pp. 271-284, Feb. 1981.
- Brogliato, B., Landau, I.-D. and Lozano-Leal, R., "Adaptive Motion Control of Robot Manipulators: A Unified Approach Based on Passivity", *ACC*, San Diego, CA, pp. 2259-2264, 1990.
- Chang, L.-W., "A versatile Sliding Control with a Second-Order Sliding Condition", *ACC*, Boston, MA, pp. 54-55, 1991.
- Chen, Y. H., "On the Robustness of Mismatched Uncertain Dynamical Systems", *J. of Dynamic Systems, Measurement and Control*, Vol. 109, pp. 29-35, March 1987.
- Chen, Y. H., "Large-Scale Uncertain System Under Insufficient Decentralized Controllers", *J. of Dynamic Systems, Measurement and Control*, Vol. 111, pp. 359-63, Sept. 1989.
- Chen, Y. H., "Adaptive Robust Observers for Nonlinear Uncertain Systems", *Int. J. of Systems Science*, Vol. 21, No. 5, pp. 803-814, May 1990a.
- Chen, Y. H., "State Estimation for Nonlinear Uncertain Systems: A Design based on Properties Related to the Uncertainty Bound", *Int. J. Control*, Vol. 52, No. 5, pp. 1131-1146, 1990b.
- Chen, Y. H. and Hsu, C., "Structural Decomposition Approach for the Stability of Uncertain Dynamic Systems", *J. of Applied Mechanics*, Vol. 55, pp. 992-4, Dec. 1988.
- Chen, Y. H. and Tomizuka, M., "Design of Adaptive Observer for Plant Under Input Disturbance and Measurement Noise", *Int. J. of Control*, Vol. 47, pp. 625-632, 1988.
- Chiang, R. Y. and Safonov, M. G., "Design of H_∞ Controller for a Lightly Damped System using a Bilinear Pole Shifting Transform", *ACC*,

- Boston, MA, pp. 1927-1928, 1991.
- Choi, B.-O. and Krishnamurthy, K., "Position and Force Control of Flexible Robotic Manipulators Using the LQG/LTR Design Methodology", *ACC*, Boston, MA, pp. 1913-1914, 1991.
- Craig, J. J., Hsu, P. and Sastry, S., "Adaptive Control of Mechanical Manipulators", *IEEE Int. Conf. Robotics Automat.*, San Francisco, CA, pp. 1986.
- Cristi, R., Healey, A. J. and Papoulias, F., "Dynamic Output Feedback by Robust Observer and Variable Structure Control", *ACC*, San Diego, CA, pp. 2649-2653, 1990.
- DeCarlo, R. A., Zak, S. H. and Mathews, G. P., "Variable Structure Control of Nonlinear Multi Variable Systems: A Tutorial", *Proceeding of the IEEE*, 212-231, 1988.
- Desoer, C. A. and Vidyasagar, M., *Feedback Systems: Input-output Properties*, Academic Press, New York, NY, 1975.
- Doyle, J. C., "Analysis of Feedback Systems with Structured Uncertainties", *IEE Proc.*, Vol. 129, Pt. D, No. 6, pp. 242-250, Nov. 1982.
- Doyle, J. C., "Structured Uncertainty in Control System Design", *Proc. of 24th Conference on Decision and Control*, Ft. Lauderdale, FL, pp. 1985.
- Doyle, J. C. and Stein, G., "Robustness with Observer", *IEEE Trans. on Autom. Contr.*, Vol. AC-24, no. 4, pp. 607-611, Aug. 1979.
- Esfandiari, F. and Khalil, H. K., "Observer-based Control of Fully-Linearized Nonlinear Systems", *the 28th IEEE Conference on Decision and Control*, Tampa, FL, pp. 84-89, 1989.
- Filippov, A. F., "Differential Equations with Discontinuous Right Hand Sides", *Am. Math. Soc. Trans.*, Vol. 42, pp. 199-231, 1964.
- Filippov, A. F., *Differential equations with Discontinuous Righthand Sides*, Kluwer Academic Publishers, 1988.
- Friedland, B., *Control System Design*, McGraw-Hill, 1986.
- Frimm, F., Evaluation of Ship's Steering Characteristics - Full Scale and Model Test, Master Thesis, Escola Politecnica da Univeridade de Sao Paulo, 1983
- Gao, Z. and Antsaklis, P. J., "New Bounds on Parameter Uncertainties for Robust Stability", *ACC*, Boston, MA, pp. 879-880, 1991.

- Gelb, A., *Applied Optimal Estimation*, MIT. Press, Cambridge, M.A., 1974.
- Gelb, A. and Vandervelde, W. E., *Multiple-Input Describing Functions and Non-linear System Design*, McGraw-Hill Book Co., New York, 1968.
- Gharban, C. K. and Cory, B. J., "Nonlinear Dynamic Power System State Estimation", *IEEE Transactions on Power Systems*, Vol. 1, pp. 276-83, Aug. 1986.
- Gibson, J. E., *Nonlinear Automatic Control*, McGraw-Hill Inc., 1963.
- Glad, S. T., "On the Gain Margin of Nonlinear and Optimal Regulators", *Proc. of 21st Conf. on Decision & Control*, Orland, FL, pp. 957-962, 1982.
- Gopalswamy, S. and Hedrick, J. K., "Robust Adaptive Control of Multivariable Nonlinear Systems", *ACC*, San Diego, CA, pp. 2247-2252, 1990.
- Grossman, W., Khorrami, F. and Friedland, B., "An Observer-Based Design for Robust Control of Robot Manipulators", *ACC*, San Diego, CA, pp. 731-736, 1990.
- Grunberg, D. B., *A Methodology for Design Robust Multivariable Nonlinear Control Systems*, MIT, 1986.
- Habibi, S. R. and Richards, R. J., "Sliding Mode Control of an Electrically Powered Industrial Robot", *IEE Proc.-D*, Vol. 139, No. 2, pp. 207-226, March 1992.
- Hached, M., Esfahani, S. M. M. and Zak, S. H., "On the Stability and Estimation of Ultimate Boundedness of Nonlinear/Uncertain Dynamic Systems with Bounded Controllers", *ACC*, San Diego, CA, pp. 1180-1185, 1990.
- Haessig, D. A., Jr., "On the Modeling and Simulation of Friction", *ACC*, San Diego, CA, pp. 1256-1261, 1990.
- Hagedorn, P., *Non-Linear Oscillations*, Oxford University Press, Oxford, 1988.
- Hermann, R. and Krener, A. J., "Nonlinear Controllability and Observability", *IEEE Trans. on Autom. Contr.*, Vol. AC-22, No. 5, pp. 728-740, Oct. 1977.
- Holmes, P., "Dynamics of a Nonlinear Oscillator with Feedback Control I : Local Analysis", *J. of Dynamic Systems, Measurement, and Control*, Vol. 107, pp. 159-165, June 1985.
- Holten, L., Gjelsvik, A. and Asm, S., "Comparison of Different Methods for

- State Estimation", *IEEE Trans. on Power Systems*, Vol. 3, pp. 1798-804, Nov. 1988.
- Hori, N., Nikiforuk, P. N. and Kanai, K., "On the Improvement of on Adaptive Observer for Multi-output Systems", *IEE Proceedings. Part D., Control Theory and Applications*, Vol. 135, pp. 67-71, Jan. 1988.
- Hsia, T. C., "Adaptive Control of Robot Manipulators - A Review", *IEEE Int. Conf. on Robotics and Automation*, 1986.
- Hu, X., "A Note on Nonlinear State Observers", *ACC*, Boston, MA, pp. 717-718, 1991.
- Hunt, L. R., Su, R. and Meyer, G., "Global Transformation of Nonlinear Systems", *IEEE Trans. on Autom. Contr.*, Vol. AC-28, No. 1, pp. 24-30, Jan. 1983.
- Hunt, L. R. and Verma, M. S., "Observers and Controllers for Feedback Linearizable systems", *ACC*, Boston, MA, pp. 546-547, 1991.
- Itkis, V., *Control Systems of Variable Structure*, John-Wiley, 1976.
- Jang, S. S., B., J. and Mukai, H., "Comparison of Two Approaches to On-line Parameter and State Estimation of Nonlinear Systems", *Ind. & Eng. Chemistry Proc. Design and Development*, Vol. 25, pp. 809-14, July 1986.
- Jazwinski, A. H., *Stochastic Process and Filtering Theory*, Academic Press, New York, 1970.
- Kailath, T., *Linear Systems*, Prentice-Hall, Inc., Englewood Cliffs, NJ, 1980.
- Kalman, R. E., "A New Approach to Linear Filtering and Prediction Problems", *Trans. ASME (J. Basic Engineering)*, Vol. 82D, no. 1, pp. 35-45, March 1960.
- Kalman, R. E. and Bucy, R. S., "New Results in Linear Filtering and Prediction Theory", *Trans. ASME (J. of Basic Engineering)*, Vol. 83D, No. 1, pp. 95-108, March 1961.
- Kanellakopoulos, I. and Kokotovic, P. V., "Observer-based Adaptive Control of Nonlinear Systems Under Matching Conditions", *ACC*, San Diego, CA, pp. 549-555, 1991.
- Kantor, J. C., "Finite Demensional Nonlinear Observer for an Exothermic Stirred-Tank Reactor", *Chemical Eng. Science*, Vol. 44, No. 7, pp. 1503-1510, 1989.
- Kao, C. K. and Sinha, A., "Sliding Mode Control of Vibration in Flexible

- Structures Using Estimated States", *ACC*, Boston, MA, pp. 2467-2474, 1991.
- Kaplan, W., *Ordinary Differential Equations*, Addition-wesley, Reading, Massachusetts, 1958.
- Keller, H., "Nonlinear Observer Design by Transformation into a Generalized Observer Canonical Form", *Int. J. Control*, Vol. 46, No. 6, pp. 1915-1930, 1987.
- Kolmogorov, A. N. and Fomin, S. V., *Introductory Real Analysis*, Dover Publications, Inc., New York, NY, 1975.
- Kolodziej, E. and Mohler, R. R., "State Estimation and Control of Conditional Linear Systems", *SIAM J. on Cont. and Optimization*, Vol. 24, pp. 497-508, May 1986.
- Krener, A. J. and Isidori, A., "Linearization by Output Injection and Nonlinear Observer", *Systems & Control Letters*, Vol. 3, pp. 47-52, June 1983.
- Krener, A. J. and Respondek, W., "Nonlinear Observers with Linearizable Error dynamics", *SIAM J. of Control and Optimization*, Vol. 23, No. 2, pp. 197-216, Mar. 1985.
- Landau, Y. D., *Adaptive Control, The Model Reference Approach*, Marcel Decker Inc., New York, 1979.
- Li, C. W. and Tao, L. W., "Observing Nonlinear Time-variable Systems Through a Canonical Form Observer", *Int. J. Control*, Vol. 44, No. 6, pp. 1703-1713, 1986.
- Li, Y. and Lee, E. B., "A Synthesis Approach to Uncertain Systems with Parametric Uncertainties", *ACC*, Boston, MA, pp. 2718-2719, 1991.
- Ljung, L., *System Identification*, Prentice-Hall, Inc., 1987.
- Ljung, L. and Soderstrom, T., *Theory and Practice of Recursive Identification*, MIT Press, Cambridge, Mass., 1983.
- Luenberger, D. G., "An Introduction to Observer", *IEEE Trans. on Autom. Contr.*, Vol. AC-16, No. 6, pp. 596-602, Dec. 1971.
- Macfarlane, A. G. J. and Postlethwaite, I., "The Generalized nyquist Stability Criterion and Multivariable Root Loci", *Int. J. of Control*, Vol. 25, No. 1, pp. 81-127, 1977.
- Masmoudi, R. A. and Hedrick, J. K., "Estimation of Vehicle Shaft Torque Using Nonlinear Observers", *ASME Winter Annual Meeting*, 1987.

- Mendel, J. M., *Lessons in Digital Estimation Theory*, Prentice-Hall, Inc., 1987.
- Minamide, N., Nikiforuk, P. N. and Gupta, M. M., "Design of a Reduced-Order Adaptive Observer", *IEE Proceedings. Part D. Control Theory and Applications*, Vol. 133, pp. 133-6, May 1986.
- Misawa, E. A., *Nonlinear State Estimation Using Sliding Observers*, Massachusetts Institute of Technology, Ph.D. Thesis, 1988
- Misawa, E. A. and Hedrick, J. K., "Nonlinear Observers-A State-of-the-Art Survey", *Trans. of the ASME*, Vol. III, pp. 344, Sept. 1989.
- Misawa, E. A., Hedrick, J. K., Slotine, J.-J. E. and Verghese, G. C., "Sliding Observer Design for Nonlinear State Estimation", *IFAC Symposium on Nonlinear Control Systems Design*, Capri, Italy, pp. 1989.
- Moher, R. R. and Bugnon, J. F., "Nonlinear System Perspective and Guaranteed State Estimation", *IEEE Int. Sympo. on Circuits and Systems 1989, the 22nd ISCAS.*, 1989.
- Moose, R. L., Sistanizadeh, M. K. and Skagfjord, G., "Adaptive State Estimation for a System with Unknown Input and Measurement Bias", *IEEE J. of Ocean Eng.*, Vol. 12, pp. 222-7, Jan. 1987.
- Nandam, P. K. and Sen, P. C., "A Comparative Study of a Luenberger Observer and Adaptive Observer-based Variable Structure Speed Control System Using a Self-Controlled Synchronous Motor", *IEEE Transactions on Industrial Electronics*, Vol. 37, pp. 127-132, Apr. 1990.
- Narendra, K. S. and Taylor, J. H., *Frequency Domain Criteria for Absolute Stability*, Academic Press, New York, 1973.
- Nayfeh, A. H. and Mook, D. T., *Nonlinear Oscillations*, John Wiley & Sons, New York, 1979.
- Nicosia, S. and Tomei, P., "State Observation of Elastic Joint Robots", *Robot Control 1988(SYROCO 1988)-Selected papers from the 2nd IFAC Symposium*, 1988.
- Nicosia, S., Tomei, P. and Tornambe, A., "A Nonlinear Observer for Elastic Robots", *Unpublished*, Vol. pp. 1986.
- Nicosia, S., Tomei, P. and Tornambe, A., "Nonlinear Control and Observation Algorithms for a Single-link Flexible Robot Arm", *Int. J. of Control*, Vol. 49, pp. 829-840, Mar. 1989.
- Nicosia, S., Tomei, P. and Tornambe, A., "Observer-based Control Law for

- a Class of Nonlinear Systems", *Int. J. of Control*, Vol. 51, pp. 553-566, Mar 1990.
- Nicosia, S. N. and Tornambe, A., "High-gain Observers in the State and Parameter Estimation of Robots Having Elastic Joints", *Systems and Control Letters*, Vol. 13, pp. 331-337, Nov. 1989.
- Niemann, H. H. N., Stroustrup, J. and Sogaard-Andersen, P., "General Conditions for Loop Transfer Recovery", *ACC*, Boston, MA, pp. 333-334, 1991.
- Ortega, R. and Spong, M. W., "Adaptive Motion Control of Rigid Robots: A Tutorial", *IEEE CDC*, Austin, TX, pp. 1988.
- Ortega, R. and Yu, T., "Robustness of Direct Adaptive Controllers: A Survey", *10th IFAC World Conf.*, Munich, FRG, pp. 1986.
- Peleties, P. and Decarlo, R., "Asymptotic Stability of m-Switched Systems using Lyapunov-Like Functions", *ACC*, Boston, MA, pp. 1679-1684, 1991.
- Phaneuf, R. J., *Approximate Nonlinear Estimation*, Massachusetts Institute of Technology, 1968
- Phelps, A. R., "Computation of Nonlinear Observers", *the 28th IEEE Conference on Decision and Control*, Tampa, FL, pp. 1989.
- Pons, M. N. and Engasser, J. M., "Comparison Between Adaptive and Model-Based Extended Kalman Filters", *ACC*, 1989.
- Raghavan, S. and Hedrick, J. K., "Sliding Compensators for a Class of Nonlinear Systems", *ACC*, San Diego, CA, pp. 1174-1179, 1990.
- Schweppe, F. C., *Uncertain Dynamic Systems*, Prentice-Hall, Inc., Englewood Cliffs, NJ, 1973.
- Sethna, P. R., "Method of averaging for systems bounded for positive time", *J. Math. Anal. Appl.*, Vol. 41, pp. 621-631, 1973.
- Shaked, U., "H- ∞ Minimum Error State Estimation of Linear Stationary Processes", *IEEE Trans. on Auto. Contr.*, Vol. 35 No.5, pp. 554-558, May 1990.
- Shamma, J. S., "The Necessity of the Small-Gain Theorem for Time-Varying and Nonlinear Systems", *IEEE Trans. on Auto. Contr.*, Vol. 36, No. 10, pp. 1138-1147, Oct 1991.
- Shamma, J. S. and Dahleh, M. A., "Time-Varying Versus Time-Invariant Compensation for Rejection of Persistent Bounded Disturbances and Robust Stabilization", *IEEE Trans. Autom. Contr.*, Vol. 36, No. 7, pp.

838-847, July 1991.

Sims, C. S. and Wilson, D., "EXtended Optimality Properties of Reduced-Order Observers", *ACC*, Boston, MA, pp. 2823-2824, 1991.

Slotine, J. and Coetsee, J. A., "Adaptive Sliding Controller Synthesis for Nonlinear Systems", *Int. J. Control*, Vol. 43, pp. 1631-1651, 1986.

Slotine, J.-J., Hedrick, J. K. and Misawa, E. A., "On Sliding Observers for Nonlinear Systems", *J. of Dynamic Systems, Measurement, and Control*, Vol. 109, pp. 245, Sept. 1987.

Slotine, J.-J. and Li, W., *Applied Nonlinear Control*, Prentice-Hall, 1991.

Slotine, J.-J. E., "Sliding Controller Design for Nonlinear Systems", *Int. J. Control*, Vol. 40, No. 2, pp. 421-434, 1984.

Sobol, I. M., *The Monte Carlo Method*, Mir Publishers, Moscow, 1987.

Sorenson, H. W., *Kalman Filtering: Theory and Application*, IEEE Press, New York, NY, 1985.

Spong, M. W. and Ortega, R., "On Adaptive Inverse Dynamics Control of Rigid Robots", *IEEE trans. on Automatic Control*, Vol. 35 No. 1, pp. 92-95, Jan. 1990.

Spong, M. W. and Vidyasagar, M., "Robust Linear Compensator Design for Nonlinear Robotic Control", *IEEE J. Robotics Automat.*, Vol. RA-3, pp. 345-351, 1987.

Spong, M. W. and Vidyasagar, M., *Robot Dynamics and Control*, Wiley, New York, NY, 1989.

Stalford, H., "Stability Conditions for Nonlinear Control Processes Using Lyapunov Functions with Discontinuous Derivatives", *J. of Mathematical Analysis and Applications*, Vol. 84, pp. 356-371, 1981.

Steinberg, A. and Corless, M., "Output Feedback Stabilization of Uncertain Dynamical Systems", *IEEE Trans. on Autom. Cont.*, Vol. 30, No. 10, pp. 1025-1027, Oct 1985.

Stephenson, A., "On a new type of dynamical stability", *Mem. Proc. Manch. Lit. Phil. Soc.*, Vol. 52, pp. 1907-1908, 1908.

Svobodny, T. P., "Stability of Nonlinear Observers for Dissipative ODEs", *Int. J. of Control*, Vol. 50, No. 4, pp. 1235-1247, Oct. 1989.

Swiniarski, R., "Adaptive Observer Application to the Estimation of Nonlinear Biotechnological Processes", *Adaptive Control of Chemical*

Processes 1988(ADCHEM 1988) - Selected Papers from the 2nd Int. IFAC Symposium, 1988.

- Taylor, J. H., "Statistical Performance Analysis of Nonlinear Stochastic Systems by the Monte Carlo Method", *Mathematics and Computers in Simulation*, Vol. XXIII, pp. 21-33, 1981.
- Thau, F. E., "Observing the State of Nonlinear Dynamical Systems", *Int. J. Control*, Vol. 17, No.3, pp. 471-479, 1973.
- Tibken, B. and Hofer, E. P., "Systematic Observer Design for Bilinear Systems", *IEEE International symposium on Circuits and Systems, the 22nd ISCAS*, 1989.
- Tkachenko, V. Y., "Simulation of Dry Friction", *Automation and Remote Control*, Vol. 35, pp. March 1974.
- Tornambo, A., "Use of Asymtotic Observers Having-high-gain in the State and Parameter Estimation", *the 28th IEEE Conference on Decision and Control*, 1989.
- Tunali, E. T. and Tarn, T.-J., "New Results for Identifiability of Nonlinear Systems", *IEEE Trans. on Autom. Contr.*, Vol. AC-32, No. 2, pp. 146-154, Feb. 1987.
- Uosaki, K. and Koketsu, Y., "Optimal Robust Transformation for Nonlinear State Estimation", *Eighth IFAC/IFORS Symposium on Identification and System Parameter Estimation*, 1988.
- Utkin, V. I., "Survey Paper: Variable Structure Systems with Sliding Modes", *IEEE Trans. on Autom. Contr.*, Vol. AC-22, No. 2, pp. 212-222, April 1977.
- Utkin, V. I., *Sliding Modes and Their Application in Variable Structure System*, MIR Publishers, Moskow, 1978.
- Utkin, V. I., "Variable Structure Systems: Present and Future", *Automation and Remote Control*, Vol. 44, No. 9, pp. 1105-1120, Sept. 1984.
- Utkin, V. I. and Drakunov, S. V., "Stochastic Regularization of Systems with Discontinuous Controls", *Sov. Phys. Dokl.*, Vol. 28(10), pp. 835-837, Oct. 1983.
- Velichenko, V. V., "Optimal Control Problems for Equations with Discontinuous Right-Hand Sides", *Automation and Remote Control*, Vol. 27, No.7, pp. 1153-1163, July 1966.
- Walcott, B. and Zak, S. H., "Combined Observer-Controller Synthesis for Uncertain Dynamical Systems with Applications", *IEEE Trans. on*

- System, Man, and Cyber.*, Vol. 18 No. 1, pp. 88-104, 1988.
- Walcott, B. L., "Nonlinear Output Stabization of Uncertain Systems", *ACC*, San Diego, CA, pp. 2253-2258, 1990.
- Walcott, B. L., Corless, M. J. and S.H. Zak, "Comparative Study of Nonlinear State-Observation Techniques", *Int. J. Control*, Vol. 45, No. 6, pp. 2109-2132, 1987.
- Walcott, B. L. and Zak, S. H., "*Observation and Control of Nonlinear Uncertain Dynamical Systems: A Variable Structure Approach*", Purdue Univ., 1986a.
- Walcott, B. L. and Zak, S. H., "Observation of Dynamical Systems in the Presence of Bounded Nonlinearities/Uncertainties", *25th CDC*, Athens, Greece, pp. 1986b.
- Walcott, B. L. and Zak, S. H., "State Observation of Nonlinear Uncertain Dynamical Systems", *IEEE Trans. Autom. Cont.*, Vol. AC-32, pp. 166-170, 1987.
- Wishner, R. P., Tabaczynski, J. A. and M. Athans, "A Comparison of Three Non-Linear Filters", *Automatica, Pergamon Press*, Vol. 5, pp. 487-496, 1969.
- Wit, C. C. D. and Alvarez, Q., "Nonlinear Observer for Robots with Flexible Joints", ?, 1988.
- Wit, C. C. D. and Slotine, J.-J. E., "Sliding Observer for Robot Manipulators", *Automatica*, Vol. 27, No. 5, pp. 859-864, 1991.
- Xia, X.-H. and Gao, W.-B., "Nonlinear Observer Design by Observer Error Linearization", *SIAM J. Control and Optimization*, Vol. 27, NO. 1, pp. 199-216, Jan. 1989.
- Yaz, E. and Azemi, A., "Variable Structure Observers for Nonlinear Models with Unbounded Noise and Measurement Uncertainties", *ACC*, Boston, MA, pp. 43-48, 1991.
- Zak, S. H., Brehove, J. D. and Corless, M. J., "Control of Uncertain Systems with Unmodeled Actuator and Sensor Dynamics and Incomplete State Information", *IEEE Trans. on Systems, Man and Cybernetics*, Vol. 19, No. 2, pp. 241-257, Mar-Apr. 1989.
- Zak, S. H. and MacCarley, C. A., "State-Feedback Control of Non-linear Systems", *Int. J. Control*, Vol. 43, No. 5, pp. 1497-1514, 1986.
- Zeitz, M., "The Extended Luenberger Observer for Nonlinear Systems", *Systems & Control Letters*, Vol. 9, pp. 149-156, 1987.

- Zhao, X., Stalford, H. L. and Hanagud, S. V., "On the μ Control of Uncertain Manipulator Arms", *ACC*, Boston, MA, pp. 2051-2056, 1991.
- Zhu, W.-h., Chen, H.-t. and Zhang, Z.-j., "A Variable Structure Robot Control Algorithm with an Observer", *IEEE Trans. on Robotics and Automation*, Vol. 8 No. 4, pp. 486-492, Aug. 1992.

APPENDIX A

MATHEMATICAL BACKGROUND

A.1 Differential Equations with Discontinuous Right-Hand Sides

The evolution of the theory of differential equations with discontinuous right-hand sides has been to a great extent motivated by its many applications. The popular usage of the switching technique in automatic control systems leads to the necessity of fabricating an intricate theory. The technique of the variable structure system with sliding motions has been developed fundamentally in the literature from Russia [Utkin, 1984]. The basic properties are explored in this chapter.

Definitions of solution

The solutions of the differential equations with discontinuous right-hand sides are studied by cases. The usual definition of a solution for a continuous differential equation cannot apply directly to the discontinuous differential equations of which are discontinuous on an arbitrary smooth line or on a surface S .

i) For the first case, the definition of a solution for continuous differential equations can be applied to the case in which the solution point approach on the surface S and leave on the other side of the surface S . Here the solution passes through S and satisfies the equation everywhere except at the

intersection point at which the solution does not have a derivative.

ii) In the other case, a solution point approaches on both sides of a line or a hyperplane S , the usual definition is unsuitable because there is no clue of how a solution point that has reached on the hyperplane S may be continued. The solution of velocity field along a surface of discontinuous, i.e. the hyperplane (in this study $x_1=0$), can be determined by the Filippov' equivalent solution.

Consider the case in which the function $f(x)$ is discontinuous on a smooth surface S that is given by the equation $y = C x = 0$. The surface S separates its neighborhood in the state space into domains Ω_- and Ω_+ . As the trajectory ξ approaches the point $x \in S$ from the domains Ω_- and Ω_+ at a given time t . let the function $f(t, \xi)$ have the limiting values:

$$\lim_{\substack{\xi \in S^- \\ \xi \rightarrow S(x)}} f(t, \xi) = f(t, x), \quad \lim_{\substack{\xi \in S^+ \\ \xi \rightarrow S(x)}} f(t, \xi) = f^+(t, x) \quad (A.1)$$

Lemma 1.1. [Filippov, 1964] Let the regions Ω_+ and Ω_- in the space x_1, \dots, x_n be separated by a smooth surface S . Suppose that the vector function $f(t, x)$ is bounded and, for any time t , its limiting values $f(t, x)$ and $f^+(t, x)$ exist when the solution point is approaches from S_- and S_+ . Let f_N^- and f_N^+ be the projections of the vectors f and f^+ on the normal to the surface S directed from S_- and S_+ . Let the vector function $x(t)$ be absolutely continuous. For $t_1 \leq t \leq t_2$, let assume $x(t) \in S$, $f_N^-(t, x) \geq 0$, $f_N^+(t, x) \leq 0$, $f_N^-(t, x) - f_N^+(t, x) > 0$. In order for $x(t)$ to be a solution of (A.1), it is necessary and sufficient that for almost all $t \in [t_1, t_2]$

$$\dot{x} = f^0(t, x), \quad f^0 \equiv \alpha f^+ + (1-\alpha) f \quad (A.2)$$

$$\text{where, } \alpha \equiv \frac{f_N^-}{f_N^- - f_N^+} \quad (A.3)$$

Proof) See Filippov pp.206.

Remark) If f and f^+ are continuous with respect to (t, x) , $x \in S$, then equation (A.2) holds for all $t \in (t_1, t_2)$. It is easy to see that the value of \dot{x} for a solution is lying on the hyperplane.

Following Figure A.1 are examples of hyperplane $H = x_1 = 0$.

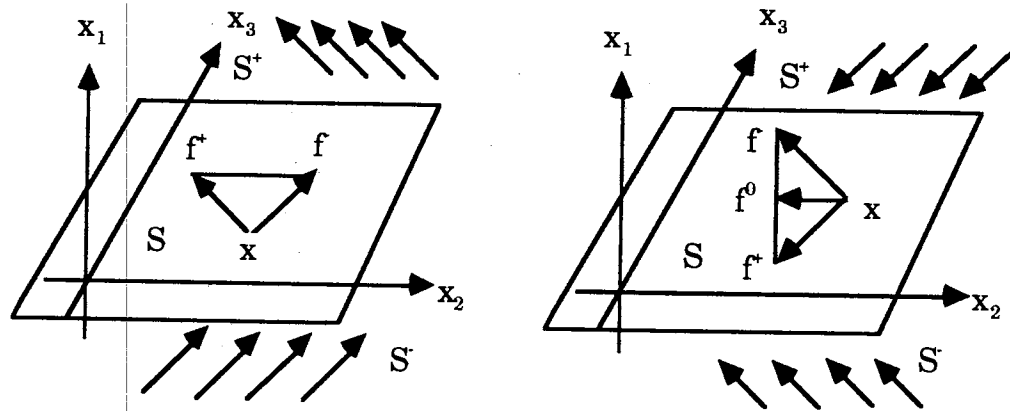


Figure A.1 The velocity field near the hyperplane

For $t_1 < t < t_2$, draw a line joining the endpoints of the vectors $f(t, x)$ and $f^+(t, x)$ that start from the point x . If this line does not intersect the hyperplane S as shown Figure A.1a, the solution is determined by the first case. In this case, the solutions pass from one side to the other of the hyperplane.

If this line intersects the hyperplane S (Figure A.1b), the intersection point is the endpoint of the vector $f^0(t, x)$ which determines the velocity of motion $\dot{x} = f^0(t, x)$ along the surface S . This is the Filippov's equivalent solution [Filippov, 1964] of the differential equation with discontinuous right-hand sides:

$$\dot{x} = f^0(t, x) \quad (\text{A.4})$$

The velocity function of this case is:

$$f^0(t, x) \neq f(t, x), \quad f^0(t, x) \neq f^*(t, x) \quad (\text{A.5})$$

This movement of the solution point is called a "sliding motion".

A.2 Differential of Signum Function

We want to apply chain rule to differentiate a signum function about time which is discontinuous at zero. The Fourier series expansion for a square wave is obtained as followings:

$$\text{sqw}(x) = \frac{4}{\pi} \sin\left(\frac{\pi x}{p}\right) + \frac{4}{3\pi} \sin\left(\frac{3\pi x}{p}\right) + \dots + \frac{4}{(2m-1)\pi} \sin\left(\frac{(2m-1)\pi x}{p}\right) + \dots \quad (\text{A.6})$$

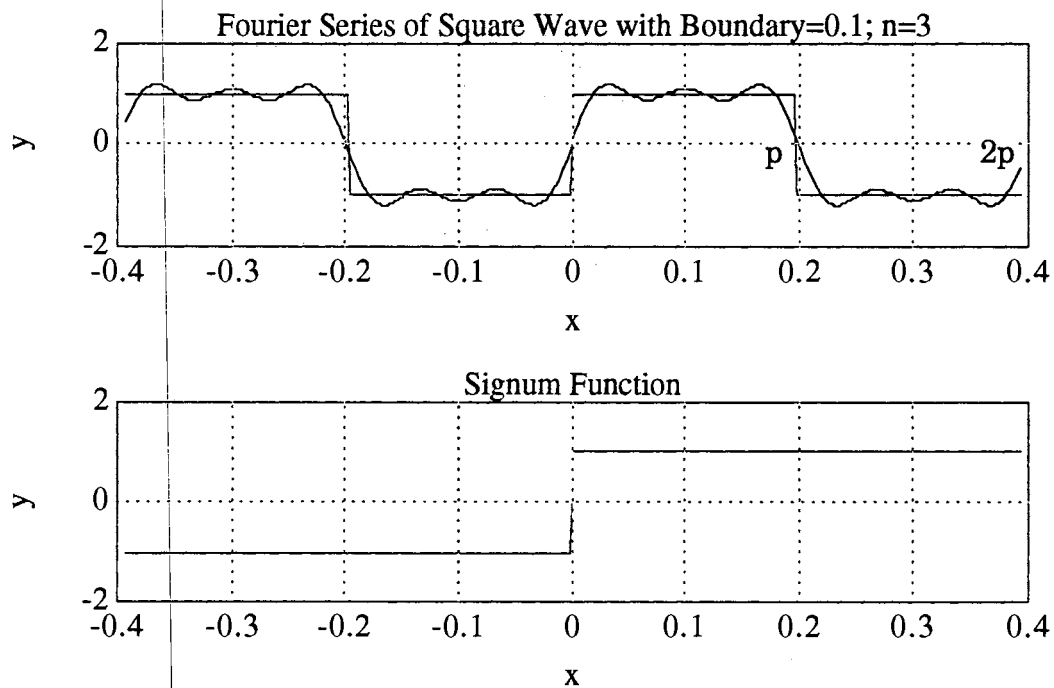


Figure A.2 Fourier series expansion of square wave and signum function

The signum function can be recomposed by using sqw(x) and sgn(x).

$$\text{sgn}(x) = \begin{cases} \text{sqw}(x) & (-\varepsilon < x < \varepsilon) \\ \text{sgn}(x) & (x < -\varepsilon, x > \varepsilon) \end{cases} \quad (\text{A.7})$$

$$\begin{aligned} \frac{d}{dt}(\text{sgn}(x)) &= \\ &= \frac{d}{dt} \left[\frac{4}{\pi} \left\{ \sin\left(\frac{\pi x}{p}\right) + \frac{1}{3} \sin\left(\frac{3\pi x}{p}\right) + \dots + \frac{1}{(2m-1)} \sin\left(\frac{(2m-1)\pi x}{p}\right) + \dots \right\} \right] \\ &= \frac{4}{\pi} \left[\frac{d}{dt} \left\{ \sin\left(\frac{\pi x}{p}\right) \right\} + \frac{1}{3} \frac{d}{dt} \left\{ \sin\left(\frac{3\pi x}{p}\right) \right\} + \dots + \frac{1}{(2m-1)} \frac{d}{dt} \left\{ \sin\left(\frac{(2m-1)\pi x}{p}\right) + \dots \right\} \right] \\ &= \frac{4}{\pi} \left[\frac{d}{dx} \left\{ \sin\left(\frac{\pi x}{p}\right) \right\} \frac{dx}{dt} + \frac{1}{3} \frac{d}{dx} \left\{ \sin\left(\frac{3\pi x}{p}\right) \right\} \frac{dx}{dt} + \dots + \frac{1}{(2m-1)} \frac{d}{dx} \left\{ \sin\left(\frac{(2m-1)\pi x}{p}\right) \right\} \frac{dx}{dt} + \dots \right] \\ &= \frac{4}{\pi} \left[\frac{\pi}{p} \left\{ \cos\left(\frac{\pi x}{p}\right) \right\} \frac{dx}{dt} + \frac{1}{3} \frac{3\pi}{p} \left\{ \cos\left(\frac{3\pi x}{p}\right) \right\} \frac{dx}{dt} + \dots + \frac{1}{(2m-1)} \frac{(2m-1)\pi}{p} \left\{ \cos\left(\frac{(2m-1)\pi x}{p}\right) \right\} \frac{dx}{dt} + \dots \right] \\ &= \frac{4}{\pi} \frac{\pi}{p} \left[\left\{ \cos\left(\frac{\pi x}{p}\right) \right\} \frac{dx}{dt} + \left\{ \cos\left(\frac{3\pi x}{p}\right) \right\} \frac{dx}{dt} + \dots + \left\{ \cos\left(\frac{(2m-1)\pi x}{p}\right) \right\} \frac{dx}{dt} + \dots \right] \\ &= \frac{4}{p} \left[\left\{ \cos\left(\frac{\pi x}{p}\right) \right\} \frac{dx}{dt} + \left\{ \cos\left(\frac{3\pi x}{p}\right) \right\} \frac{dx}{dt} + \dots + \left\{ \cos\left(\frac{(2n-1)\pi x}{p}\right) \right\} \frac{dx}{dt} + \dots \right] \\ &= \frac{4}{p} \left[\cos\left(\frac{\pi x}{p}\right) + \cos\left(\frac{3\pi x}{p}\right) + \dots + \cos\left(\frac{(2m-1)\pi x}{p}\right) + \dots \right] \frac{dx}{dt} \end{aligned}$$

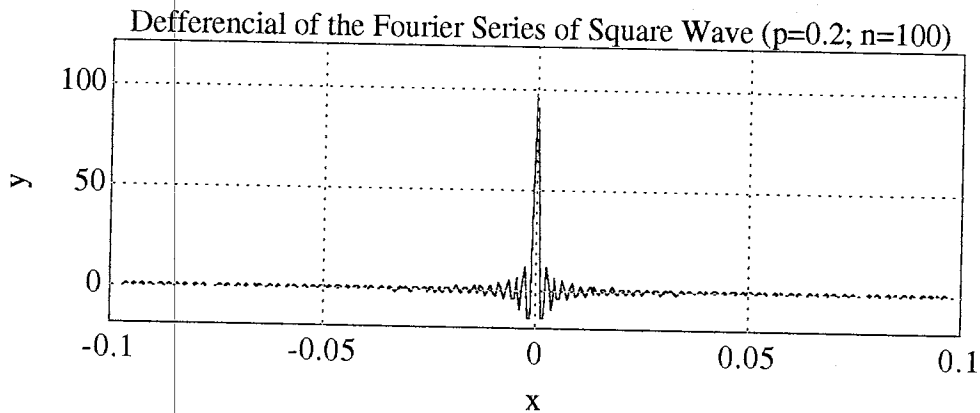


Figure A.3 Differential of the Fourier Series of Square Wave

For finite p , $4/p$ is also finite. Hence, we need to evaluate the rest term.

$$\text{Let } y = \left[\cos\left(\frac{\pi x}{p}\right) + \cos\left(\frac{3\pi x}{p}\right) + \dots + \cos\left(\frac{(2m-1)\pi x}{p}\right) + \dots \right] \quad (\text{A.8})$$

If x equals zero, then y will be infinite as n goes infinite. If x does not equal zero, then y will converge zero as n goes infinite. We can define $\delta(x)$ as following:

$$\delta(x) = \begin{cases} \infty, & (x = 0) \\ 0, & (x \neq 0) \end{cases} \quad (\text{A.9})$$

Let us consider a following function:

$$f_p(x) = \begin{cases} \frac{1}{\epsilon} & (-\epsilon < x < \epsilon) \\ -\frac{1}{\epsilon} & (-p < x < -p + \epsilon, p - \epsilon < x < p) \\ 0 & \text{elsewhere} \end{cases} \quad (\text{A.10})$$

$$f(x) = \frac{a_0}{2} + \sum_{n=1}^{\infty} \left(a_n \cos\left(\frac{n\pi x}{p}\right) + b_n \sin\left(\frac{n\pi x}{p}\right) \right) \quad (\text{A.11})$$

$$\text{where } a_0 = 0, a_n = \frac{2}{p} \int_0^{\epsilon} \frac{1}{\epsilon} \cos\left(\frac{n\pi x}{p}\right) dt + \frac{2}{p} \int_{p-\epsilon}^p \frac{-1}{\epsilon} \cos\left(\frac{n\pi x}{p}\right) dt \quad (\text{A.12})$$

i) $n = 2m$

$$a_{2m} = 0 \quad (\text{A.13})$$

ii) $n = 2m-1$

$$a_{2m-1} = \frac{4}{p} \left[\frac{\sin\left(\frac{(2m-1)\pi\epsilon}{p}\right)}{\frac{(2m-1)\pi\epsilon}{p}} \right] \quad (\text{A.14})$$

It is well known that a delta function is mathematically defined as a limit of the above function. Take the limit and we get the coefficient:

$$\lim_{\epsilon \rightarrow \infty} a_{2m-1} = \frac{4}{p} \quad (\text{A.15})$$

We can see this coefficient is exactly same as the former one.

A.3 Differential of Saturation Function

The differential of saturation function is:

$$\frac{d}{dt}(\text{sat}(x_1)) = \begin{cases} \frac{1}{\varepsilon} \dot{x}_1, & (-\varepsilon < x_1 < \varepsilon) \\ 0, & (|x_1| > \varepsilon) \end{cases} \quad (\text{A.16})$$

Definition A.1

$$\delta_\varepsilon(x) = \begin{cases} \frac{1}{\varepsilon}, & \text{for } -\varepsilon < x < \varepsilon \\ 0, & \text{for } |x| > \varepsilon \end{cases} \quad (\text{A.17})$$

By using definition A.1, the derivative of $\text{sat}(x_1)$ is:

$$\frac{d}{dt}(\text{sat}(x_1)) = \delta_\varepsilon(x_1) \dot{x}_1 \quad (\text{A.18})$$

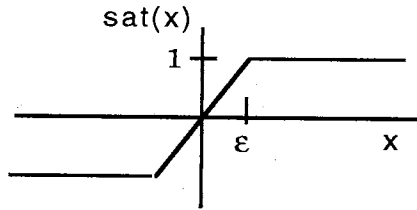


Figure A.4 A saturation function

A.4 Bilinear Form Matrix Function

Definition A.2

A $n \times n$ matrix P whose diagonal elements $|p_{ii}| > \sum_{j \neq i}^n |p_{ij}|, \forall i$, is said diagonally dominant (row dominance) [Strang, 1976].

A $n \times n$ matrix P whose diagonal elements $|p_{ii}| > \sum_{j \neq i}^n |p_{ji}|, \forall i$, is said diagonally dominant (column dominance).

For any symmetric matrix P , the product $Q(x)=x^t Px$ is a *quadratic form*.

Theorem A.1

A necessary and sufficient condition that the real quadratic form $Q(x)=x^t Px$ be positive-definite is that every principal minor of P be positive. ■

Closely associated with quadratic form is what is known as bilinear form.

Definition A.3

If P is a symmetric matrix, the expression $B(x,y) = x^t Py$ is said as a bilinear form. ■

Consider a simple conjecture that every element of x,y and every principal minor of P of a bilinear form $B(x,y)$ is positive. However, following example shows this conjecture is not true.

$$B(x,y) = x^t Py = [1 \ 5] \begin{bmatrix} 9 & -5 \\ -5 & 3 \end{bmatrix} \begin{bmatrix} 1 \\ 1 \end{bmatrix} = -6$$

Let us consider a special form $J = K^T P x = D x$ where $D = K^T P$. If every element D and x is positive then J is positive. For the sliding observer, matrix P is obtained from Lyapunov equation with the Hurwitz matrix A_m and the positive coefficient K is another design coefficient. For designing a sliding observer we can easily check the matrix D . However, a diagonal dominant matrix P and positive coefficient K will make a positive matrix D .

APPENDIX B

STABILITY THEOREMS

B.1 Linear Stability Theorem

Time-invariant case

Although various stability conditions have been obtained for linear, time-varying dynamical equations, they can hardly be used, because all the conditions are stated in terms of state transition matrices, which are very difficult, if not impossible, to obtain. In the stability study of linear time-invariant dynamical equations, the knowledge of the state transition matrix is, however, not needed. The stability can be determined directly from the system matrix A . Consider the n -dimensional linear time-invariant dynamical equation

$$\dot{x} = A x + B u \quad (B.1)$$

$$y = C x \quad (B.2)$$

where A , B , C are $n \times n$, $n \times p$, $q \times n$ real constant matrices, respectively. As in the time-varying case, first, we study the zero-state response and the zero-input response and then the total response. The zero-state response of the system is characterized by

$$G(s) = C (s I - A)^{-1} B \quad (B.3)$$

From theorem , the forced response of system is BIBO stable if and only if all the poles of $G(s)$ have negative real parts.

A linear dynamical equation is said to be totally stable if and only if for any initial state and for any bounded input, the output as well as all the state variables are bounded [Chen, 1970]. ■

Theorem B.1

The forced response (zero state) of $\dot{x} = A x$ is asymptotically stable if and only if all the eigenvalues of A have negative real parts. □

Proof Let P be the nonsingular matrix such that $\hat{A} = PAP^{-1}$ and \hat{A} is in the Jordan form. For the zero state response, in order to be asymptotically stable, in addition to the bound of $\|e^{At}\|$, it is required that $\|e^{At}\|$ tends to zero as $t \rightarrow \infty$, or equivalently, that $\|\hat{e}^{At}\| \rightarrow 0$ as $t \rightarrow \infty$. Since every entry of \hat{e}^{At} is of the form $t^k e^{a_j t + i\omega_j t}$, we conclude that $\|\hat{e}^{At}\| \rightarrow 0$ as $t \rightarrow \infty$ if and only if all the eigenvalues of \hat{A} have negative real parts. Consequently the eigenvalues of A have negative real parts. ■

If a linear time-invariant system is asymptotically stable, its zero-input response will approach zero exponentially; thus it is also said to be exponentially stable. It is clear that total stability implies BIBO stability. However, BIBO stability may not imply total stability. If a linear time-invariant dynamical equation is controllable and observable, then the characteristic polynomial of A is equal to the characteristic polynomial of $G(s)$. Consequently, we have the following theorem [Chen, 1970].

If a linear time-invariant dynamical equation is controllable and observable, then the following statements are equivalent:

1. The dynamical equation is totally stable.
2. The forced response is BIBO stable.
3. The forced response is asymptotically stable.

4. All the poles of the transfer function matrix have negative real parts.
5. All the eigenvalues of the matrix A have negative real parts.

B.2 Dynamics of Saturation Nonlinear Observer

Rewrite the suggested sliding observer (2.6) with the saturation functions instead of the signum functions. Consider a 3-dimensional system:

$$\begin{cases} \dot{x}_1 = x_2 - h_1 x_1 - k_1 \text{sat}(x_1) \\ \dot{x}_2 = x_3 - h_2 x_1 - k_2 \text{sat}(x_1) \\ \dot{x}_3 = -h_3 x_1 - k_3 \text{sat}(x_1) + w \end{cases} \quad (\text{B.4})$$

If the switching term 1_s is a saturation function, the equivalent gain is

$$\hat{\dot{x}} = A \hat{x} + B u + H \tilde{y} + K 1_s(\tilde{y}) \quad (\text{B.5})$$

$$\text{where } 1_s(\tilde{y}) = \begin{cases} \frac{\tilde{y}}{\epsilon} & , \quad |\tilde{y}| \leq \epsilon \\ \frac{\tilde{y}}{|\tilde{y}|} & , \quad |\tilde{y}| > \epsilon \end{cases}$$

$$|\tilde{y}| \leq \epsilon, \quad \hat{\dot{x}} = A \hat{x} + B u + \left(H + \frac{K}{\epsilon} \right) \tilde{y} \quad (\text{B.6})$$

$$|\tilde{y}| > \epsilon, \quad \hat{\dot{x}} = A \hat{x} + B u + \left(H + \frac{K}{|\tilde{y}|} \right) \tilde{y}$$

The robust property of the saturation function needs to be studied to design a quasi-optimal filter. The equivalent gain h^* is plotted as:

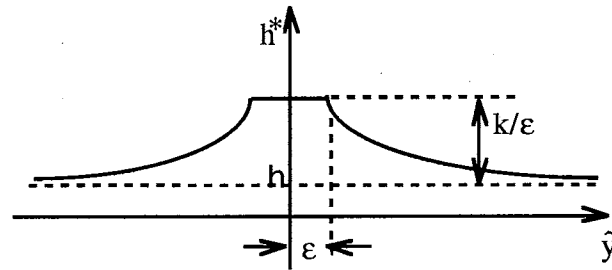


Figure B.1 The equivalent gain profile

The derivative of $\text{sat}(x_1)$ is expressed by using definition A.17:

$$\frac{d}{dt}(\text{sat}(x_1)) = \delta_\epsilon(x_1) \dot{x}_1 \quad (\text{B.7})$$

Differentiate the first equation and plug in the second equation:

$$\ddot{x}_1 = -h_1 \dot{x}_1 - h_2 x_1 - k_1 \delta_\epsilon(x_1) \dot{x}_1 - k_2 \text{sat}(x_1) + x_3 \quad (\text{B.8})$$

Differentiate again and plug in the third equation:

$$x_1^{(3)} = -h_1 \ddot{x}_1 - h_2 \dot{x}_1 - h_3 x_1 - k_1 \delta_\epsilon(x_1) \ddot{x}_1 - k_2 \delta_\epsilon(x_1) \dot{x}_1 - k_3 \text{sat}(x_1) + w \quad (\text{B.9})$$

Combine the same order terms and rewrite the equation then we have the dynamics of the sliding observer with saturation functions:

$$x_1^{(3)} = -(h_1 + k_1 \delta_\epsilon(x_1)) \ddot{x}_1 - (h_2 + k_2 \delta_\epsilon(x_1)) \dot{x}_1 - h_3 x_1 - k_3 \text{sat}(x_1) + w \quad (\text{B.10})$$

For convenience, we can rewrite (B.10) for the outside and for the inside of the boundary layer. For the outside of the boundary layer:

$$x_1^{(3)} = -h_1 \ddot{x}_1 - h_2 \dot{x}_1 - h_3 x_1 - k_3 \text{sgn}(x_1) + w \quad (\text{B.11})$$

Within the boundary layer:

$$x_1^{(3)} = -(h_1 + \frac{k_1}{\epsilon}) \ddot{x}_1 - (h_2 + \frac{k_2}{\epsilon}) \dot{x}_1 - (h_3 + \frac{k_3}{\epsilon}) x_1 + w \quad (\text{B.12})$$

Outside the boundary layer, the sliding observer with saturation functions behaves exactly the same as the signum function observer. Within the boundary layer, the sliding observer with saturation functions behaves like a high gain system.

B.3 Sliding Observer using the Absolute Stability Theorem

In this section, the sliding observer by Misawa [1988] is summarized. Let us consider the robust nonlinear observer in the presence of only output measurement, rather than full state feedback. Since, the measured output provides only partial information about the system state, the additional observer structure must be used. Misawa [1988] proved the stability of the sliding observer by using the Passivity theorem [Astrom, 1989] that guarantees the L_2 -stability of the estimation error. In order to maintain generality, we need to consider the following conditions:

- Define the terms 1_s such that $\tilde{y}^T 1_s > 0$, and $k_n^* > 0$ (B.13)

With these conditions, one can combine the disturbance and "switching" term $1_s(\tilde{y})$, resulting in the estimation error dynamics described by:

$$\dot{\tilde{x}} = (A - HC) \tilde{x} - K^* \alpha(\tilde{y}) \tilde{y} \quad (B.14)$$

This equation is described in the block diagram as Figure B.2. One can readily see that the equation (B.5) is now given in the exact form required by the Passivity theorem.

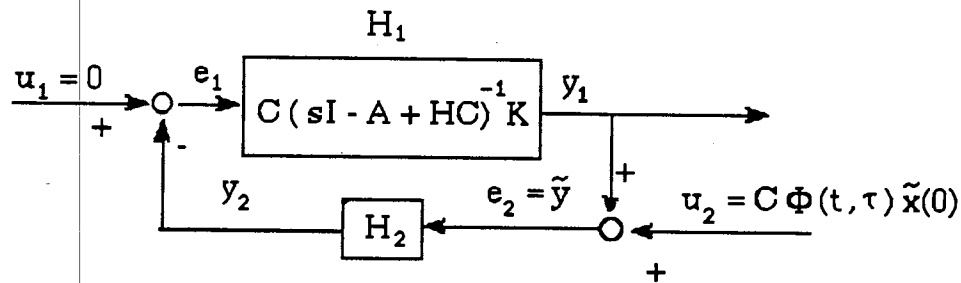


Figure B.2 Estimation error dynamics

The operators H_1 and H_2 , and the input u_2 are defined as follows:

$$H_1 e_1 := C \int_0^t \Phi(t, \tau) K(\tau) e_1(\tau) d\tau \quad (B.15)$$

$$H_2 e_2 = H_2 \tilde{y} := \alpha(\tilde{y}) \tilde{y} \quad (B.16)$$

$$u_2 := C \Phi(t, \tau) \tilde{x}(0) \quad (B.17)$$

where $\Phi(t) = e^{(A-HC)t}$ is the state transition matrix.

In this scheme, e_1 and e_2 are defined as: $e_1 = u_1 - H_2 e_2$ and $e_2 = u_2 + H_1 e_1$.

In order to introduce the main result, it is necessary to define the sets \mathcal{H} and \mathcal{H}_e :

$$\mathcal{H} = \left\{ x(t) \mid \|x\|^2 = \int_0^\infty x(t)^T x(t) dt < \infty \right\} \quad (B.18)$$

$$\mathcal{H}_e = \left\{ x(t) \mid \|x\|_T^2 = \int_0^T x(t)^T x(t) dt < \infty \right\} \quad \forall T \geq 0 \quad (B.19)$$

The main estimation convergence (stability) results can now be stated as a theorem.

Theorem B.2

- $(A - H C)$ is made stable;
- The gain matrices H and K , and the function 1_s are chosen such that there are constants α_i and β_i , ($i=1,2,3$), so that:

$$\|H_1 z\|_T \leq \alpha_1 \|z\|_T + \beta_1$$

$$\int_0^T z(t)^T (H_1 z) dt =: \langle z | H_1 z \rangle_T \geq \alpha_2 \|z\|_T^2 + \beta_2$$

$$\int_0^T (H_2 z)^T z(t) dt =: \langle H_2 z | z \rangle_T \geq \alpha_3 \|H_2 z\|_T^2 + \beta_3$$

$\forall z \in \mathcal{H}_t, \forall T \in [0, \infty);$

- $\alpha_2 + \alpha_3 > 0$;

Then: $e_1, e_2 = \tilde{y}$, $H_1 e_1, H_2 e_2 \in \mathcal{H}$, and $\tilde{y} = C \tilde{x} \Rightarrow 0$ as $t \Rightarrow \infty$. \square

The main result stated in this section gives a fairly general result for the problem at hand.

First Design Procedure

The first design procedure shows the observed states to be asymptotically convergent if the transfer function matrix

$$H_1(s) = C (sI - A + H C)^{-1} D \quad (B.20)$$

can be made strictly positive real.

- 1) Let the function $1_s(\cdot)$ be

$$1_s(\tilde{y})^T = [\text{sign}(\tilde{y}_1), \text{sign}(\tilde{y}_2), \dots, \text{sign}(\tilde{y}_m)]$$

where $\text{sign}(\tilde{y}_i) = \tilde{y}_i / |\tilde{y}_i|$

- 2) Choose the gain matrices H and ρ so that the following conditions are satisfied:

$$\begin{aligned} P(A - H C) + (A - H C)^T P &= -Q \\ K^T P &= C \\ K &= D \rho \end{aligned} \quad (B.21)$$

for some symmetric positive definite matrices P and Q .

- 3) If these conditions are met, then the design is complete. If they are not met one can iterate by changing the matrices D and ρ , or iterate using the multiplier theory [Desoer, 1975] trying to meet the conditions given in this design procedure. If these changes do not work, then one can try the

method described in Second Design Procedure.

The second conditions is usually hard to verify and can be too restrictive for particular problems. When it works, this design procedure guarantees that $\tilde{y} \Rightarrow 0$ and $\hat{x} \Rightarrow 0$ as $t \Rightarrow \infty$.

For systems with a single measurement, the definition of strictly positive real linear systems [Desoer, 1975] give an easier way to check whether the operator H_1 is strictly positive real. In this case, by placing the eigenvalues of $A - H C$ in the open left half plane, the operator H_1 is strictly positive real if and only if the following transfer function

$$H_1(s) = C (sI - A + H C)^{-1} K \quad (B.22)$$

evaluate at all $s=j\omega$ is completely contained in the open right half plane:

$$\text{Re} [G(j\omega)] > 0 \quad \text{for all } \omega \in \mathbb{R} \quad (B.23)$$

If this approach does not work, one still has the option to design the observer using a following alternative method.

Second Design Procedure

The previous design procedure was restricted by the Positive Real Lemma, which resulted from the strict passivity condition imposed by the use of pure switching (signum function) for the function $1_s(\tilde{y})$. This suggests that by using the saturation function for $1_s(\tilde{y})$, a less restrictive condition may be found. This is the case, and the design procedure uses the circle criterion [Landau, 1979] for the single measurement case, and the extension of circle criterion to the multivariable case [Luenberger, 1966].

In this case the design process has two parts. The first part guarantees that the output estimation error $\tilde{y} = y - C \tilde{x}$ remains inside the boundary layer once it gets into it and the second part guarantees that the boundary

layer is attractive.

1) Let $1_s(\tilde{y})$ be the vector function whose components are saturation functions defined in the usual way:

$$1_s(\tilde{y})^T = [\text{sat}(\tilde{y}_1/\varepsilon_1), \text{sat}(\tilde{y}_2/\varepsilon_2), \dots, \text{sat}(\tilde{y}_m/\varepsilon_m)] \quad (\text{B.24})$$

and

$$\text{sat}(\tilde{y}_i/\varepsilon_i) = \begin{cases} \tilde{y}_i/|\tilde{y}_i| & \text{if } |\tilde{y}_i| \geq \varepsilon_i \\ \tilde{y}_i/\varepsilon_i & \text{if } |\tilde{y}_i| < \varepsilon_i \end{cases} \quad (\text{B.25})$$

2) Set the gain matrix K as:

$$K = D \rho \quad (\text{B.26})$$

$$\rho = \text{diag}(\rho_1, \dots, \rho_m), \quad \rho_i \geq 1 \quad (\text{B.27})$$

3) Choose the width of boundary layer for \tilde{y}_i called ε_i , and which coincides with the saturation limit ε_i in the sat-function defined by (B.25); define the matrix

$$\Delta = \text{diag}(\varepsilon_1, \varepsilon_2, \dots, \varepsilon_m) \quad (\text{B.28})$$

The choice of ε_i is arbitrary, to some extent, but one might want to have it as small as possible as long as the particular choice does not conflict with the next steps.

4) Design for boundedness inside the boundary layer. Choose the gain matrices H and ρ such that for all $t \in \mathbb{R}_+$ and for all $\omega \in \mathbb{R}$:

$$\begin{aligned} & \max [\sigma_{\max} (C (j\omega I - A + (H + K\Delta^{-1}) C)^{-1} D) + \\ & + \sigma_{\max} (C e^{(A - (H + K\Delta^{-1}) C)t}) \max_i(\tilde{x}_0)] \leq \min_i(\varepsilon_i) \end{aligned} \quad (\text{B.29})$$

In practice this test has to be verified in the time interval of interest, typically during the initial transient. This method may be very conservative, as the usual singular analysis is.

5) Check whether the state estimation error bounds are within desirable

limits:

$$|\tilde{x}(t)| \leq \max_{0 < \omega < +\infty} [\sigma_{\max}((j\omega I - A + (H + K\Delta^{-1})C)^{-1}D)] \quad (B.30)$$

Clearly, if the transfer function matrix

$$G(s) = C(sI - A + (H + K\Delta^{-1})C)^{-1}D \quad (B.31)$$

has finite transmission zeros then the desired convergence time and the desired accuracy can be difficult to achieve. In particular, if the zeros turn out to be in the closed right half plane, then the problem may become particularly difficult, even impossible in some cases.

6) Check for stability outside the boundary layer (single measurement systems). The error dynamics can be written as:

$$\begin{aligned} \tilde{y} &= C \tilde{x} \\ \dot{\tilde{x}} &= (A - H C) \tilde{x} - K \phi \tilde{y} \end{aligned} \quad (B.32)$$

It is necessary to verify that (A.8) is stable for ϕ such that ϕ is constrained in the sector:

$$0 < \phi < \frac{1}{\epsilon} \left(1 + \frac{1}{\rho}\right) = \overline{G} \quad (B.33)$$

For instance, if the circle criterion is used, then it is sufficient to show that the Nyquist Plot of the transfer function

$$H_1(s) = C(sI - A + H C)^{-1}K \quad (B.34)$$

is to the right of the vertical line that intersects the real axis at $-\frac{1}{G}$

7) Check for stability outside the boundary layer (systems with multiple measurements). The matrices H and K must be such that:

- $(A - H C - K M C)$ has eigenvalues in the open left half plane ; the matrix M is a diagonal matrix whose entries are $m_{ii} = \frac{1}{2\epsilon_i} \left(1 + \frac{1}{\rho_i}\right)$

• The following condition is verified for all values of $\omega \in \mathcal{R}$ at which H_1^{-1} exists:

$$\sigma_{\min} ([M + H_1^{-1}(j\omega)] M^{-1}) \geq 1 \quad (\text{B.35})$$

where $H_1(s) = C (sI - A + H C)^{-1} K$

8) If this last condition is satisfied, then the design is complete. Otherwise, one has to iterate changing the width of boundary layers and the choice of matrices D , ρ and H .

B.4 Alimov's Transformation

The sliding observer error dynamics without disturbance is:

$$\dot{x} = A_m x - K 1_s(\tilde{y}) \quad (\text{B.36})$$

where K is a $n \times 1$ column matrix whose elements are positive and $1_s(s)$ is a signum function.

With a nonsingular Hurwitz system matrix A_m , we are investigating the effect of a discontinuous switching surface.

$$s(t) = \tilde{y} = C x(t) \quad (\text{B.38})$$

We denote by $x_+(x^0, t)$ and $x_-(x^0, t)$ the trajectories of the systems

$$\begin{aligned} \dot{x} &= f_+(x) = A x - K, \\ \dot{x} &= f_-(x) = A x + K \end{aligned} \quad (\text{B.39})$$

passing for $t=0$ through the initial point x^0 of the space x .

For the studying of the system, it is convenient to rewrite (B.39) in a new coordinate [Alimov, 1960] $x_+ = x - A^{-1} K$, $x_- = x + A^{-1} K$:

$$\begin{cases} \dot{x}_+ = A x_+, \\ \dot{x}_- = A x_-, \end{cases} \quad (\text{B.40})$$

We denote by $\dot{s}_+(x)$ and $\dot{s}_-(x)$ the derivatives with respect to time of the function $s(x) = C x(t)$ according to the system.

$$\begin{aligned}\dot{s}_+(x) &= C A x - C K 1_s(s) \\ \dot{s}_-(x) &= C A x + C K 1_s(s)\end{aligned}\tag{B.41}$$

Switching plane = Sliding zone + Passing zone

1) In the space $s(x) > 0$, we assume that $x(x^o, t) = x_+(x^o, t)$, (for $s(x) < 0$, $x(x^o, t) = x_-(x^o, t)$).

2) At any point σ_t of the set $s(x)=0$, $\dot{s}_+(x) \dot{s}_-(x) > 0$ which represents two half-planes $(C K)^{-1} C A x < -1$, $C x = 0$ and $(C K)^{-1} C A x > +1$, $C x = 0$, the trajectories $x_+(\sigma_t, t)$, $x_-(\sigma_t, t)$ go through the surface $s(x) = 0$ in the same direction. We determine $x(\sigma_t, t)$ by connecting continuously at σ_t those half-trajectories $x_+(\sigma_t, t)$ and $x_-(\sigma_t, t)$ which lie close to σ_t in the regions $s(x) > 0$ and $s(x) < 0$, respectively.

3) At any point σ_s of the set $s(x)=0$, $\dot{s}_+(x) \dot{s}_-(x) < 0$, the trajectories $x_+(\sigma_s, t)$ and $x_-(\sigma_s, t)$ go through the surface $s(x)=0$ in the opposite direction. The hyperplane is:

$$C x = 0 \text{ and } -1 < (C K)^{-1} C A x < +1\tag{B.42}$$

Example B.2

$$C=[1 \ 0 \ 0], K=[k_1 \ k_2 \ k_3]^T, (C K)^{-1} C A x = \frac{h_1 x_1 + x_2}{k_1}$$

$$\text{i.e. } -k_1 < x_2 < k_1, \text{ for } s=0 (|x_1| \ll 1)$$

The representative point of the system moves according to the equations

$$\dot{x} = A x - K 1_s(0) = A x - K \zeta(t)\tag{B.43}$$

where $\zeta(t)$ is chosen so that the derivative with respect to time $\dot{s}_o(x)$ of the function $s(x)$ is obtained as in the above equation. It satisfies the equality

$$\dot{s}_0(x) = C A x(t) + C K \zeta(t) = 0 \quad (B.44)$$

Combine (B.42) and (B.43), we obtain

$$\begin{aligned} s(x) &= C x = 0, \\ \dot{x} &= f_0(x) = R x, \quad R = A - (C K)^{-1} K C A \end{aligned} \quad (B.45)$$

For the trajectories of the sliding dynamics, we will use the notation $x_0(x^0, t)$.

By using the equation (B.44), we can extend the definition of a switching function.

$$1_s(s) = \begin{cases} -1 & \text{for } s < 0, \\ \zeta & \text{for } s = 0 \\ +1 & \text{for } s > 0 \end{cases}$$

The essence of Filippov's equivalent dynamics is precisely the definition of the discontinuous right hand side, including infinite valued functions, continuous in the same sense as the extended definition. The fact that the solution $x(x^0, t)$ can be continued for $t \Rightarrow +\infty$, its uniqueness, and the property for are obvious; the continuity relative to x^0 and t can easily be proved by using (B.41) and (B.44). The solution $x(x^0, t)$ of the system (B.44), determined as above, is also a generalized solution of this system in the sense of the definition of Filippov.

We consider finally the boundary $s(x)=0$, $\dot{s}_+(x) \dot{s}_-(x) = 0$ of the zone of the sliding regime, represented by the two hyperlines

$$C x = 0, \quad \dot{s}_+(x) = C A x - C K 1_s(s) = 0 \quad (B.49)$$

$$C x = 0, \quad \dot{s}_-(x) = C A x + C K 1_s(s) = 0 \quad (B.50)$$

We will form the Lyapunov function $V(x)$ for the system with Hurwitz system matrix by linking on the surface $s(x)=0$. The Lyapunov functions:

$$V_+(x) = X_+^T P X_+, \quad x_+ = x - A^{-1} K \quad (B.51)$$

$$V_-(x) = X_-^T P X_-, \quad x_- = x + A^{-1} K \quad (B.52)$$

For the systems (P is a symmetric matrix of the n th order), respectively:

$$V(x) = \begin{cases} V_+(x) - V_+(0) & \text{for } s(x) \geq 0, \\ V_-(x) - V_-(0) & \text{for } s(x) \leq 0 \end{cases} \quad (B.53)$$

The continuity of $V(x)$ is established if $V_+(x)$ and $V_-(x)$ are chosen so that the equality

$$V_+(x) - V_+(0) = V_-(x) - V_-(0) \quad \text{for } s(x) = 0 \quad (B.54)$$

holds, since the relation $V_+(x) - V_+(0) = V_-(x) - V_-(0)$ is equivalent to $x^T P A^{-1} K = 0$. The connecting equation (i.e., so-called matching condition) can be rewritten in the form

$$P A^{-1} K = \rho C^T \quad (\rho = \text{const} \neq 0) \quad (B.55)$$

It is evident from the relation

$$V(x) = x^T P x + 2\rho S 1_s(s) \quad (B.56)$$

that follows from (B.53) and (B.55). If the function $x^T H x$ that is satisfying the condition (B.55) is positive definite, then the function $V(x)$ will also be positive definite for $\rho > 0$.

For any solution $x(x^0, t)$ everywhere except possibly at points of intersection of $x(x^0, t)$ with the surface $s(x)=0$, the derivative $\dot{V}(x)$ with respect to time of the function along $x(x^0, t)$ exists and satisfies the relations

$$\dot{V}(x) = \begin{cases} \dot{V}_+(x) = x_+^T (PA + A^T P) x_+ & \text{for } s(x) > 0, \\ \dot{V}_-(x) = x_-^T (PA + A^T P) x_- & \text{for } s(x) < 0, \\ \dot{V}_o(x) = x^T (PR + R^T P) x & \text{for } s(x) = 0, \dot{s}_+(x) \dot{s}_-(x) < 0 \end{cases} \quad (\text{B.57})$$

where $PA + A^T P = -Q$ (B.58)

Let the Q matrix is a symmetric positive definite matrix. Then, with the Hurwitz system matrix, there exists a unique matrix P by the equation. It is apparent that the function $\dot{V}_+(x)$ or $\dot{V}_-(x)$ is negative definite and the function $V(x)$ decreases along any trajectory $x_+(x_+^o, t)$ or $x_-(x_-^o, t)$. Finally, we need to show the $V(x)$ also decreases in sliding mode.

APPENDIX C

SIGN EQUALIZATION OF PASSING STATES

C.1 Transient State of the Reaching Dynamics

At the passing instance, even though the velocity field is discontinuous, the trajectory of the solution point in the reaching domain is continuous. Consequently the dynamical characteristic for the half domain can be extended to the whole domain directly. Hence let us review the reaching dynamics in the view point of a linear system theory as follows:

$$\mathbf{x}(t) = \underbrace{e^{A(t-\tau)} \mathbf{x}(\tau)}_{\text{Zero-input response}} + \underbrace{\int_{\tau}^t e^{A(t-\lambda)} B u(\lambda) d\lambda}_{\text{zero-state response}} \quad (\text{C.1})$$

A very important property of any linear system is that the responses of the system can be decomposed into two parts, as follows:

$$\begin{aligned} & \text{Responses due to } \{\mathbf{x}(t_0), u(t_0, \infty)\} \\ &= \text{responses due to } \{\mathbf{x}(t_0), 0\} + \text{responses due to } \{0, u(t_0, \infty)\} \end{aligned}$$

The responses due to $\{\mathbf{x}(t_0), 0\}$ are called the zero-input response or a transient term: they are generated exclusively by the nonzero initial state $\mathbf{x}(t_0)$. The responses due to $\{0, u(t_0, \infty)\}$ are called as the zero-state response or the forced term: they are excited exclusively by the input $u(t_0, \infty)$. Hence, for linear systems, we can consider the zero-input response and the zero-state

responses independently. Reset the initial time zero at the passing instance and rewrite the equation (2.17):

$$\mathbf{x}(t) = e^{At} \mathbf{x}^i + e^{At} \int_0^t e^{-A\lambda} B u(\lambda) d\lambda \quad (\text{C.2})$$

The disturbance input u_d of the reaching dynamics is composed of the disturbance w and $-k_n \text{sign}(x_1)$. If the disturbance input can be assumed as a white noise (or normal distributed random noise with zero mean) then the disturbance output of a high order system is much smaller than the output by the switching term $-k_n \text{sign}(x_1)$. Hence, the transient response for the step input is useful to understand the reaching dynamics.

Transient responses of 2 order systems

The transient response of the reaching dynamics may be described in terms of the rise time t_r which is the time for the step response to reach from 10 to 90 percent of its final value, the exact values can again be obtained directly from the simulated results. The approximate relation between the rise time versus ζ is known for the 2-order system [Kuo, 1982]. For the range of $0 < \zeta < 1$, the rise time approximated by the first order equation is

$$t_r \approx \frac{0.8 + 2.5 \zeta}{w_n} \quad (0 < \zeta < 1)$$

The rise time approximated by the second order equation is

$$t_r \approx \frac{1 + 1.1 \zeta + 1.4 \zeta^2}{w_n}$$

For the overdamped range ($1 < \zeta$), the rise time is approximately [Friedland, 1986]:

$$t_r = \frac{2\zeta}{\omega_n}$$

Transient responses of higher order systems

Some more detail descriptions of the transient response of the 2-order system can be found in the book of Clark [1962]. However, it is hard to find a paper which explicitly mentions the complex phenomena of the transient response for a higher order system including the zero input response. From the general solution (C.2), both terms have the same transient factor $e^{\lambda t}$ so that the transient times of the step input response and zero input response should be the same order. With the special initial condition, the specific eigenmode only will be excited.

Example C.1

Consider the third order sliding observer reaching error dynamics:

$$\begin{cases} \dot{x}_1 = x_{2s} - h_1 x_1 \\ \dot{x}_{2s} = x_{3s} - h_2 x_1 \\ \dot{x}_{3s} = -h_3 x_1 + u_d \end{cases}$$

where $H=[.8 \ .31 \ .05]^T$, $w=0$, initial states: $x_1:0$, $x_2:3$, $x_3:5$, $u_d = -\text{sgn}(x_1)$

The simulation results are shown in the Figure C.1. As it is expected, the transient time of the noised disturbance input is approximately the same as the step response. The transient time t_t for the zero input response can be defined as the time for the initial state to reach from 10 to 90 percent of its equilibrium state. The transient time t_t can be obtained directly from the simulated results Figure C.1. The transient time is approximately 10 second for all. Figure C.1 (d) is the superposition of Figure C.1 (a) and (b).

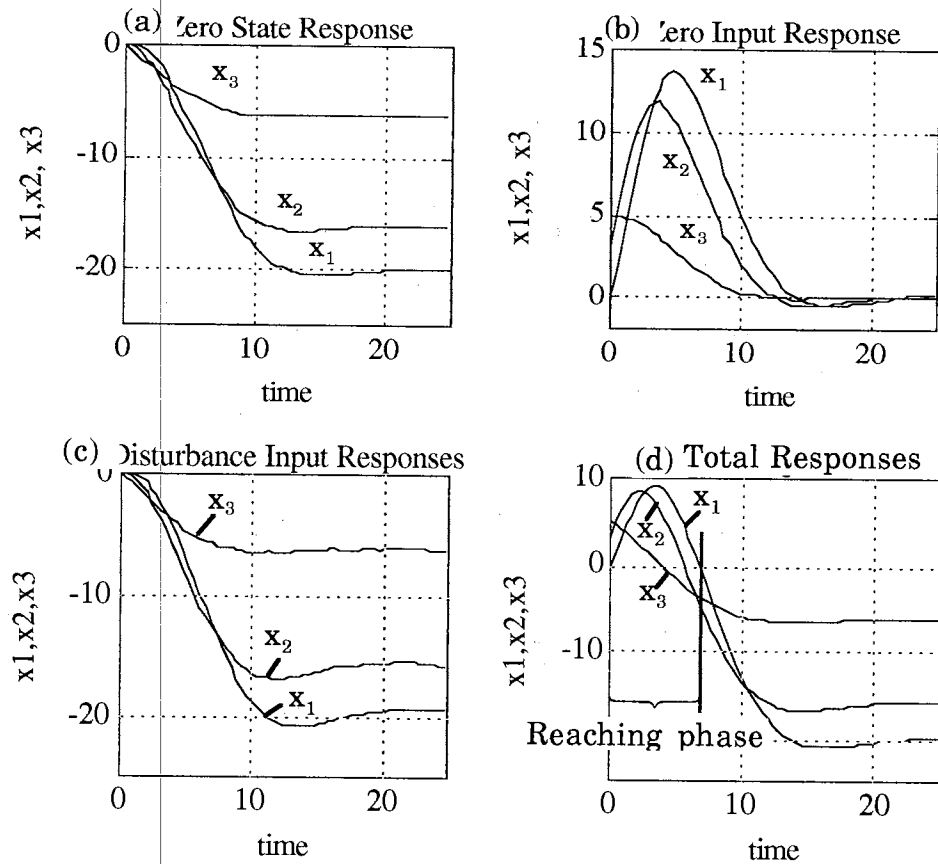


Figure C.1 Transient responses of reaching dynamics

- a) Zero state response (Step input) b) Zero input response
c) Random noise disturbance input response d) Total response

Conjecture C.1

For the zero input response, the last state x_3 is a strictly decreasing function and reaches the minimum value when the state x_1 is zero. If all the initial states are positive at the hyperplane ($x_1 = 0$), then all of the initial velocity field is positive except \dot{x}_n . The conceptual diagram is shown in Figure C.2. In the Figure C.2, the reaching time of x_n is less than the reaching time of x_1 .

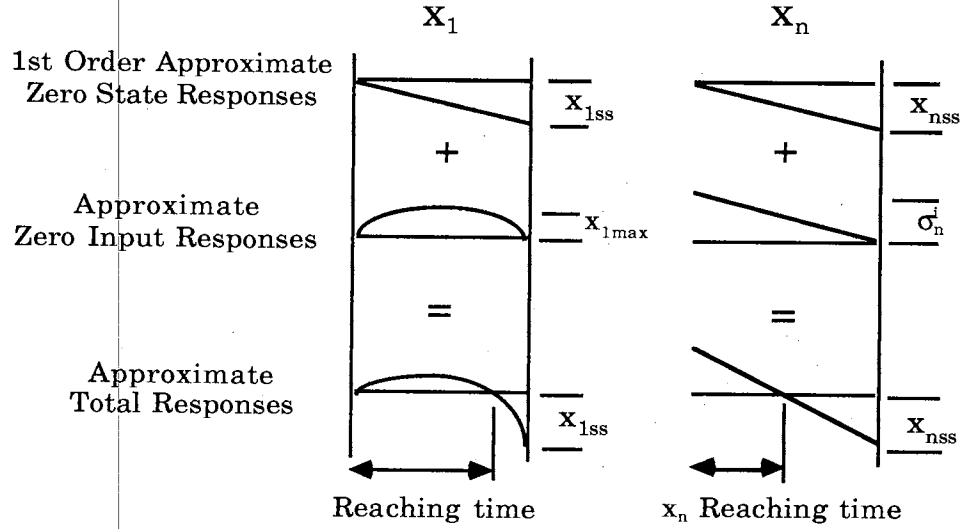


Figure C.2 The conceptual diagram of the reaching time

Minimum Phase Transfer Function

The transfer functions for the each state are

$$\left\{ \begin{array}{l} x_{2s}(s) = (s + h_1) x_1(s) \\ x_{3s}(s) = (s^2 + h_1s + h_2) x_1(s) \\ \dots \\ x_{ns}(s) = (s^{n-1} + h_1s^{n-2} + \dots + h_{n-1}) x_1(s) \\ u_d(s) = (s^n + h_1s^{n-1} + \dots + h_n) x_1(s) \end{array} \right. \quad (C.3)$$

The transfer functions between the state are

$$\left\{ \begin{array}{l} \frac{x_1(s)}{x_{2s}(s)} = \frac{1}{(s + h_1)} \\ \frac{x_{2s}(s)}{x_{3s}(s)} = \frac{(s + h_1)}{(s^2 + h_1s + h_2)} \\ \dots \\ \frac{x_{(n-1)s}(s)}{x_{ns}(s)} = \frac{(s^{n-2} + h_1s^{n-3} + \dots + h_{n-2})}{(s^{n-1} + h_1s^{n-2} + \dots + h_{n-1})} \\ \frac{x_{ns}(s)}{u_d(s)} = \frac{(s^{n-1} + h_1s^{n-2} + \dots + h_{n-1})}{(s^n + h_1s^{n-1} + \dots + h_n)} \end{array} \right. \quad (C.4)$$

Even though the reaching dynamics cannot be settle down to its steady state, the ratio between the steady states are helpful to understand the characteristic of the reaching dynamics. Apply the final value theorem and we get:

$$\left\{ \begin{array}{l} \lim_{s \rightarrow 0} \frac{x_1(s)}{x_{2s}(s)} = \frac{1}{h_1} \\ \lim_{s \rightarrow 0} \frac{x_{2s}(s)}{x_{3s}(s)} = \frac{h_1}{h_2} \\ \dots \\ \lim_{s \rightarrow 0} \frac{x_{(n-1)s}(s)}{x_{ns}(s)} = \frac{h_{n-2}}{h_{n-1}} \\ \lim_{s \rightarrow 0} \frac{x_{ns}(s)}{u_d(s)} = \frac{h_{n-1}}{h_n} \end{array} \right. \quad (C.5)$$

For the transfer function between the input and output state is

$$\lim_{s \rightarrow 0} \frac{x_1(s)}{u_d(s)} = \frac{1}{h_n} \quad (C.6)$$

A transfer function whose poles and zeros all lie in the left-half s-plane is called a minimum phase transfer function. The steady state value of the nonminimum phase system is negative for the case of a simple transfer function that has a zero and a pole. If any of the coefficient h_i is negative then some of the final value ratio of equation should be negative so that some the zero state responses move to different sign direction. Therefore the superposition of the zero state responses and zero input responses does not guarantee the sign equalization of all states x_2, \dots, x_n at the final passing point.

C.2 Eigen structure

The characteristic equation is

$$|\lambda I - A_m| = \lambda^n + h_1 \lambda^{n-1} + \dots + h_{n-1} \lambda + h_n \quad (C.7)$$

$$\text{where } A_m = \begin{bmatrix} -h_1 & 1 & 0 & \dots & 0 & 0 \\ -h_2 & 0 & 1 & & & \\ \vdots & & & & & \\ \vdots & & & & 0 & 1 \\ -h_n & 0 & & \dots & 0 & 0 \end{bmatrix} \quad (\text{C.8})$$

The Routh-Hurwitz stability method provides an answer to the question of stability by considering the characteristic equation of the system.

$$\begin{aligned} & (\lambda - \lambda_1)(\lambda - \lambda_2) \dots (\lambda - \lambda_n) \\ &= \lambda^n - (\lambda_1 + \lambda_2 + \dots + \lambda_n) \lambda^{n-1} + (\lambda_1 \lambda_2 + \dots + \lambda_n \lambda_1) \lambda^{n-2} + \dots + (-1)^n (\lambda_1 \lambda_2 \dots \lambda_n) \end{aligned} \quad (\text{C.9})$$

By comparing the two equations, we obtain the coefficients:

$$h_1 = (-1)^1 (\text{sum of all the eigenvalues})$$

$$h_2 = (-1)^2 (\text{sum of the products of the eigenvalues taken 2 at a times})$$

...

$$h_n = (-1)^n (\text{products of all } n \text{ eigenvalues})$$

For the canonical form system, the eigen structure has special form as follows:

$$\begin{bmatrix} -h_1 & 1 & 0 & \dots & 0 & 0 \\ -h_2 & 0 & 1 & & & \\ \vdots & & & & & \\ \vdots & & & & 0 & 1 \\ -h_n & 0 & & \dots & 0 & 0 \end{bmatrix} \begin{bmatrix} x_1 \\ x_2 \\ \vdots \\ x_n \end{bmatrix} = \lambda_j \begin{bmatrix} x_1 \\ x_2 \\ \vdots \\ x_n \end{bmatrix} \quad (\text{C.10})$$

For $\lambda = \lambda_j$ case ($j=1, 2, \dots, n$)

From the 1st equation of (C.10), the eigenvector x_2 is obtained as follows:

$$\begin{aligned} x_2 &= h_1 x_1 + \lambda_j x_1 \\ &= \{-(\lambda_1 + \lambda_2 + \dots + \lambda_n) + \lambda_j\} x_1 \end{aligned} \quad (\text{C.11})$$

From the following equations of equation (C.10), the remaining eigenvectors are also expressed as function of the state x_1 and the eigenvalues:

$$\begin{aligned}
 x_3 &= h_2 x_1 + \lambda_j x_2 \\
 &= \left\{ (\lambda_1 \lambda_2 + \dots + \lambda_n \lambda_1) - \lambda_j (\lambda_1 + \lambda_1 + \dots + \lambda_n - \lambda_j) \right\} x_1 \\
 &= \left\{ \sum_{\substack{k \neq j, l \neq j, k \neq l}} \lambda_k \lambda_l \right\} x_1 \\
 x_4 &= h_3 x_1 + \lambda_j x_3 \\
 &= \left\{ -(\lambda_1 \lambda_2 \lambda_3 + \dots + \lambda_n \lambda_1 \lambda_2) + \lambda_j (\lambda_1 + \lambda_1 + \dots + \lambda_n - \lambda_j) \right\} x_1 \\
 &= \left\{ - \left(\sum_{m \neq n \neq o} \lambda_m \lambda_n \lambda_o \right) + \lambda_j \sum_{\substack{k \neq j, l \neq j, k \neq l}} \lambda_k \lambda_l \right\} x_1 \\
 &= - \sum_{\substack{k \neq j, l \neq j, m \neq j, \\ k \neq l \neq m}} \lambda_k \lambda_l \lambda_m x_1 \\
 &\dots \\
 x_n &= \frac{-h_n}{\lambda_j} x_1 = (-1)^{n+1} \frac{(\lambda_1 \lambda_2 \dots \lambda_n)}{\lambda_j} x_1
 \end{aligned}$$

If all the eigenvalues are negative, all the coefficient of the above equations are positive. Therefore, all the eigenvector have the same sign as x_1 .

If all eigenvalues of A are distinct, the response of $\dot{x} = Ax$ due to $x(0) = x_0$ can be written as:

$$\hat{x}(s) = (sI - A)^{-1} x_0 = \sum_j \frac{1}{s - \lambda_j} q_j p_j x_0 \quad (\text{C.13}) \text{ where } q_j \text{ and } p_j \text{ are,}$$

respectively, right and left eigenvector of the system matrix A which is associated with λ_j . In the time domain, the equation becomes:

$$x(t) = \sum_j (p_j x_0) e^{\lambda_j t} q_j \quad (\text{C.14})$$

If x_0 is chosen so that $p_j x_0 = 0$ for all j except $j=i$, then the equation (C.14)

diminishes to

$$\mathbf{x}(t) = (\mathbf{p}_i \mathbf{x}_0) e^{\lambda_i t} \mathbf{q}_i$$

For this initial state, only the mode $e^{\lambda_i t}$ is excited and $\mathbf{x}(t)$ will travel along the direction of the eigenvector \mathbf{q}_i .

C.3 3-order System

Rewrite a 3-order right reaching dynamics:

$$\begin{cases} \dot{x}_1 = -h_1 x_1 + x_{2+} \\ \dot{x}_{2+} = -h_2 x_1 + x_{3+} \\ \dot{x}_{3+} = -h_3 x_1 + u_d \end{cases} \quad (\text{C.15})$$

where $u_d = w - k_n \operatorname{sgn}(x_1)$

Since the state x_1 is not changed by the coordinate transformation in each domain Ω_+ , Ω_0 , Ω_- , it is noted without a sign of + or -. It is obvious that, in the shifted coordinate, the above system is a linear system and it is asymptotically stable and attractive to the shifted origin. Since the right half domain Ω_+ and the left half domain Ω_- are symmetric to each other about the origin of original coordinate, let us consider the half domain Ω_+ only. If the initial states are not on the sliding patch, then the solution point needs to be attracted to the sliding patch. Hence, for the stability analysis purpose, it is assumed that the initial point is satisfying the passing condition $\sigma_{2+}^i > 0$ without loss of generality.

Case 1)

With the initial condition $\sigma_{3+}^i > 0$, the initial velocity field of the reaching dynamics is obtained from (C.15):

$$\begin{cases} \dot{x}_1^i > 0 \\ \dot{x}_{2+}^i > 0 \\ \dot{x}_{3+}^i < 0 \end{cases} \quad (C.16)$$

We can do pole placement to choose the linear correction coefficients. Let us assume that the system is underdamped or critically damped. Since the Hurwitz system is asymptotically stable, the velocity of x_1 is negative as it approaches the switching plane. The velocity field, $\dot{x}_1^f < 0$, is due to the state x_2 in the equation (C.15).

$$\text{Hence, } \dot{x}_1^f < 0 \text{ implies } \sigma_{2+}^f < 0 \quad (C.17)$$

$$\text{where } \begin{cases} \text{if } 0 > \sigma_{2+}^f > -2 k_1 : \text{satisfy sliding condition} \\ \text{if } \sigma_{2+}^f < -2 k_1 : \text{passing the hyper plane} \end{cases}$$

The initial passing point with $\sigma_{3+}^i > 0$ arrived at final point, $\sigma_{2+}^f < 0$. The associated velocity field is $\dot{x}_{2+} = -h_2 x_1 + x_{3+}$ in which the first term $-h_2 x_1$ is always negative and x_{3+} is strictly decreasing. Consequently, the direction of velocity \dot{x}_{2+} can be changed only once and the velocity of x_{2+} is negative at the final passing time.

$$\sigma_{2+}^f < 0 \text{ implies } \dot{x}_{2+}^f < 0 \quad (C.18)$$

The approaching velocity $\dot{x}_{2+}^f < 0$ near the switching plane $x_1 \approx 0$ is due to the negative state of x_{3+} .

$$\dot{x}_{2+}^f < 0 \text{ implies } \sigma_{3+}^f < 0 \quad (C.19)$$

The equation (C.17) and (C.19) shows that both of the final passing state are negative ($\sigma_{2+}^f < 0$ and $\sigma_{3+}^f < 0$). The general shearing effect of the sliding observer can be explained by the "sign equalization" of the final passing state.

Let us consider the other case $\sigma_{3+}^i < 0$.

Case 2)

With the initial condition $\sigma_{3+}^i < 0$, the initial velocity field of the reaching dynamics is

$$\begin{cases} \dot{x}_1^i > 0 \\ \dot{x}_{2+}^i < 0 \\ \dot{x}_{3+}^i < 0 \end{cases} \quad (C.20)$$

With the initial passing point $\sigma_{3+}^i < 0$, the final state is negative because the \dot{x}_3 is strictly decreasing.

$$\dot{x}_{3+}^i < 0 \text{ implies } \sigma_{3+}^f < 0 \quad (C.21)$$

The approaching velocity $\dot{x}_{1+}^f < 0$ near the switching plane $x_1 \approx 0$ is due to the negative of state x_{2+} .

$$\dot{x}_{1+}^f < 0 \text{ implies } \sigma_{2+}^f < 0 \quad (C.22)$$

We can see here the "sign equalization" of the states of the final passing point as it is in the equation (C.21) and (C.22). For the case of passing right, the unified sign of final passing state is positive ($\sigma_{2+}^f > 0$ $\sigma_{3+}^f > 0$). The sign equalization is due to the characteristic of the sliding observer velocity field. The direction of each state \dot{x}_j is the function of x_1 and x_{j+1} (for the last state: u_d) only. Since, in the right reaching domain, x_1 is positive only and the velocity of last state \dot{x}_{3+} is strictly decreasing, each direction sign can change only once or not at all. This special feature of the sliding observer guarantees the sign equalization in 2- and 3-order cases.

It is useful to note that σ_{2s}^f of the final passing point has the opposite sign of σ_{2s}^i :

$$\sigma_{2s}^i \sigma_{2s}^f < 0 \quad (s=+ \text{ or } -) \quad (\text{C.23})$$

When the solution point passes left, the succeeded initial state in the shifted-coordinate is obtained by the equation (2.60). Particularly the second state determines that the solution point pass through the hyperplane or not.

$$\begin{cases} \sigma_{1-}^i(\tau_j) = \sigma_{1+}^f(\tau_j) \\ \sigma_{2-}^i(\tau_j) = \sigma_{2+}^f(\tau_j) + 2 k_1 \\ \dots \\ \sigma_{n-}^i(\tau_j) = \sigma_{n+}^f(\tau_j) + 2 k_{n-1} \end{cases} \quad (\text{C.24})$$

If the sign of the second state in the following shifted-coordinate does not change, then the solution point crosses the hyperplane. If the sign is changed, then the sliding motion starts because the solution point moves to the hyperplane from the both sides.

C.4 High Order System

In the previous sections, the transient and the final states were reviewed. For the minimum phase LTI systems, the sign of final values are unity as shown in the previous section. The eigen structure of the reaching dynamics shows sign equalization also. However, since the reaching dynamics is only some part of the transient period, it is a subtle problem to prove the sign equalization of the reaching dynamics.

Conjecture C.1 Initially unified sign case.

If the initial signs are the same each other then the sign of the velocity changes only once.

Justification) Consider a n-order right reaching dynamics in the shifted-

coordinate.

$$\begin{cases} \dot{x}_1 = -h_1 x_1 + x_{2+} \\ \dot{x}_{2+} = -h_2 x_1 + x_{3+} \\ \dots \\ \dot{x}_{n+} = -h_n x_1 + u_d \end{cases}$$

Let assume the sign of all of the initial states are positive except $x_1 = 0$. At the hyperplane ($x_1 = 0$), all of the velocity field are positive direction except the last velocity.

Let assume the sign of \dot{x}_1 changes only once then the state x_1 is convex over the right reaching domain as followings:

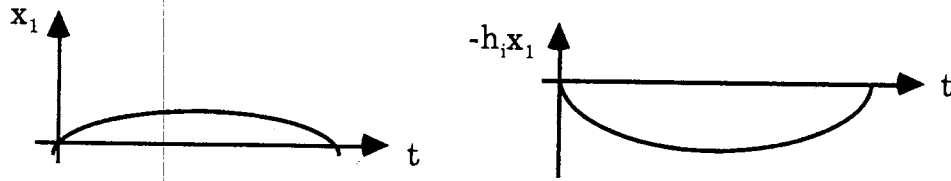


Figure C.3 a) Convexity of x_1 b) Concavity of $-h_i x_1$

For the i -th equation, the first term in the RHS, $-h_i x_1$, is concave over the right-reaching domain. The last state x_n that is initially positive decreases strictly and the sign of the final passing point of x_n is negative (see detail Chapter C.1).

The initial velocity direction of the second last state, i.e., $\dot{x}_{(n-1)+}$ is positive and becomes negative when $h_{n-1} x_1$ is greater than the state x_n . Since the last state x_n strictly decreases and the term, $-h_{n-1} x_1$, is concave over the time domain, the sign of $\dot{x}_{(n-1)+}$ changes only once. Therefore the second last state, $x_{(n-1)+}$ is concave. Let assume the state decreases enough so that it

becomes negative as plotted in Figure C a).

The initial velocity of the third last state, i.e., $\dot{x}_{(n-2)+}$ is positive and becomes negative when $h_{n-2} x_1$ is greater than the state x_{n-1} . Since the second last state x_{n-1} convex and the term, $-h_{n-2} x_1$, is concave over the whole time domain, the sign of $\dot{x}_{(n-2)+}$ changes only once. Therefore the third last state, $x_{(n-2)+}$ is concave. The sign change of the rest velocity can be explained as the same way as the former ones. Therefore, the assumption of convexity of x_1 is valid.

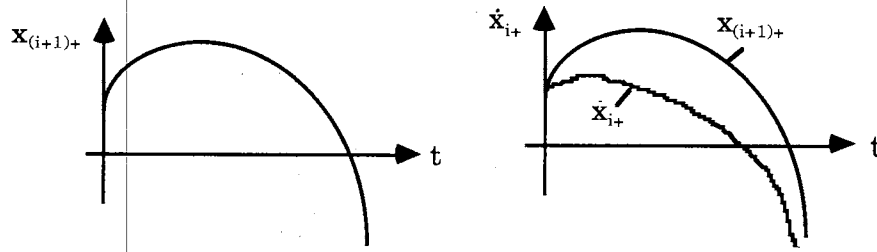


Figure C.4 a) Convexity of the state b) Sign Change of the state

Each state decreases enough to be negative as the state x_1 approaches to the hyperplane. If the state x_2 is positive when the state x_1 decreases and approaches to the hyperplane, then the velocity \dot{x}_1 is positive and the state x_1 increases again. Therefore, x_1 cannot be zero with the positive state x_2 and this is contradict to the convexity of x_1 .

Conjecture 2

All the final signs are changed from the initial sign

Justification) If any state x_{i+} has the same sign at the approaching the hyperplane instance then it will change the sign of velocity of the previous

state $\dot{\mathbf{x}}_{(i-1)+}$ again. This is contradiction to the Lemma 1)

Sign Alternating (For right-reaching domain)

Rewrite the reaching dynamics:

$$\dot{\mathbf{x}}_+ = -H \mathbf{x}_1 + \begin{pmatrix} \mathbf{x}_{2+} \\ \mathbf{x}_{3+} \\ \dots \\ \mathbf{x}_{n+} \\ \mathbf{u}_d \end{pmatrix} \quad (\text{C.25})$$

where $H = [h_1 \ h_2 \ , \dots \ , h_n]^T$

The initial velocity field is function of σ_+^i and \mathbf{u}_d only. The signs of the initial state are

$$(\sigma_+^i)^T = [\underbrace{0 \ + \dots \ +}_{\text{part I}} \underbrace{- \ ? \ \dots \ -}_{\text{part II}}]$$

The j-th equation of the reaching dynamics has the first negative state \mathbf{x}_{j+1} :

$$\dot{\mathbf{x}}_{j+} = -h_j \mathbf{x}_1 + \mathbf{x}_{(j+1)+}$$

Part I) If \mathbf{x}_{j+1} is negative all the time until \mathbf{x}_1 become 0, the first negative state \mathbf{x}_{j+1} do the same role as \mathbf{u}_d in the initial sign unity case. Hence, the number N_I is increased at least 1. If \mathbf{x}_{j+1} become positive at the instance \mathbf{x}_1 arriving the hyperplane then the N_I does not change in the next reaching domain.

Part II) The disturbance input also unifies the sign of the state in descending order so that the system will satisfy the sliding condition or on the way to the sign unity of the passing point.

C.5 Numerical Search Program

C.5 Numerical Search Program

The source code of the MATLAB program SOON and the SIMNON program Reaching are listed for the third order case only because the extension to the higher order system is straight forward.

C.5.1 SOON (for MATLAB)

```
%-----
%                               SOON.M
%-----
%   Sliding Observer design by worst reaching dynamics
%   for Nonlinear/ uncertain system
%   PURPOSE: Known Bounded Disturbance and
%   Known Bounded Initial States
%   Design the sliding observer coefficients in order to
%   converge to the sliding patch directly.
%-----
% For 3rd order only
odr=input('System Order=')
w=input('Wmax=')
w11=1.1*w
k3=max(1.1,w11);
% Select the proper Linear Coefficients
disp('Choose H so that the system is critically damped or slightly under
      damped');
h1=input('h1=')
h2=input('h2=')
h3=input('h3=')

% Save data for the Simnon program Reaching
save d_reaching
!ren d_reaching.mat d_reaching.t
% Run the Simnon Program Reaching
mreaching
% Get the Output of mreaching
!Ren o_reaching.t o_reaching.mat
load o_reaching

% Steady State with constant disturbance
x2ss=w*k1/k3;
x3ss=w*k2/k3;
```

```

%disp('Sliding dynamics e.v. ');
%As=[-k(2,1)/k(1,1) 1;-k(3,1)/k(1,1) 0];
As=[-k2/k1 1;-k3/k1 0];
eas=eig(As);
if re(eas) > 0 then disp('Warning:Unstable Equivalent Dynamics!!')
subplot(122);grid;
axis([-0.5 0.1 -1.5 1.5]);
plot(eas,'*');
xlabel('Re');ylabel('Im');
title('E.V. of sliding dynamics');
end

```

C.5.2 Reaching (for SIMNON)

```

"-----
MACRO M_REACHING
"-----
" Plot whole step at once : for third order system only
syst sys3 cost3 gold3 conn3 " *3.t: 3rd order system
store x1 x2 x3 t [sys3] tau j[cost3]
error 1e-6
init x2in[gold3]:3 "The initial bound of the states
init x3in[gold3]:2
" Estimates the proper number of the evaluations of the cost function
" in the GOLD.T search.
let plow=0
let phigh=2
let acc=.01
let unc0.=phigh-plow "Initial uncertainty.
let f1.=1.
let f2.=1.
free qf1.
free qf2.
free x. "Ratio fn-1/fn.
free uncn. "Uncertainty after N evaluations.
free n. "Required number of evaluations.
free p0. "Initial optimization starting point.
free teval. "Simulation time for evaluation.
free toptim. "Total simulation time.
default nmax.=20 "Maximal number of evaluations.

"-----Calculation of required number of evaluations
for i=1. to nmax.
let qf2.=f1.+f2.
let qf1.=f2.
let f1.=qf1.
let f2.=qf2.

```

```

let x.=f1./f2.
let uncn.=unc0./f1.
let n.=i
let nacc=-.05

if uncn. le nacc goto exit
next i
"-----
label exit
"-----

let p0.=x.*unc0.
let p0.=plow+p0.
init p:p0.
init pmin:p0.
init phi:phigh
init plo:plow
disp teval/teval
let toptim.=n.*teval.
let tperid.=12*teval.

simu 0 toptim. .001 /dz31 tperid.
init x1in[gold3]:x1in[gold3]
init x2in[gold3]:x2in[gold3]
init x3in[gold3]:x3in[gold3]
init jmin[gold3]:1e33
init m[gold3]:m[gold3]
export dz31<dz31

    let dat=dz3
"-----
"      Step by step
"-----

    default step.=30
    for jj=2 to step.
    let datjj=dat+jj
let p0.=x.*unc0.
let p0.=plow+p0.
let nn.=jj*n.
let jj1=jj-1
let nn0.=jj1*n.
disp teval/teval "from gold3
disp x1/x1

let toptim.=nn.*teval.
let tbgn.=nn0.*teval.

simu tbgn. toptim. 0.0001 /datjj tperid.
init x1in[gold3]:x1in[gold3]
init x2in[gold3]:x2in[gold3]

```

```

init x3in[gold3]:x3in[gold3]
init jmin[gold3]:1e33
init m[gold3]:nn.
init p:p0.
init pmin:p0.
init phi:phigh
init plo:plow
  free unc0.
"suspend
export datjj<datjj
if x1. le acc goto exitj
  next jj
"-----
label exitj

split 2 2
area 1 1
ashow x2(x1)
turn dark on
area 1 2
ashow x3(x1)
area 2 1
ashow x3 x2 "y
area 2 2
turn dark off
ashow T
end

"-----
"          CONTINUOUS SYSTEM SYS3
"-----
input T alarm
output y1 y2 y3 e1 e2 e3
state x1 x2 x3
der dx1 dx2 dx3

"Disturbance Input :T
dx1 = if alarm<0.5 then -h1*x1 + x2 else 0
dx2 = if alarm<0.5 then -h2*x1 + x3 else 0
dx3 = if alarm<0.5 then -h3*x1 -kn*T else 0
st= CTERM(t>t0 or (dx1<0 and x1 < eps) )
eps:-.001
t0:300

"Output
mag = sqrt(dx1*dx1+dx2*dx2 + dx3*dx3)
e1 = x1 + dx1/mag
e2 = x2 + dx2/mag
e3 = x3 + dx3/mag

```

```

y1 = x1
y2 = x2
y3 = x3

```

```

"parameters
h1:6 "1.8 ---data1.8
h2:12.2 ".95 "12.2
h3:8.4" .25 "8.4
kn:.023
end

```

```

"-----
"                                CONTINUOUS SYSTEM COST3
"-----
"Evaluates the cost function
input e1 e2 e3 tau
output j alarm
state s1
der ds1

```

```

" Measure distance
ds1 = if not alarm then e1*e1 + e2*e2 + e3*e3 else 0
v = s1+.01
j = 1/v
"Alarm test:
alarm = if j>jmax then 1 else 0
"parameters:
Jmax : 1000
end

```

```

"-----
"                                DISCRETE SYSTEM GOLD3
"-----

```

```

"Discrete system to perform optimination of one parameter
input j y1 y2 y3
output peval tbegin
state plo phi pmin p jmin  x1in x2in x3in m n
new qplo qphi qpmin qP qJmin qx1in qx2in qx3in qm qn
time t
tsamp ts

```

```

"Update the search state:
left = P<mid
decr = J<Jmin
stepn=qm-qn
t15 = stepn+1.5
t05 = stepn+0.5
PloFix = if t<t15*teval then 1 else mod(left+decr+1,2)
PhiFix = if t<t15*teval then 1 else mod(left+decr,2)

```



```

unc = newPhi-newPlo "Uncertainty interval.
mid = (Phi+Plo)/2 "Midpoint of the interval
newPlo = if PloFix then Plo else if decr then Pmin else P
newPhi = if PhiFix then Phi else if decr then Pmin else P
newPmin = if decr then P else Pmin
qJmin = if t>t05*teval and decr then J
        else Jmin
qPlo = if t>t15*teval then newPlo else Plo
qPhi = if t>t15*teval then newPhi else Phi
qPmin = if t>t05*teval then newPmin else Pmin
qP = Peval
"Calculate the new evaluation point Peval:
Peval = if t>t05*teval then newPhi+newPlo-newPmin else Pmin

"Reset process and loss-function after each test
qm = m+1 "Counter
qn = if n<11.5 then n+1 else 1 "Numbering in each step
qx1in = if mod(m+1,nmax)>0 then x1in else y1
qx2in = if mod(m+1,nmax)>0 then x2in else y2
qx3in = if mod(m+1,nmax)>0 then x3in else y3

x1[sys3] = x1in
x2[sys3] = x2in
x3[sys3] = x3in
s1[cost3]=0
"New sample:
ts = t+teval
tbegin = t

"Initial values that should be set by the user
nmax:12 "Max number of evaluation in each step
n:0
m:0
Plo :0.0 "Lower bound of parameter
Phi :1.0 "Upper bound of parameter
P : 0.61803 "Golden section ratio
"Jmin :1E33 "Max real value
teval : .05 "Simulation time for evaluation
end

"-----
" CONNECTING SYSTEM CONN3
"-----
time t
T[sys3] = Peval[gold3]
e1[cost3] = e1[sys3]
e2[cost3] = e2[sys3]
e3[cost3] = e3[sys3]
y1[gold3] = y1[sys3]

```

```
y2[gold3] = y2[sys3]
y3[gold3] = y3[sys3]
J[gold3] = J[cost3]
tau[cost3] = t - tbegin[gold3]
alarm[sys3] = alarm[cost3]
end
```

VITA 2

JinHee Choi

Candidate for the Degree of
Doctor of Philosophy

Thesis: A STUDY ON SLIDING MODE STATE ESTIMATION

Major Field: Mechanical Engineering

Biographical:

Personal Data: Born in Pusan, Korea, August 15, 1956, the son of Mr. and Mrs. JongKwan Choi.

Education: Received the Bachelor of Science degree in Mechanical Design and Production Engineering from Seoul National University in February, 1979; received the Master of Science degree in Mechanical Engineering from Korea Advanced Institute of Science and Technology in February, 1981; completed the requirements for the Doctor of Philosophy degree at Oklahoma State University in May, 1993.

Professional Experience: Lecturer, Korea Military Academy, June 1981 - February 1983; Instructor, Korea Military Academy, March 1983 - April 1986; Assistant Professor, Korea Military Academy, May 1986 - present.